1968

A study of the anodic oxidation of ethylene on gold and gold-platinum alloys

San-Cheng Lai

Department: Chemical and Biochemical Engineering

A STUDY OF THE ANODIC OXIDATION OF ETHYLENE ON GOLD AND GOLD-PLATINUM ALLOYS

by

SAN-CHENG, LAI 1968

An Abstract of a Dissertation

Presented to the Faculty of the Graduate School of the

UNIVERSITY OF MISSOURI-ROLLA

In Partial Fulfillment of the Requirements for the Degree

DOCTOR OF PHILOSOPHY

IN

CHEMICAL ENGINEERING

1968

The anodic oxidation of ethylene on Au and Au-Pt alloys was studied at 80°C in solutions of H_2SO_4, K_2SO_4, K_2CO_3, and KOH with pH's ranging from 0.35 to 12.7. Reaction rates were measured as a function of potential, pH, temperature, and partial pressure of ethylene. A transition region (apparently a change in the mechanism) was found in the Tafel plots.

The following parameters were found in acid solutions on Au and above the transition region on Au-rich alloys,

$$\left(\frac{\partial V}{\partial \log i}\right)_{P_E,T,pH} \sim 70 \text{ mv}, \qquad \left(\frac{\partial i}{\partial P}\right)_{V,T,pH} > 0$$

$$\left(\frac{\partial \log i}{\partial pH}\right)_{V,T,P_E} \sim 0 \; ; \qquad \left(\frac{\partial E_a}{\partial V}\right)_{P_E,pH} \sim -23 \text{ Kcal/volt}$$

Below the transition region and in basic solutions on all electrodes, the following parameters were found

$$\left(\frac{\partial V}{\partial \log i}\right)_{P_E,T,pH} \sim 140 \text{ mv}, \qquad \left(\frac{\partial i}{\partial P}\right)_{V,T,pH} > 0$$

$$\left(\frac{\partial \log i}{\partial pH}\right)_{V,T,P_E} \sim \begin{cases} 0 \text{ (in acid)} \\ 1 \text{ (in base)} \end{cases} ; \left(\frac{\partial E_a}{\partial V}\right)_{P_E,pH} \sim -11 \text{ Kcal/volt}$$

The efficiency studies in 1 N H_2SO_4 showed that the relative amounts of CO_2 produced decreased with decreasing Pt content in the alloys. Acetaldehyde was the only other product detected. No CO_2 was produced on Au.

The reaction mechanism in acid solutions on Au and above the transition region on Au-rich alloys is interpreted in terms of the following sequence:

$$C_2H_4\ (sol) \rightleftharpoons C_2H_4\ (ads)$$

$$C_2H_4\ (ads) \rightleftharpoons C_2H_4^+\ (ads) + e$$

$$C_2H_4^+\ (ads) + H_2O \xrightarrow{r.d.s.} C_2H_4OH\ (ads) + H^+$$

$$C_2H_4OH\ (ads) \longrightarrow CH_3CHO + H^+ + e$$

or,

$$C_2H_4OH\ (ads) \xrightarrow{H_2O} \cdots \rightarrow CO_2, CH_3CHO,\ H^+,\ \text{and electrons}$$

The corresponding rate equation is

$$i = nFk\ a_{H_2O}\ \Theta_E\ \exp(FV/RT)$$

Below the transition region and in basic solutions on all electrodes, the reaction sequence proposed is

$$C_2H_4\ (sol) \rightleftharpoons C_2H_4\ (ads)$$

r.d.s.
$$\begin{cases} C_2H_4\ (ads) + H_2O\ (sol) \longrightarrow C_2H_4OH\ (ads) + H^+ + e \\ C_2H_4\ (ads) + OH^-\ (sol) \longrightarrow C_2H_4OH\ (ads) + e \end{cases}$$

$$C_2H_4OH\ (ads) \xrightarrow{H_2O} \cdots \rightarrow CO_2,\ CH_3CHO,\ H^+,\ \text{and electrons}$$

The rate equation for this sequence is represented by

$$i = nF(k\ a_{H_2O} + k'\ a_{OH^-})\ \Theta_E\ \exp\left(\frac{\alpha FV}{RT}\right)$$

ACKNOWLEDGEMENTS

The author wishes to thank Dr. J. W. Johnson, Professor of Chemical Engineering, who served as research advisor, and Dr. W. J. James, Professor of Chemistry and Director of the Graduate Center for Materials Research, Space Sciences Research Center, University of Missouri-Rolla. Their help, guidance, and encouragement are sincerely appreciated.

The author gratefully acknowledges a Research Assistantship from the Space Sciences Research Center.

The author is deeply indebted to his parents for their encouragement while pursuing advanced studies in the United States.

A STUDY OF THE ANODIC OXIDATION OF ETHYLENE ON GOLD AND GOLD-PLATINUM ALLOYS

by

SAN-CHENG LAI

A Dissertation

Presented to the Faculty of the Graduate School of the

UNIVERSITY OF MISSOURI-ROLLA

In Partial Fulfillment of the Requirements for the Degree

DOCTOR OF PHILOSOPHY

IN

CHEMICAL ENGINEERING

1968

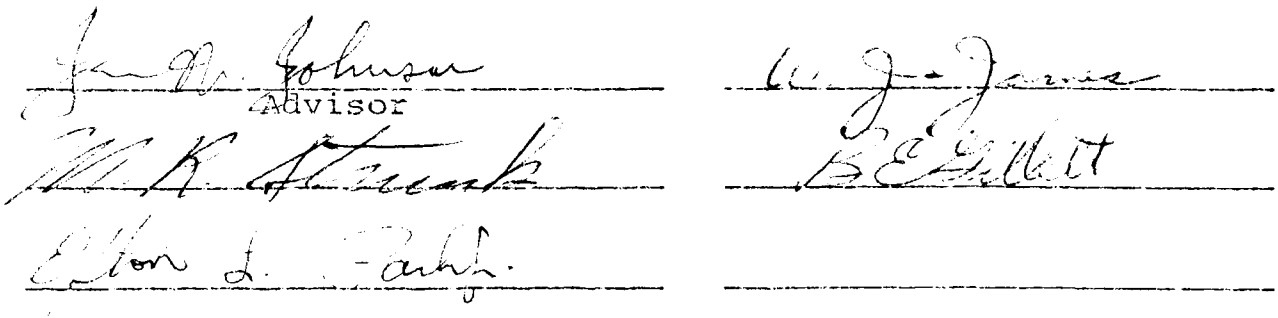

TABLE OF CONTENTS

LIST OF FIGURES

LIST OF TABLES

Chapter I

INTRODUCTION

The distinctive features of electrochemical energy conversion is the direct conversion of the chemical energy of a reaction into electrical energy without going through the intermediary of heat, thereby avoiding the Carnot limitation. Since it is theoretically possible to obtain electrical energy to the extent of the free energy change of the chemical reaction, the overall thermal efficiencies expected are nearly 100 percent. However, the observed efficiencies of most electrochemical energy converters are considerably lower than this due to a slowness of one or more of the intermediate steps of the overall reaction.

There has been a recent surge of studies on the electrooxidation of hydrocarbons because of their possible use as fuels in electrochemical conversion. The widespread use of fuel cells hinges on a cheap and readily available fuel such as natural gas, propane, or methane that can be oxidized at moderate temperatures. From the economic standpoint, hydrocarbons have a clear advantage over other fuels suggested for use. They also have a further advantange of being easily handled and distributed through established systems. Therefore, it is important that these specialized fuel cells are developed and commercialized.

Since most fuel cells studies[1,2] have been concerned with technological aspects, the results are usually too complex to allow electrode kinetic analysis. The more fundamental

aspects of several organic systems have been studied[3,4,5,6]. Previous studies of the electro-oxidation of ethylene on Au in acid[7] had not been directed toward determining all the reaction parameters which are useful in diagnosing a mechanism.

It has been reported[8] that Pt alloys have shown an even higher catalytic activity than pure Pt black. This refers particularly to alloys of the Pt-Ru system and to a lesser degree of alloys with Ir and Rh. These catalysts were found to be active for the oxidation of a number of organic fuels such as methanol and selected hydrocarbons.

The object of this reported investigation was to establish the mechanisms for the anodic oxidation of ethylene on Au and Au-Pt alloy electrodes in aqueous solutions. It was believed that this research would lead to a better understanding of the rate processes of electrochemical reactions in general on alloy electrodes.

Chapter II

LITERATURE REVIEW

Since electrocatalysis plays an important role in electro-organic reactions, the literature reviewed for this investigation is divided into two parts: (1) electrocatalysis in electrochemical reactions, and (2) anodic oxidation of ethylene on various metals.

A. Electrocatalysis in Electrochemical Reactions

Electrocatalysis has been defined as the influence of an inert metal electrode upon a reaction rate, when the influence of mass transfer to or from active sites is eliminated. Electrocatalysis is closely related to the field of chemical catalysis, but with two major differences: (1) an influence of an applied electric field, and (2) an influence of the electrolyte on the reaction rate. The potential as an additional variable is in many ways an advantage, since the rate of the reaction may be varied over a wide range simply by varying the potential. A considerable increase in temperature would be necessary in order to change the rate of non-electrochemical reactions by the same magnitude.

One problem in electrocatalysis is that electrochemical reactions are generally carried out in aqueous or non-aqueous solutions. Thus, the solvent may play a role in the overall reaction. In addition, it is necessary to study the reaction in highly purified solutions. Otherwise, impurities may affect the kinetics of the desired reactions so that the real

mechanism is obscured. As in chemical catalysis, the nature of electronic interactions between the metal surface and reacting molecules play an important role in electrocatalysis. Factors that should be considered are: the magnitude of electronic work functions, the number of unfilled electron levels in d-bands, the structure of the adsorbing crystal planes, the electron affinity of the adsorbing species, the presence of unpaired and π electrons, the effect of steric hindrance, and the energies of the adsorbing species. A brief consideration of these follows.

1. Electronic Factors

The principal electronic factors associated with active metal catalysts, particularly the transition metals, are the electronic work function and the number of unfilled electron levels in the d-bands. Three distinctive groups of metals have been obtained when the exchange current (i_o) for the hydrogen evolution reaction is compared to the work function of the metal[9]. The high overpotential metals fall in one group, the medium overpotential metals in another, and the low overpotential metals in a third. These three groups are associated with the slow discharge, slow electrochemical desorption, and slow recombination mechanisms, respectively. In another study, plots of overpotential at a constant current density versus the heat of adsorption of hydrogen on the metal (the percent d-band character increases as the heat of adsorption decreases) showed a separation into two distinct groups[10].

The effect of d-band character (or d-vacancies) on the hydrogen electrode reaction is also illustrated in the work of Damjanovic et al., using Au, Pd (or Pt), and their alloys[11]. With an increasing Au-content of the alloy, i_o decreases fairly sharply until at 60 percent Au, whereafter the change is considerably slower. At 60 percent Au the d-band is completed and no further change in activity would be expected above this composition. A linear relationship was found between log i_o and the number of unpaired d-electrons/atom in these alloys. In another study, Conway et al., also found a similar relationship for hydrogen evolution on Cu, Ni, and their alloys[12].

Rao et al., coulometrically determined the oxygen coverage at one atmosphere pressure on a number of metals[13]. The results showed that unpaired d-electrons participated directly in the bonding of the metal atom to oxygen (Table I.) Au, with no unpaired d-electrons, had the lowest oxygen coverage, while Ru with the highest number of unpaired electrons had the highest.

The influence of electronic factors on the electroreduction rate of oxygen has been studied on a number of metals and alloys[14]. From the Tafel curves for the metals Pt, Pd, Ir, Rh, and Au in acid solutions, it appears that Au with no unpaired d-electrons has a significantly lower exchange current density than the other metals. Rh and Ir which have the same number of unpaired electrons show essentially identical current-potential behavior.

TABLE I

RELATIONSHIP OF OXYGEN COVERAGES TO NUMBER OF UNPAIRED d-ELECTRONS/ATOM FOR THE NOBLE METALS[13]

Metal	Observed Oxygen Coverage	Calculated Oxygen of a Monolayer	Fraction of Surface Covered by Oxygen	Number of Unpaired d-Electrons/Atom
	$\mu C/cm^2$	$\mu C/cm^2$		
Pd	110	510	0.22	0.55
Pt	110	500	0.22	0.55-0.6
	135	500	0.27	0.55-0.6
Rh	480	530	0.90	1.7
Ir	440	525	0.84	1.7
Ru	500	530	0.95	2.2
Au	<15		<0.03	0

The current-potential behavior of a series of Au-Pd alloys shows (1) the value of the rest potential decreases in going from Pd to Au, and (2) Au and 75Au-25Pd alloy have considerably higher Tafel slopes than Pd and the other alloys which exhibit nearly the same slope. Thus, a change in mechanism occurs at approximately the composition where the d-bands are filled.

A proposed explanation of the influence of the d-vacancy on the electrocatalysis of oxygen reduction is that chemisorbed oxygen is an intermediate in the reaction and that the M-O bond strength varies with the percent d-vacancy.

Recently, a parabolic (volcano type) relationship between the exchange current density for ethylene oxidation and the latent heat of sublimation of the electrode metal was obtained by Kuhn and Bockris (See Figure 1)[15]. A similar relationship was found for alloys of Pd and Rh. This was proposed as a possible method to determine the composition of alloys to substitute for the pure metals.

From the parabolic relationship, it may be inferred that on the left-hand side of the peak that adsorption is rate determining since there is an increase of rate with heat of sublimation. This can be shown with the Pauling equation which relates the strength of an adsorption bond with the heat of sublimation[16]. Using similar reasoning, a desorption step would control the rate of the overall reaction on the right-hand side of the peak.

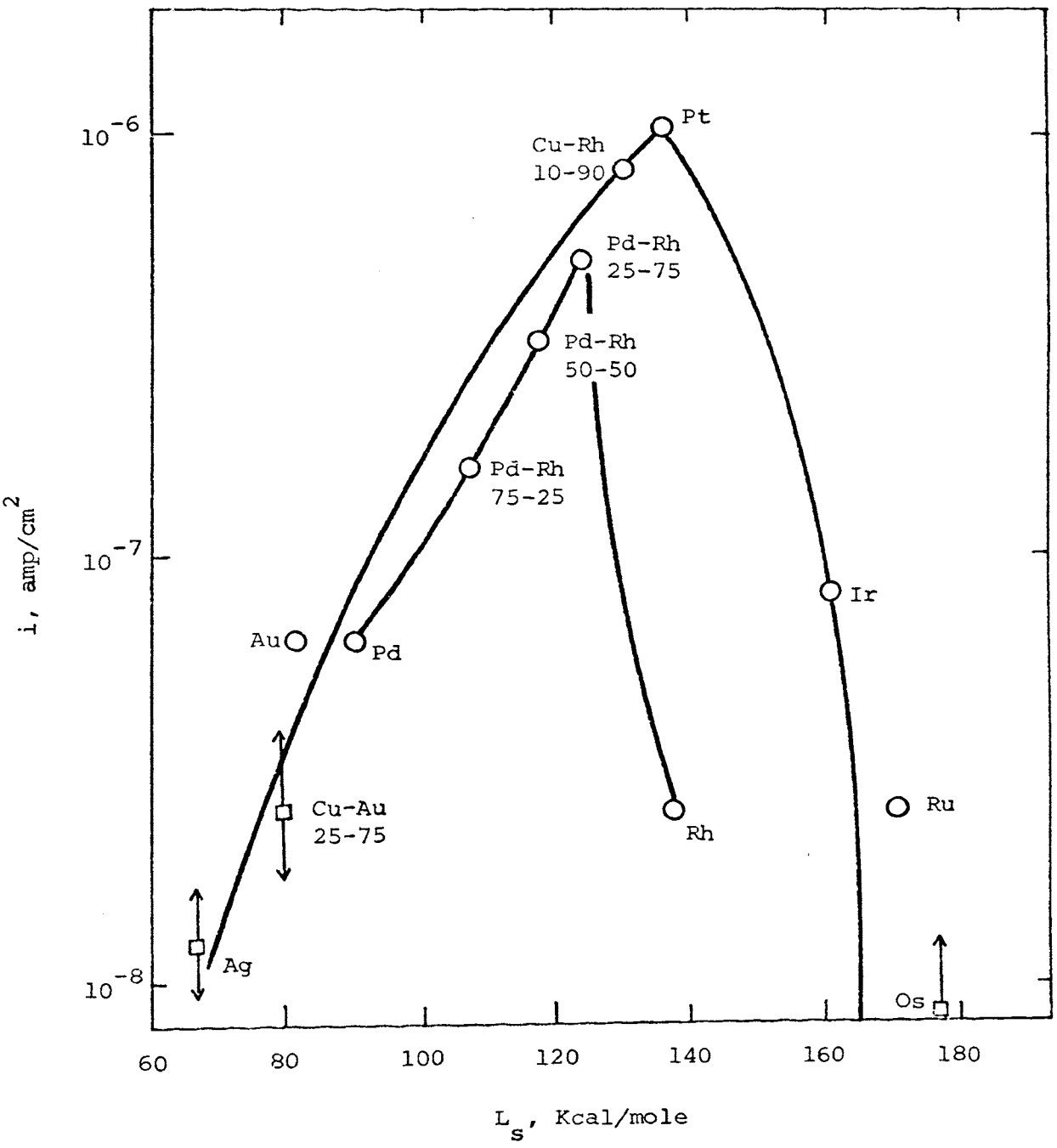

Figure 1. Effect of latent heat of sublimation on catalytic activity for the anodic oxidation of ethylene.[15]

2. Geometric Factors

Only a small amount of work has been done to examine the influence of geometric factors on electrochemical reactions. The metals usually studied in the electro-oxidation of organic compounds (Pt, Pd, Rh, Ir, and Au) have similar lattice parameters. They all have face-centered cubic structure and their atomic radii do not vary over 0.1 Å.

Hydrogen overpotential measurements have been made on the various crystal planes of Ni[17]. The (III) plane, which is the most densely packed plane, showed the highest activity. No effect of grain size on the rate of hydrogen evolution on platinized Pt has been observed, however, small grain sizes were not used[18].

In a study of formic acid oxidation, Gottlieb found that the only effect of the platinization of Pt was to increase the true area of the electrode[19]. Similar results were obtained for the oxidation of other hydrocarbons[20]. This indicates that increased roughness of the electrode surface does not affect the catalytic activity. The effect of defect concentration in electrocatalysis has not been studied for organic oxidations. One study of hydrogen evolution on iron showed a ten-fold increase in the rate factor when 0.1 percent C was introduced into zone-refined iron[21]. In general, geometric factors play a small role and in many cases cannot be separated from the electronic factors. However, they can become important if the internuclear distances of the metal atoms are not within a certain range, particularly if more than one site

attachment is involved in adsorption[22].

B. Anodic Oxidation of Ethylene

1. Ethylene Oxidation on Platinum

Ethylene oxidation in alkaline solution of Pt has been studied by Green et al.[5] Their current-voltage curves indicate Tafel slopes of (2)(2.3 RT/F). They reported no significant influence of ethylene partial pressure on the Tafel slope or the exchange current. There were upper limits on the Tafel curve. Limiting currents were attributed to both electrode passivation and transport of ethylene to the electrode. In the latter case, the limiting current was dependent on stirring and the partial pressure of ethylene. Measurements made over extended periods of time showed that the electrode became continuously less active. This phenomenon was attributed to the formation of an oxide layer on which the rate of ethylene oxidation was significantly lowered. Experiments were also carried out in a closed cell arrangement, where ethylene consumed at the anode and coulombs of charge passed could be measured simultaneously. Within experimental error, it was found that one mole of ethylene involved the passage of twelve Faradays of charge showing the ethylene was totally oxidized, i.e.,

$$C_2H_4 + 16\ OH^- \longrightarrow 2\ CO_3^{=} + 10\ H_2O + 12\ e \qquad (2.1)$$

The following mechanism was proposed:

$$OH^-(sol) \xrightarrow{r.d.s.} OH\ (ads) + e \qquad (2.2)$$

$$C_2H_4\ (sol) \rightleftharpoons C_2H_4\ (ads) \qquad (2.3)$$

$$C_2H_4\ (ads) + OH\ (ads) \longrightarrow C_2H_4OH\ (ads)\ \cdots \qquad (2.4)$$

The formation of oxide films in alkaline solution was taken as strong evidence for the occurrence of OH^- discharge. It was postulated that oxide formation commenced only when the surface concentration of hydroxyl radicals achieved a sufficiently high coverage, i.e.,

$$2\ M\text{-}OH\ (\text{high coverage}) \longrightarrow 2\ M\text{-}O + H_2O \qquad (2.5)$$

Thus, extensive OH^- discharge lead to surface oxide formation and passivation.

Wroblowa et al., studied the oxidation of ethylene on platinized Pt in acid and alkaline media[6]. They found the faradaic efficiency for oxidation of the ethylene to carbon dioxide in acid solutions to be 100 ± 1 percent. In 1 N NaOH, the efficiency was 90 ± 5 percent. The values for complete oxidation were calculated according to the reactions:

$$C_2H_4 + 4\ H_2O \longrightarrow 2\ CO_2 + 12\ H^+ + 12\ e \quad (\text{in acid solutions}) \qquad (2.6)$$

$$C_2H_4 + 12\ OH^- \longrightarrow 2\ CO_2 + 8\ H_2O + 12\ e \quad (\text{in basic solutions}) \qquad (2.7)$$

For 1 atm ethylene partial pressure, linear Tafel regions with slopes of 140-160 mv were found over the pH range 0.5 to 12.5.

At higher potentials, the current rapidly decreased to negligible values. This was explained as passivation of the electrode, similar to that proposed by Green, et al.[5]

Current-potential relations were determined at ethylene partial pressures of 10^{-1}, 10^{-2}, 10^{-3}, and 10^{-4} atm. The length of the linear Tafel region decreased considerably at lower pressures due to the current becoming diffusion limited. For a constant potential, the current was found to increase with decreasing ethylene partial pressure, in other words,

$$\left(\frac{\partial\ i}{\partial\ P_E}\right)_{V,T,pH} < 0 \qquad (2.8)$$

This inverse pressure effect showed that the rate determining step involved a substance whose adsorption required a surface free of ethylene (or any intermediate derived therefrom).

The current-pH relationship was found to be

$$\left(\frac{\partial\ \log\ i}{\partial\ pH}\right)_{V,T,P_E} = -0.45 \qquad (2.9)$$

A study of the temperature effect in 1 N H_2SO_4 for an ethylene pressure of 1 atm was made. An apparent activation energy of 20.5 ± 1 Kcal at 0.380v was calculated. No systematic change with potential was found. This was attributed to experimental error arising from the limited temperature and potential range over which the measurements could be carried out. The activation energy at the reversible potential

was calculated as 17 ± 2 Kcal .

The most probable mode of ethylene adsorption is

$$C_2H_4 + 2\ M \longrightarrow \underset{\underset{M}{|}}{H_2C} \text{——} \underset{\underset{M}{|}}{CH_2} \qquad (2.10)$$

Evidence was given that ethylene adsorbed onto Pt with a four point attachment. Thus, the isotherm employed was of the form

$$(\theta_E)/(1-\theta_E)^4 = K_c C_E \qquad (2.11)$$

or,

$$= K_p P_E \qquad (2.12)$$

Experimental values of K_p were reported as

$$2.3 \leq K_p \leq 150$$

The reaction sequence was represented as

$$C_2H_4\ (sol) \rightleftharpoons C_2H_4\ (ads) \qquad (2.13)$$

r.d.s.

$$H_2O\ (sol) \longrightarrow OH\ (ads) + H^+\ (sol) + e \qquad (2.14a)$$

$$OH^-\ (sol) \longrightarrow OH\ (ads) + e \qquad (2.14b)$$

$$C_2H_4\ (ads) + OH\ (ads) \longrightarrow C_2H_4OH\ (ads),$$

$$\text{or } C_2H_3\ (ads) + HOH \qquad (2.15)$$

$$C_2H_4OH\ (ads) \longrightarrow \overset{H_2O}{\cdots} \longrightarrow 2\ CO_2\ (sol) + 11\ H^+\ (sol) + 11\ e \qquad (2.16)$$

The coverage of all intermediates would be small in comparison with the coverage of the ethylenic radical, since they would be formed after the rate determining step and not in equilibrium due to the constant removal of the final product. From this reasoning, it was concluded that $\theta_T \sim \theta_E$. Thus, the rate equation was expressed as

$$i = k_{2.14a} a_{H_2O} (1-\theta_E) \exp\left(\frac{\alpha FV}{RT}\right) \tag{2.17}$$

or

$$i = k_{2.14b} a_{OH^-} (1-\theta_E) \exp\left(\frac{\alpha FV}{RT}\right) \tag{2.18}$$

It was necessary to modify this mechanism in order to explain the observed pH effect. For this modification, it was assumed: (1) H_2O undergoes charge transfer only when oriented with the O atoms toward the electrode, thus increasing the fraction of water molecules which could react at increasing pH. (2) The potential of zero charge of Pt changes with pH according to the equation

$$V_{pzc} = V°_{pzc} + \frac{RT}{F} \ln a_{H^+} \tag{2.19}$$

Introducing these assumptions into the rate equation gives

$$i = k_{2.14a} a_{H_2O} (1-\theta_E) \exp\left[\{V - (V°_{pzc} + \frac{RT}{F} \ln a_{H^+})\}\frac{\alpha F}{RT}\right] \tag{2.20}$$

It was further concluded that since the variation of log i with pH remained constant throughout the entire pH range and since H_2O discharge was the only way to supply adsorbed

OH in acid solutions, H_2O discharge was the rate determining step for the entire pH range.

2. Ethylene Oxidation on Various Noble Metals

Dahms and Bockris studied the electro-oxidation of ethylene on noble electrodes (Pt, Ir, Rh, Au, and Pd) in sulfuric acid solutions at 80°C[7]. The primary objective of this investigation was to determine the relative electrocatalytic activity of the metals; however, some mechanisms were suggested. A summary of their results is presented in Table II. Pt, Ir, and Rh were found to behave somewhat similarly, as did Au and Pd.

In 1 N Na_2SO_4 solutions in which the concentration of H_2SO_4 varied from 0.01 to 1 M, the reaction rates for the group Pt, Ir, and Rh were found to vary in the order Pt > Rh > Ir. Other parameters such as the extent of oxidation, Tafel slopes, pH effects, partial pressure effects, and temperature effects were found to be consistent with the results presented by Wroblowa et al., earlier in the discussion of the anodic oxidation on Pt. Therefore, it was concluded that water discharge was the rate determining step for the anodic oxidation of ethylene on metals of this group.

A differing behavior was found within the groups in that the lengths of the linear Tafel region for Ir and Rh were very short compared to Pt and similarly the length for Pd was shorter than for Au. The limited linear region was attributed to oxide formation which tended to passivate the

TABLE II

ETHYLENE OXIDATION AND CHARACTERISTIC PROPERTIES OF THE METALS[7]

Metal	Reaction Product	"Chemical" Reaction Rate at P.Z.C.	pH Dependence $\left(\frac{\partial V}{\partial pH}\right)_i$	Tafel Slope $\left(\frac{\partial V}{\partial \log i}\right)_{pH}$	P.Z.C.	Vacant d-Orbitals per Atom	Heat of Sublimation
		amp/cm^2	mv	mv	v(SHE)		Kcal/gmole
Pt	CO_2	$1x10^{-7}$	70	160	+0.30	0.55	135
Ir	CO_2	$1x10^{-11}$	75	132	+0.05	1.5	165
Rh	CO_2	$5x10^{-11}$	70	155	+0.05	1.5	138
Au	No CO_2 Aldehydes	$1x10^{-11}$	0	72	+0.30	0	84
Pd	As Au	$7x10^{-10}$	0	80-110	+0.25	0.55	91

electrode.

Vastly different results from those on the Pt, Rh, Ir group were obtained for Au and Pd. For these, the predominant reaction products were aldehydes and ketones with apparently no CO_2 production. Thus, the approximate number of electrons transferred per ethylene molecule was two.

Current-potential plots of Au and Pd in 1 N Na_2SO_4 solutions, in which the concentration of H_2SO_4 ranged from 0.1 to 2 M H_2SO_4 indicated that pH had essentially no effect on the Tafel curves. The slopes of the linear Tafel region were found to be 70 mv for the Au electrode and 80-110 mv for Pd.

For a constant potential, the current was found to decrease with decreasing ethylene partial pressure, i.e., a positive pressure effect:

$$\left(\frac{\partial\, i}{\partial\, P_E}\right)_{V,T,pH} > 0 \qquad (2.21)$$

The mechanism proposed for the Au, Pd group was

$$C_2H_4\ (sol) \rightleftharpoons C_2H_4\ (ads) \qquad (2.22)$$

$$C_2H_4\ (ads) \rightleftharpoons C_2H_4^+\ (ads) + e \qquad (2.23)$$

$$C_2H_4^+\ (ads) + H_2O\ (sol) \xrightarrow{r.d.s.} C_2H_4OH\ (ads) + H^+\ (sol) \qquad (2.24)$$

$$C_2H_4OH\ (ads) \longrightarrow C_2H_4O\ (sol) + H^+\ (sol) + e \qquad (2.25)$$

It was emphasized that further work was needed to verify

the above mechanism, but that it was consistent with the limited results that were obtained.

A hypothesis was presented to explain the differences in the oxidation products of the two groups. As seen in Table II, there is a large difference in the heats of sublimation of the first and second groups. Using these data and Pauling's equation, it was found that the bond strengths between the carbon atoms and the metals in the first group were about 20 Kcal higher than those of the second group. Consequently, the bonds between the metal-organic intermediates on the Au, Pd metals could be broken more easily, resulting in a higher rate of desorption which would yield intermediate oxidation products.

Dahms and Bockris also determined the oxygen coverage at various potentials for the five metals involved in their study. It was concluded that the rate at which the oxidation could occur is limited primarily by a competing oxide formation at higher potentials in the order Rh > Ir > Pt, Pd > Au. This conclusion was consistent with the experimental results.

3. Ethylene Oxidation on Noble Metals and Alloys

Kuhn et al., studied the anodic oxidation of ethylene on smooth noble metals and certain binary alloys in aqueous solutions at 80°C (See Table III)[15]. Attempts were made to correlate catalytic activities from heterogeneous gas reactions. Homogeneous, non-porous metallic phases were considered and variations in these single phases on the reaction

TABLE III

PARAMETERS IN THE ELECTROCHEMICAL OXIDATION OF ETHYLENE[15]

Metal or Alloy	Tafel Slope	$\left(\frac{\partial \log i}{\partial P_E}\right)$	$\left(\frac{\partial \log i}{\partial pH}\right)_V$	Reaction Product	Coverage with Ethylene	$\left(\frac{i_{H_2O}}{i_{D_2O}}\right)$	i (0.6 v)
	mv	atm^{-1}					amp/cm^2
Pt	140	-0.2	0.45	CO_2	1	1.5-2.5	5×10^{-6}
Pd	190	+0.5	0.5	50% CO_2 Balance Aldehydic			2×10^{-7}
Rh	160	+0.5	0.5	CO_2	0.02	4-5	1×10^{-7}
Ir	160	+0.5	0.5	CO_2			3×10^{-7}
Au	200	+0.5	0.5	As Pd	0.3	4-6	2×10^{-7}
Os							$<1\times10^{-8}$
Ru	165						1×10^{-7}
Ag							5×10^{-8}
Hg							$<1\times10^{-8}$
Pd-Au							
20-80							6×10^{-7}
46-54	160	+0.5					3×10^{-7}
78-22							4×10^{-7}
Rh-Pd							
25-75							7×10^{-7}
50-50	170						1.5×10^{-6}
75-25							3×10^{-8}
Cu-Rh							
10-90	160	+0.5					4×10^{-6}
Cu-Au							1×10^{-7}
Pt-Rh							
80-20	160						8×10^{-7}
50-50							5×10^{-7}
Pt-Ni							
85-15	170						4×10^{-7}

mechanisms were examined. The choice of substrates was limited to metals and their alloys which neither corrode nor passivate in the potential range for ethylene oxidation (0.3-0.9v SHE). For alloys, such as those containing Ni or Cu, increasing amounts of the non-noble constituent were introduced so that the highest possible amount of non-noble component could be determined which did not result in dissolution of the alloy during passage of an anodic current.

Studies in isotopic substitution also were carried out. A comparison of anodic reaction rates occurring on the same metals in aqueous and deuterated electrolytes offered an additional criterion in the elucidation of reaction mechanisms under conditions where the electrolyte was the only source of hydrogen/deuterium atoms. The isotope effects were estimated for various possible rate determining steps and are presented below:

(1) Rate determining or preceding steps do not involve the breaking of bonds in water molecules. This type of mechanism was postulated by Bagotsky and Vasiliev[23] for oxidation of organic alcohols and acids of the type R-H where the r.d.s. is

$$R\text{-}H + H_2O \longrightarrow R\ (ads) + H_3O^+ + e \qquad (2.26)$$

or

$$R\text{-}H + D_2O \longrightarrow R\ (ads) + HD_2O^+ + e \qquad (2.27)$$

No primary isotope effect would be expected, and only a

secondary isotope effect would result from the slight difference in the reduced masses of species H_3O^+ and DH_2O^+ with correspondingly small frequency differences. The effect on the rate of reaction of this is negligible.

(2) Rate determining step involves the breaking of bonds in a water molecule.

(a) R.d.s. is water discharge. Both the transition states,

$$M + O\begin{<}{H}{H} \longrightarrow M\cdots O\begin{<}{H^+}{H} + e \qquad (2.28)$$

$$M + O\begin{<}{D}{D} \longrightarrow M\cdots O\begin{<}{D^+}{D} + e \qquad (2.29)$$

and hydration of the proton and deuteron formed, i.e., formation of the $H^+\cdots O\begin{<}{H}{H}$ and $D^+\cdots O\begin{<}{D}{D}$ bonds, will contribute to the isotope effect. The ratio of current densities is estimated to be $1 < i_H/i_D \leq 2.7$.

(3) R.d.s. involves an OH$^\cdot$ radical following water discharge.

$$2\ H_2O \rightleftharpoons OH\ (ads) + H_3O^+ + e \qquad (2.30)$$

$$R\ (ads) + OH\ (ads) \xrightarrow{r.d.s.} ROH \qquad (2.31)$$

Under Langmuir conditions, at constant temperature, pH, and potential for a given metal, $\theta_{OH}/\theta_{OD} = K_H/K_D$, the current density ratios are calculated to be $i_H/i_D = \theta_{OH}/\theta_{OD} = K_H/K_D = 3.1$.

(c) <u>R.d.s. occurs after n OH radical groups have reacted with the hydrocarbon</u>. For this case, $i_H/i_D = (K_H/K_D)^n$.

The kinetics of ethylene oxidation were summarized in the form of three empirical equations:

$$\text{rate on Pt} = k_{Pt}\, C_E^{1/n}\, C_{H^+}^{-0.5}\, \exp(FV/2KT) \qquad (2.32)$$

$$\text{rate on } M_i = k_{M_i}\, C_E^{1/m_i}\, C_{H^+}^{-0.5}\, \exp(FV/2RT) \qquad (2.33)$$

$$\text{rate on Pd, Au} = k_{Pd,Au}\, C_E^{1/m_{Pd,Au}}\, C_{H^+}^{-0.5}\, \exp(FV/3RT) \qquad (2.34)$$

Equation 2.32 applies to Pt, equation 2.34 to Au and Pd, and equation 2.33 to all other substrates used.

Interpretation of the empirical equation 2.32 has been given previously in terms of a reaction path in which water discharge was the rate determining step. The value of the isotopic effect $i_H/i_D \simeq 1.5\text{-}2$, tended to confirm this mechanism.

For equation 2.33, both the adsorbed organic and the OH radicals must be involved in the rate determining step. The mechanism which corresponds to this condition is:

$$C_2H_4\ (sol) \rightleftharpoons C_2H_4\ (ads) \qquad (2.35)$$

$$H_2O \rightleftharpoons OH\ (ads) + H^+ + e \qquad (2.36)$$

$$C_2H_4\ (ads) + OH\ (ads) \xrightarrow{r.d.s.} CH_2\text{-}CH_2OH\ (ads) \qquad (2.37)$$

The isotope effect was predicted to be approximately 4.8.

The unusual Tafel slope, 3RT/F, was observed for Au and Pd. Assuming a reaction path, as shown in equation 2.35 through 2.37, followed by parallel reactions:

$$M\text{-}CH_2\text{-}CH_2\text{-}OH \xrightarrow{\text{desorption}} CH_3\text{-}C(=O)H + H^+ + e \qquad (2.38)$$

$$M\text{-}CH_2\text{-}CH_2\text{-}OH \xrightarrow{\text{oxidation}} H\text{-}CH\text{-}CH_2^{\cdot} + H_2O \cdots CO_2 \qquad (2.39)$$

One may write for the steady state (assuming back reactions to be negligible).

$$\frac{-d\theta_{C_2H_4OH}}{dt} = 0 = V_{r.d.s.} - V_{des} - V_{ox} \qquad (2.40)$$

At constant pH, P_E and T.

$$k_{r.d.s.} \exp\left(\frac{\alpha FV}{RT}\right) = k_{des}\, \theta_{C_2H_4OH} \exp\left(\frac{\alpha FV}{RT}\right) + k_{ox}\, \theta_{C_2H_4OH} \qquad (2.41)$$

The total current i_T observed is the sum of currents leading to aldehydic products and CO_2.

$$i_T = i_{ald} + i_{CO_2} = \theta_{C_2H_4OH} \left(2\, k_{des} \exp\left(\frac{\alpha FV}{RT}\right) + 12\, k_{ox}\right) \qquad (2.42)$$

Substituting in equation 2.41 and differentiating with respect to potential gives

$$\left(\frac{\partial \log i_T}{\partial V}\right)_{p_H, p_E, T} = \frac{\alpha F}{RT}\left[\left(1 + 6\,\frac{k_{ox}}{k_{des}\,\exp\left(\frac{\alpha FV}{RT}\right)}\right)^{-1} + \left(1 + \frac{k_{des}\,\exp\left(\frac{\alpha FV}{RT}\right)}{k_{ox}}\right)^{-1}\right] \qquad (2.43)$$

The term $k_{ox}/k_{des}\ \exp(\alpha FV/RT) \equiv Z$ is the ratio of the rates of the parallel oxidation and desorption reactions, which must be close to one if both parallel reactions are to take place with significant efficiencies. From equation 2.43 it follows that for $0.1 \leq Z \leq 4$, the apparent Tafel slope will be close to 3RT/F (with maximum deviation less than 20 percent over a range of more than 220 mv. This seems to confirm earlier work on Pt, and shows the observed Tafel slope on Au and Pd to be an apparent step for substrates other than Pt.

Chapter III

EXPERIMENTAL

The experimental plan for this investigation consisted of the following major phases:

(1) Current-Potential Studies. Tafel curves were obtained for solutions whose pH ranged from 0.35 to 12.7. The necessary quantities of H_2SO_4, K_2SO_4, K_2CO_3, KOH, and distilled water were used to obtain a desired pH. The normality of solutions was kept constant at 1 N.

(2) Current-Temperature Studies. The temperature dependence of the current was studied under conditions of constant potential and ethylene partial pressure. The temperature was varied from 80°C to 55°C.

(3) Current-Partial Pressure Studies. The effect of ethylene partial pressure on the current was studied at constant potential, temperature, and pH.

(4) Coulombic Efficiency Studies. The efficiency of conversion of ethylene to CO_2 and H_2O (or H^+) was studied galvanostatically. Reaction by-products were also analyzed with a gas chromatograph.

Five electrodes from the Pt-Au system were used. Their composition (atomic percent) were 80Pt-20Au, 60Pt-40Au, 40Pt-60Au, 20Pt-80Au, and 100 Au. All studies were made at 80°C except for the activation energy determinations.

A complete discussion of each section, including apparatus, procedure, results, and sample calculations is presented in this chapter.

A. Materials

A complete list of the materials and reagents used in this investigation is contained in Appendix B.

B. Electrodes

The working electrode, or anode, was Au or an Au-Pt alloy. The cathode was platinized Pt. Two reference electrodes were used, calomel (1 N KCl) for alkaline solutions and mercurous sulfate (1 N H_2SO_4) for acid solutions.

1. Anodes

The anodes were made of Au sheet with 15.08 cm^2 area (3.45 cm width by 4.37 cm height) or Au-Pt alloy sheet with 15 cm^2 area (3.75 cm width by 4.00 cm height). A small hole was drilled near the top and a thin wire (of the same composition as the anode) looped through it and securely fastened. The wire lead outside the electrolytic cell was through a sealed four mm glass tube.

X-ray diffraction analysis showed that the alloy electrodes were two phase, α_1(Pt-rich) and α_2(Au-rich). The relative amounts of the two phases were: 80Pt-20Au($82\alpha_1$,$18\alpha_2$), 60Pt-40Au($67\alpha_1$,$33\alpha_2$), 40Pt-60Au($25\alpha_1$,$75\alpha_2$), and 20Pt-80Au ($2\alpha_1$,$98\alpha_2$).

2. Cathode

The cathode was a piece 52 mesh Pt gauze folded on a Pt wire frame for support. The Pt lead wire was also sealed in a four mm glass tube. The electrode was platinized using a

platinic chloride solution to which a trace of lead acetate had been added. The cathode geometric area was approximately 15 cm^2.

C. Current-Potential Studies

1. Apparatus

A list of the apparatus used in this study is in Appendix C. A diagram of the cell and electronic equipment is shown in Figure 2. The cell of Pyrex glass had three compartments: anodic, cathodic, and reference. The anodic and cathodic compartments (capacity 600 ml) were separated by a water-sealed stopcock which was open for potentiostatic and closed for galvanostatic operation. The reference electrode was connected to the anodic compartment through a water-sealed stopcock and Luggin capillary. The reference electrodes were at room temperature during the experiments. All potentials of the working electrode were referred to the SHE at zero at the temperature of the experiment by means of a procedure described previously[24]. Both electrode compartments contained inlets and water-sealed outlets for the nitrogen and/or ethylene flow. The temperature in the anodic compartment was controlled to within ± 0.5 C°. Heat was supplied by an electric heating tape wrapped around the compartment. The heating and cooling cycles were made approximately the same by adjusting the voltage to the tape with a variable transformer.

A dual-flow proportioner was used to control the gas

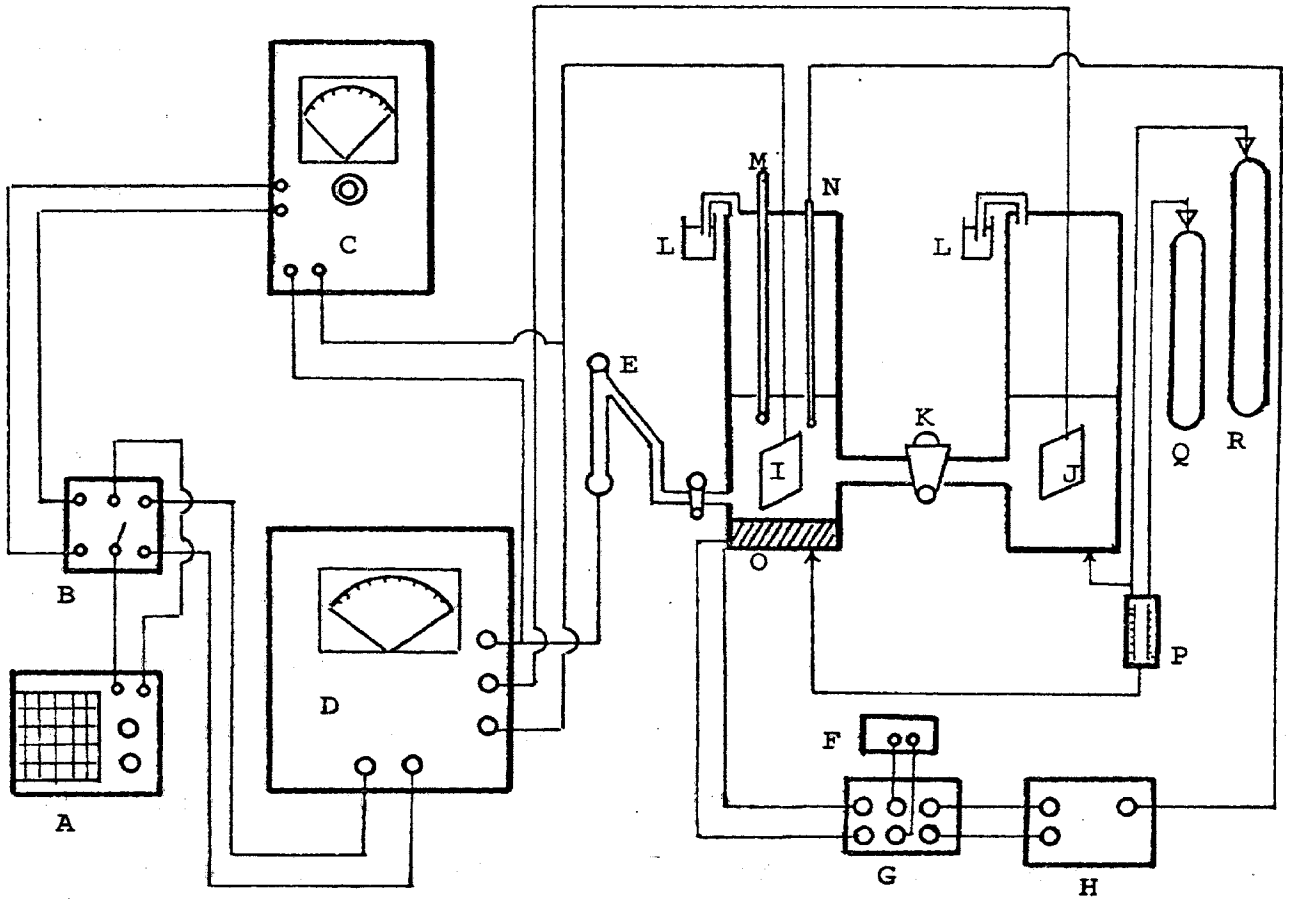

A. Recorder
B. D.P.D.T. Switch
C. Electrometer
D. Potentiostat
E. Reference Electrode
F. Variac
G. Electrical Relay
H. Temperature Controller
I. Anode
J. Cathode
K. Electrolytic Cell
L. Water-sealed Gas Exit
M. Thermometer
N. Temperature Sensor
O. Heating Tape
P. Gas Proportioner
Q. Ethylene Tank
R. Nitrogen Tank

Figure 2. Diagram of the apparatus used for potentiostatic studies in the anodic oxidation of ethylene.

flow rate into the anode compartment. It could be used to meter both nitrogen and ethylene flow rates independently. All measurements were made with constant flow rates into the cell.

A potentiostat was used to maintain a constant potential difference between the working and reference electrodes. The current was recorded from the potentiostat output.

2. Procedure

An important part of the procedure was the anode activation before each experiment. The Au electrode was placed in 1 N H_2SO_4 solution along with a small Au strip which acted as a counter-electrode. A power supply was connected to the electrodes through a double-pole double-throw switch so that the polarity of the current could be reversed rapidly. The electrode was alternately made cathodic (hydrogen evolution) and anodic (oxygen evolution) with a constant current of two amperes for pulses of ten seconds during a one minute period. The pulsing was stopped on a cathodic pulse and hydrogen was evolved for two minutes. For the Au-Pt alloy electrodes, the counter-electrode used in activation was a small strip of platinized Pt. Because of the possibility of selective dissolution of one component of the alloy, the pulse technique was not applied. The electrodes were activated by passing four amperes cathodic current (hydrogen evolution) for ten minutes. After activation, the anode was immediately removed, rinsed with distilled water, and transferred to the cell. The cell had been previously charged with sufficient

electrolyte to completely cover the electrode. The electrode was adjusted so that its bottom edge was very near the Luggin capillary. Nitrogen purging and heating was started and after one hour, the nitrogen flow to the anode compartment was stopped and ethylene was introduced. Potential measurements were begun when nitrogen flow and heating commenced. The potential was allowed to come to a steady state with no current flowing (rest potential). The potential on the anode was then increased approximately 0.05 to 0.10 v above the rest potential and held constant by means of the potentiostat. The current was recorded continuously and after it had come to a steady state, the potential was again increased by 0.025 v or 0.050 v, (the steady state was arbitrary defined as that value of current which changed less than 10 percent in one hour). This procedure was continued until a limiting value of current was reached.

3. Data and Results

Current-potential relationships were determined in solutions with pH's 0.35, 1.4, 3.0, 10.1, 10.9, and 12.7 at 80°C. The normality of the various solutions was kept constant at 1 N. The ethylene pressure was 1 atm and its flow rate was 100 cm^3/min.

The data are tabulated in Appendix D. Tafel plots are shown in Figures 3 to 8. There is an apparent transition in the curves of acid solutions on Au-Pt alloy electrodes. Linear Tafel regions above and below the transistion region

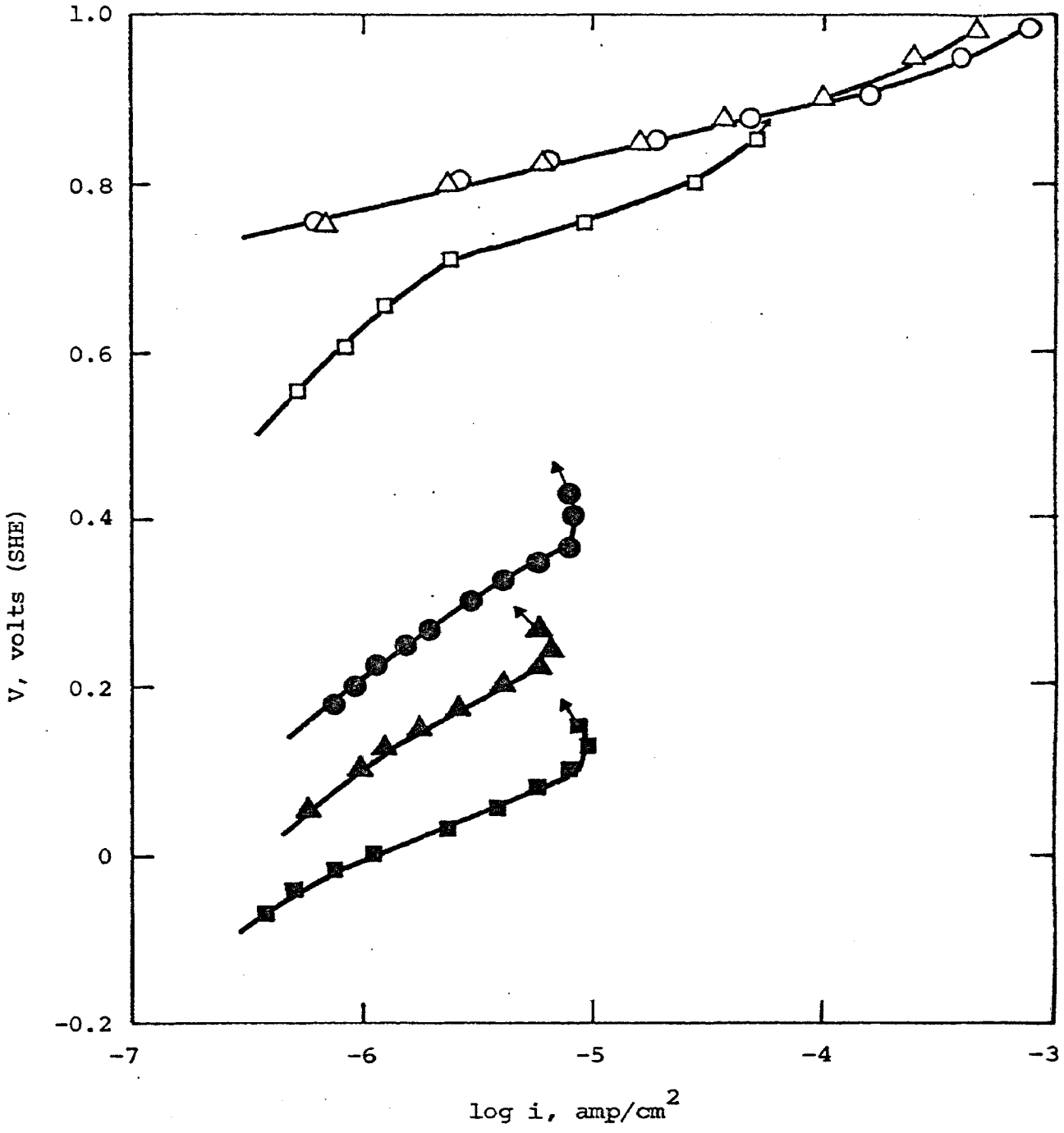

Figure 3. Tafel curves for the anodic oxidation of ethylene on Au at 80°C (P_E = 1 atm). (pH = ○, 0.35; △, 1.4; □, 3.0; ●, 10.1; ▲, 10.9; ■, 12.7)

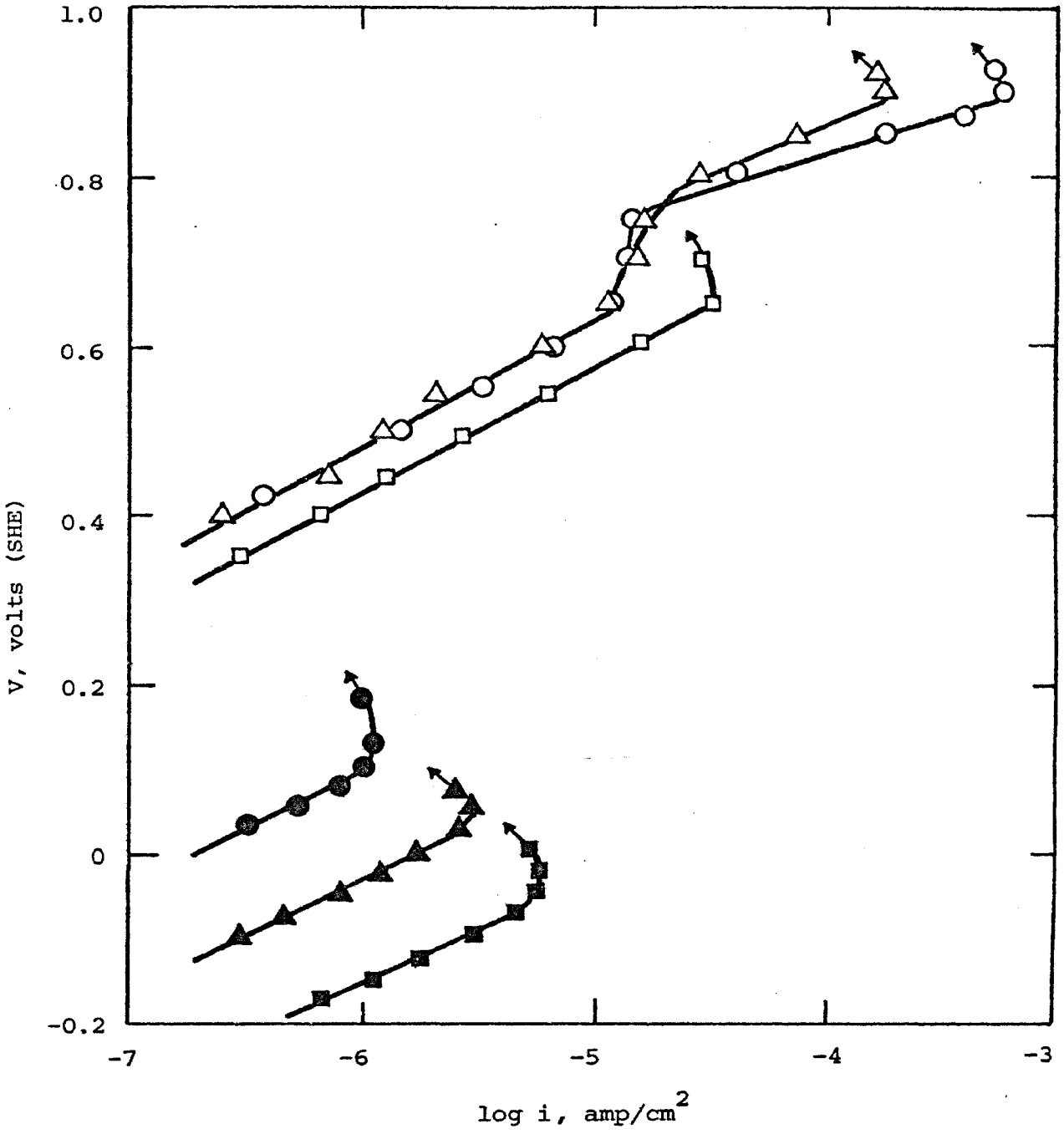

Figure 4. Tafel curves for the anodic oxidation of ethylene on 80Au-20Pt alloy at 80°C (P_E= 1 atm). (pH = ○, 0.35; △, 1.4; □, 3.0; ●, 10.1; ▲, 10.9; ■, 12.7)

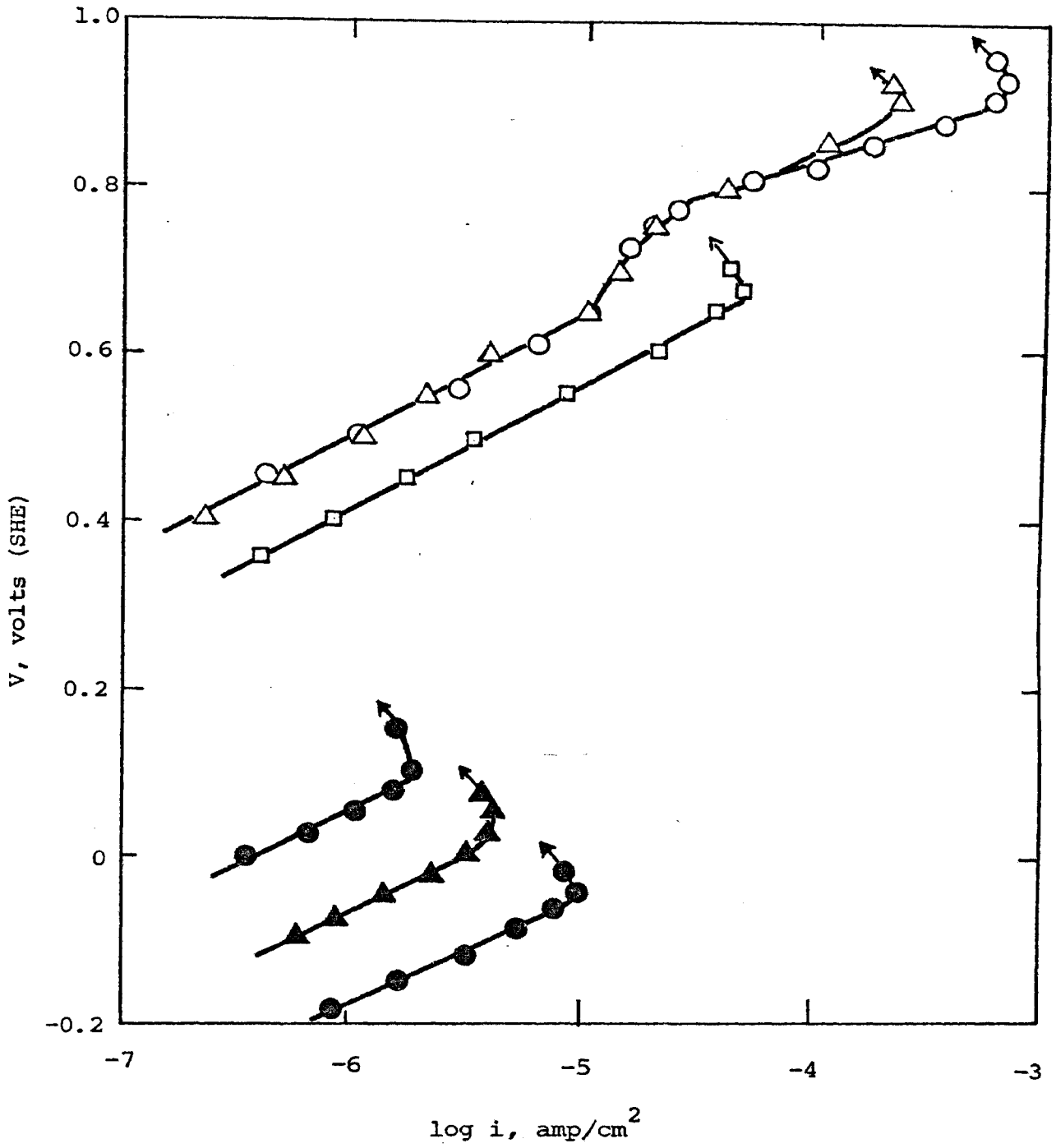

Figure 5. Tafel curves for the anodic oxidation of ethylene on 60Au-40Pt alloy at 80°C (P_E = 1 atm). (pH = ○, 0.35 ; △, 1.4; □, 3.0; ●, 10.1; ▲, 10.9; ■, 12.7)

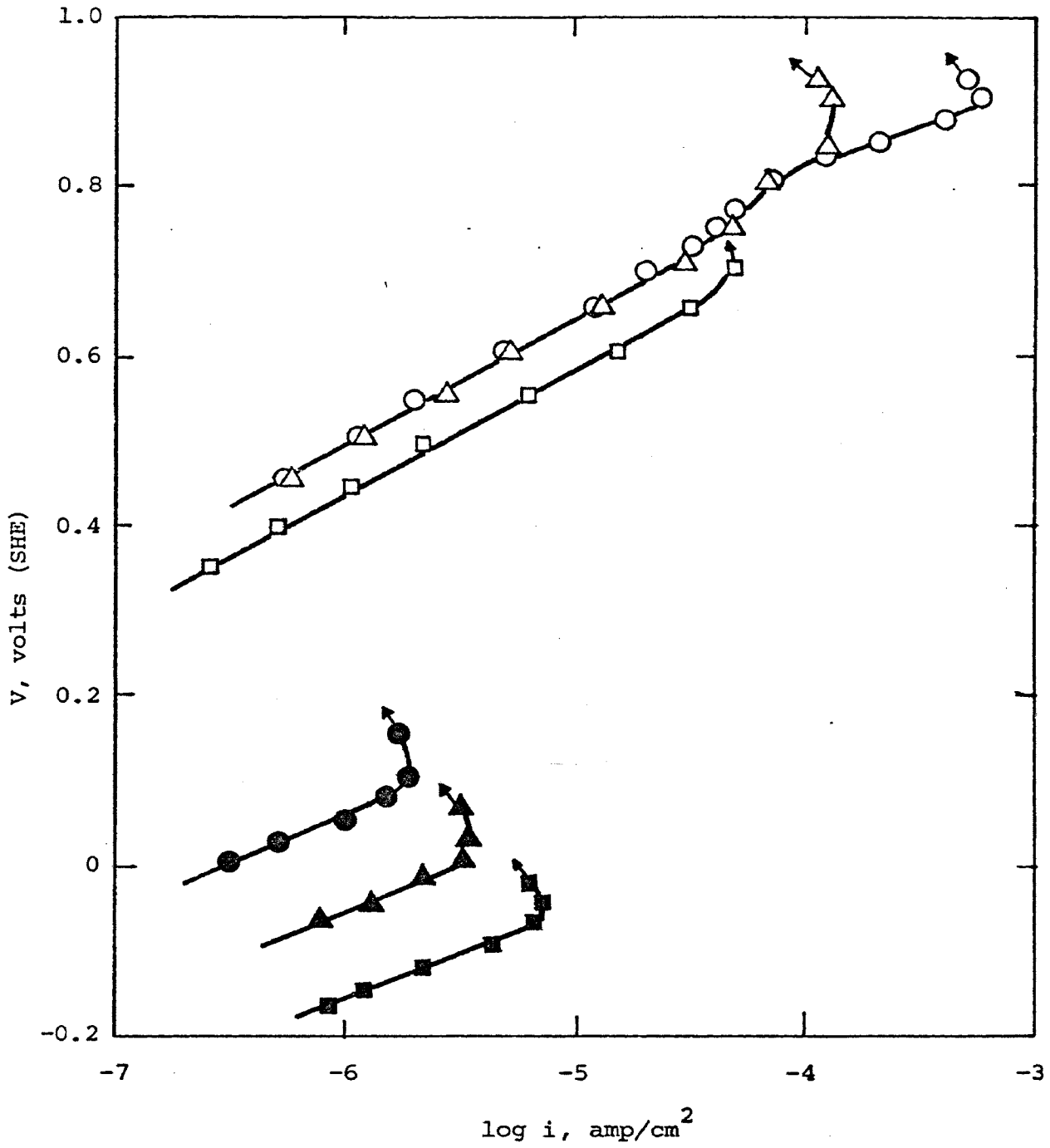

Figure 6. Tafel curves for the anodic oxidation of ethylene on 40Au-60Pt alloy at 80°C (P_E = 1 atm). (pH = ○, 0.35; △, 1.4; □, 3.0; ●, 10.1; ▲, 10.9; ■, 12.7)

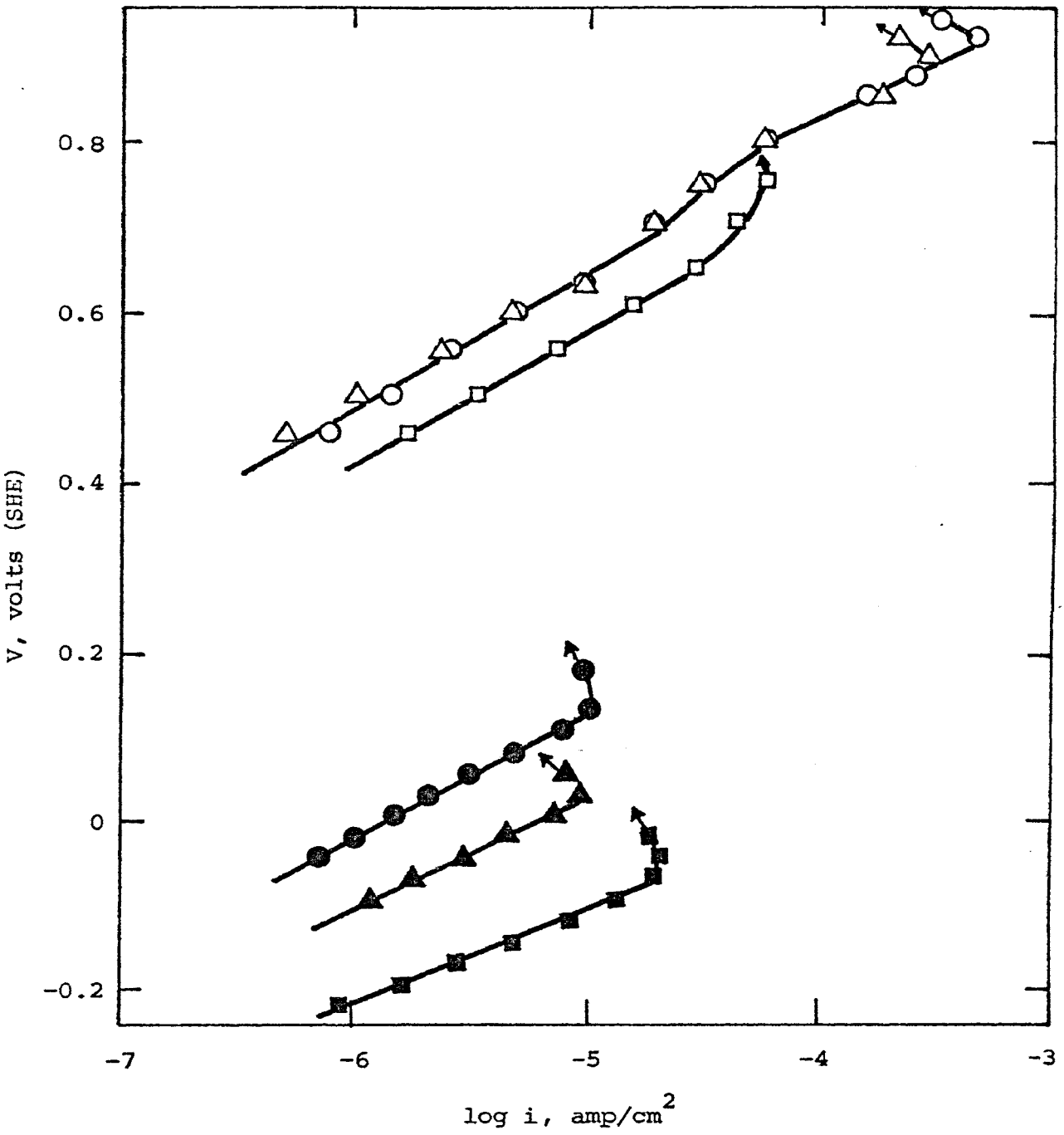

Figure 7. Tafel curves for the anodic oxidation of ethylene on 20Au-80Pt alloy at 80°C (P_E = 1 atm). (pH = ○, 0.35; △, 1.4; □, 3.0; ●, 10.1; ▲, 10.9; ■, 12.7)

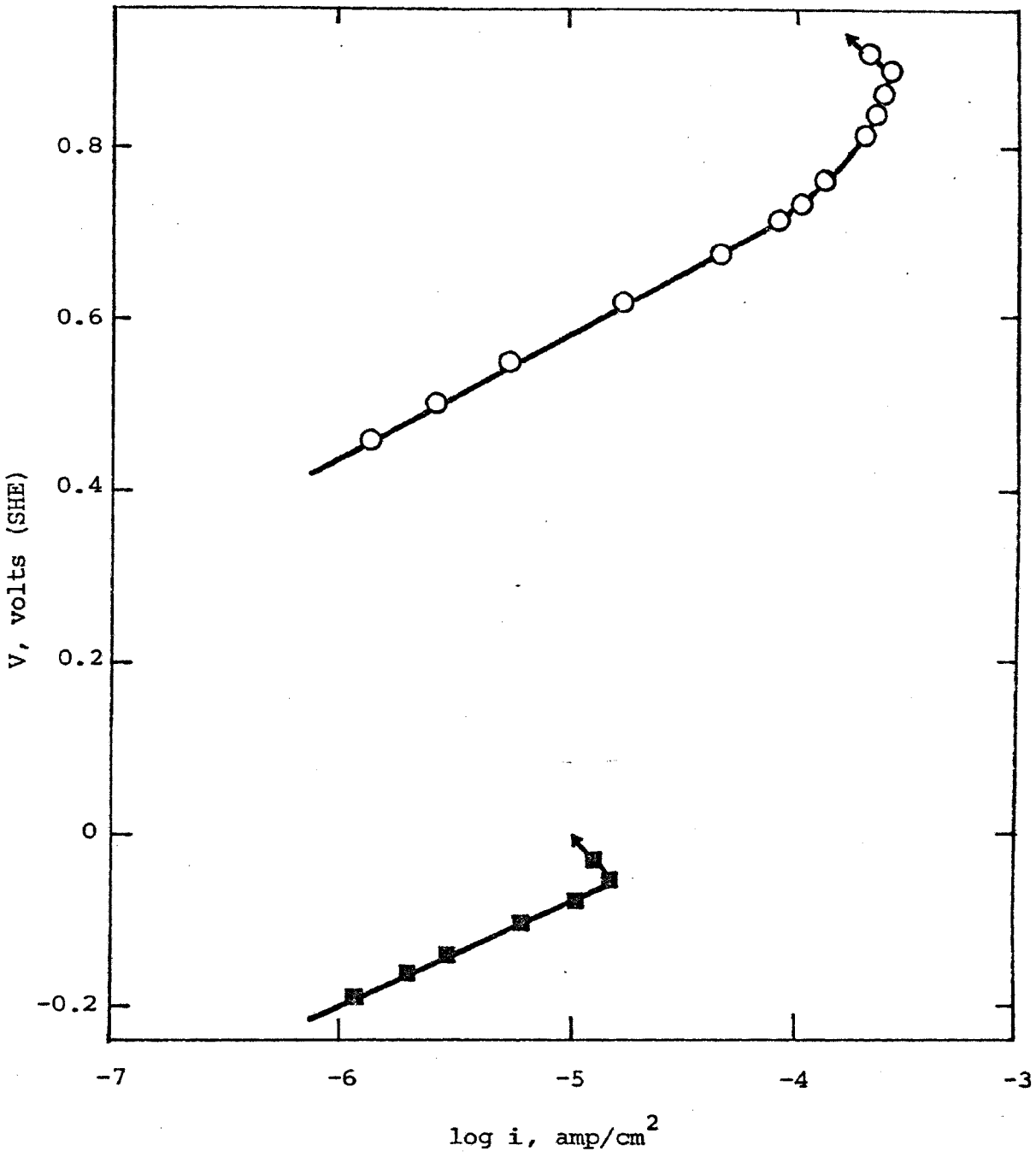

Figure 8. Tafel curves for the anodic oxidation of ethylene on smooth Pt at 80°C (P_E = 1 atm). (pH = ○, 0.35; ■, 12.7)

have different slopes. The values of the slopes are approximately 70 mv (70 to 80 mv) in acidic solutions on Au and above the transition region on Au-rich alloys. In basic solutions and below the transition region, the slopes are approximately 140 mv (130 to 150 mv) on all electrodes. The linear Tafel region was very short in basic solutions compared to acid. Increasing the potential above the linear region indicated the electrode to be passivated.

The rest potential obtained for the various electrolytes are shown in Table IV. They decreased with increasing pH.

After each run, the anode was observed to be as clean as before the run. There was no evidence of formation of any polymerization products on the anode and no discoloration of the anolyte during extended periods of operation.

D. Current-Temperature Studies

1. Apparatus

The apparatus employed in this section was the same as that described in the previous section.

2. Procedure

The cell was charged with solution, and the anode was activated and positioned as described previously. The potential was held constant at values within the linear Tafel region. The ethylene pressure was kept constant at 1 atm. The temperature was adjusted with the temperature controller while the current was continuously recorded. A

TABLE IV

REST POTENTIALS FOR ETHYLENE ON Au AND Au-Pt ALLOYS IN AQUEOUS SOLUTIONS AT 80°C (P_E = 1 atm)

pH	Rest Potentials, v(SHE)				
	Au	80Au-20Pt	60Au-40Pt	40Au-60Pt	20Au-80Pt
0.35	0.605	0.397	0.417	0.397	0.357
1.4	0.597	0.357	0.362	0.367	0.317
3.0	0.407	0.287	0.257	0.267	0.257
10.1	-0.053	-0.001	-0.001	-0.011	-0.153
10.9	-0.113	-0.111	-0.116	-0.091	-0.213
12.7	-0.196	-0.181	-0.201	-0.176	-0.291

thermometer was also incorporated in the cell to check the temperature of the solution. The temperature was varied from 80 to 55 or 60°C depending on the magnitude of the current at the lower value by increments of 5 C°.

3. Data and Results

The temperature studies were conducted in 1 N H_2SO_4 (both below and above the transition region) and 1 N KOH solutions. The experimental data are tabulated in Appendix D. Arrhenius plots have been prepared and are shown in Figures 9 to 13.

The slopes of the curves were determined and the apparent activation energy calculated for each. These values and the change in the activation energy with respect to the potential ($\partial E_a/\partial V$) are shown in Table V. This latter quantity ($\partial E_a/\partial V$) will be referred to later in the discussion as it can be derived from the reaction mechanism.

4. Sample Calculations

The sample calculations for this section are based on the data in Table XVIII. The data for the test in 1 N H_2SO_4 at a potential of 0.897 v on the Au electrode were selected for the sample calculations.

The Arrhenius equation involving the activation energy is

$$\log k = - \frac{E_a}{2.303\ RT} + \log A \qquad (3.1)$$

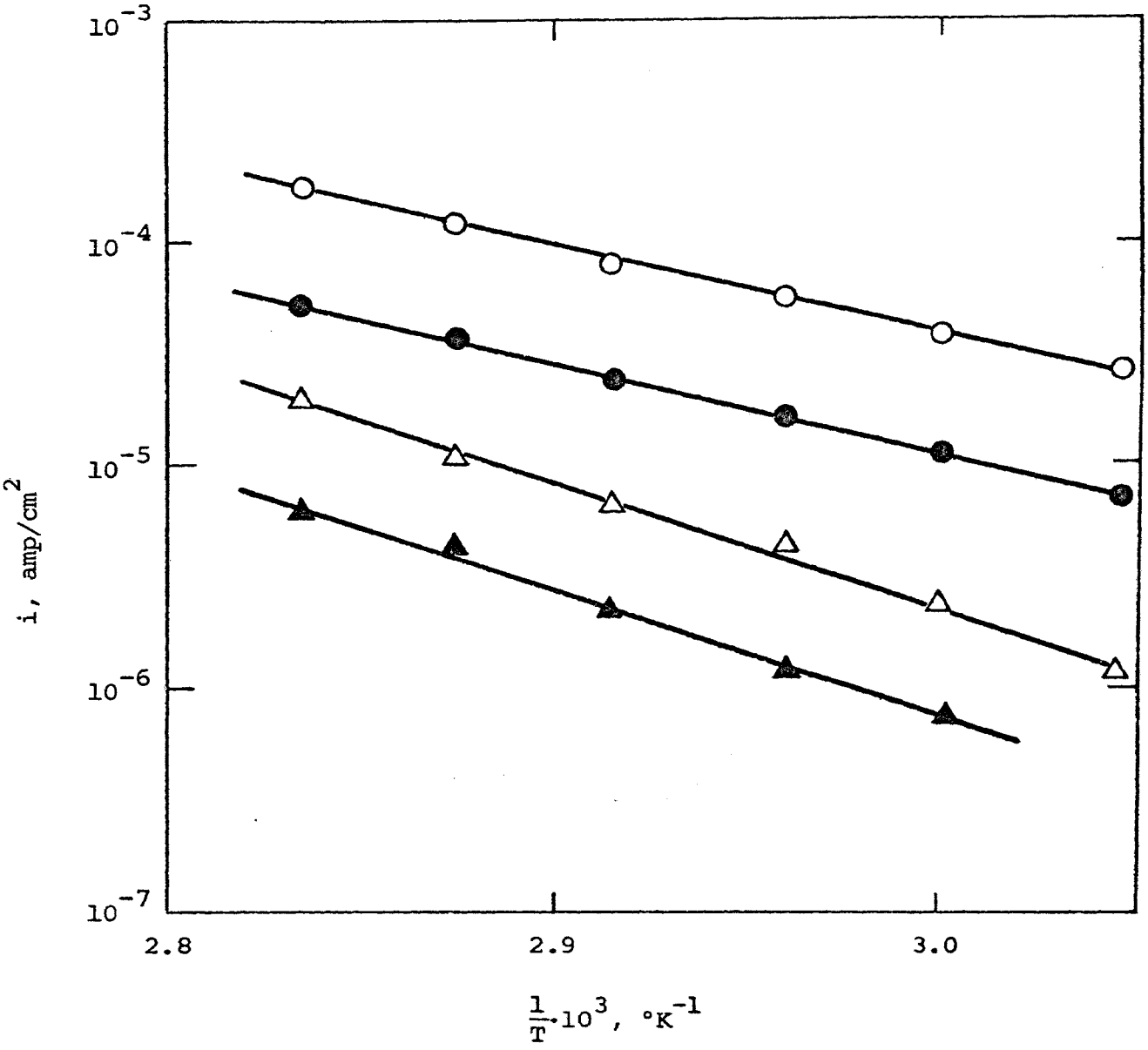

Figure 9. Current-temperature relation for the anodic oxidation of ethylene on Au (P_E = 1 atm). (○ , 0.897 v, 1 N H_2SO_4; ● , 0.847 v, 1 N H_2SO_4; △ , 0.104 v, 1 N KOH; ▲ , 0.054 v, 1 N KOH)

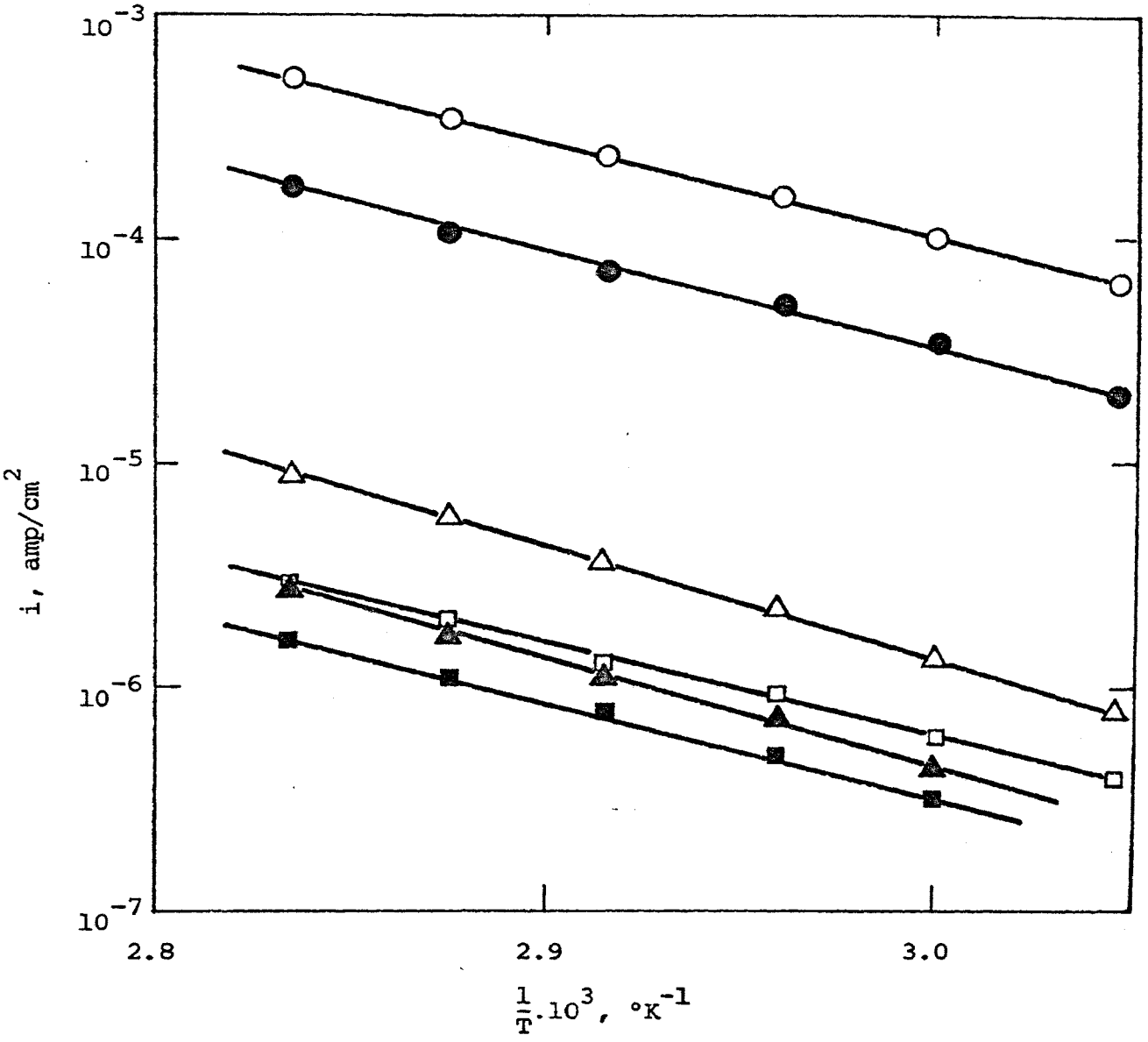

Figure 10. Current-temperature relation for the anodic oxidation of ethylene on 80Au-20Pt alloy (P_E = 1 atm).
(○ , 0.897 v, 1 N H_2SO_4; ● , 0.847 v, 1 N H_2SO_4;
△ , -0.071 v, 1 N KOH; ▲ , -0.121 v, 1 N KOH;
□ , 0.597 v, 1 N H_2SO_4; ■ , 0.547 v, 1 N H_2SO_4;
○ , ● , a.t.r.; □ , ■ , b.t.r.)

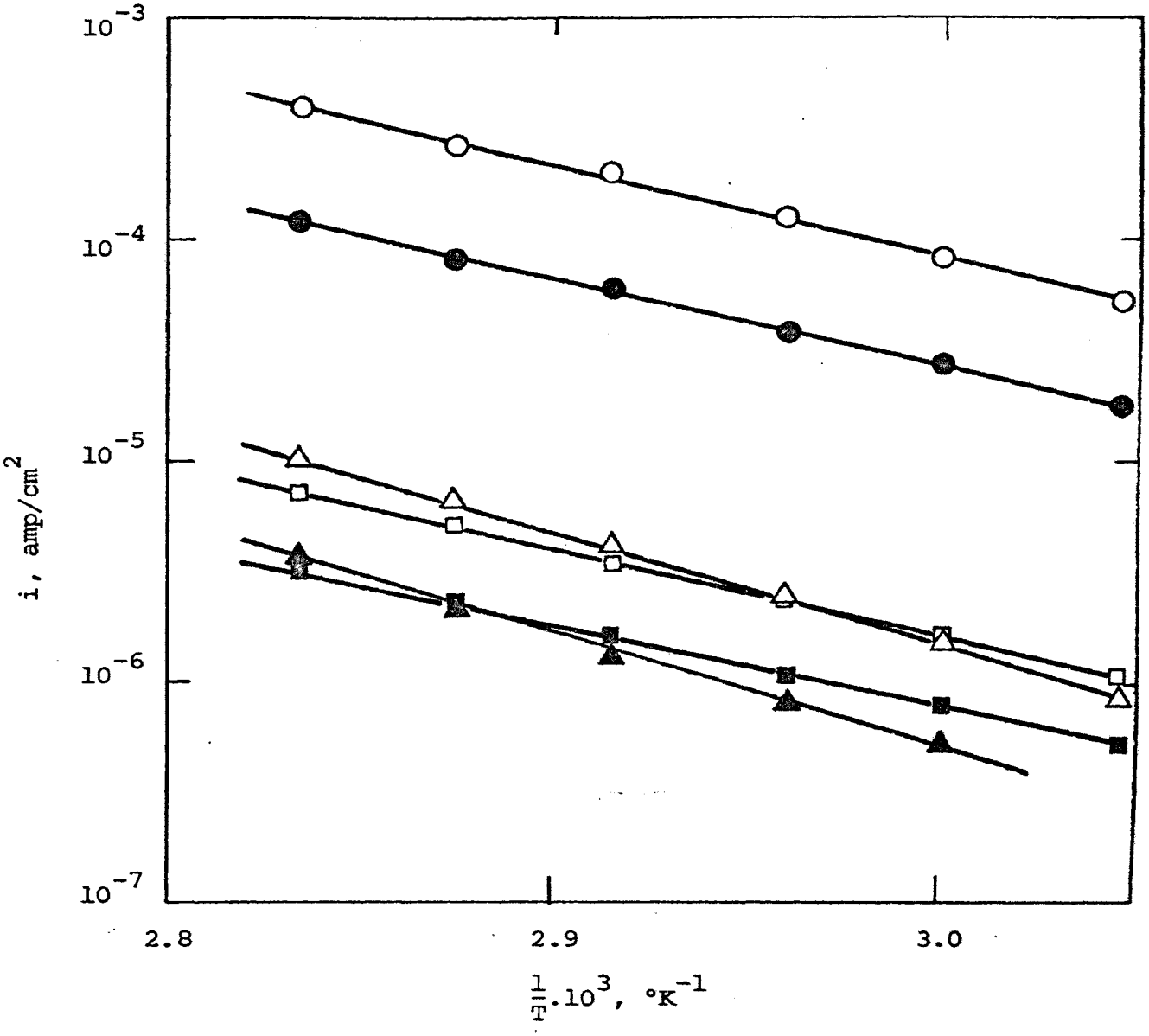

Figure 11. Current-temperature relation for the anodic oxidation of ethylene on 60Au-40Pt alloy (P_E = 1 atm).
(○, 0.872 v, 1 N H_2SO_4; ●, 0.822 v, 1 N H_2SO_4;
△, -0.071 v, 1 N KOH; ▲, -0.121 v, 1 N KOH;
□, 0.597 v, 1 N H_2SO_4; ■, 0.547 v, 1 N H_2SO_4;
○, ●, a.t.r.; □, ■, b.t.r.)

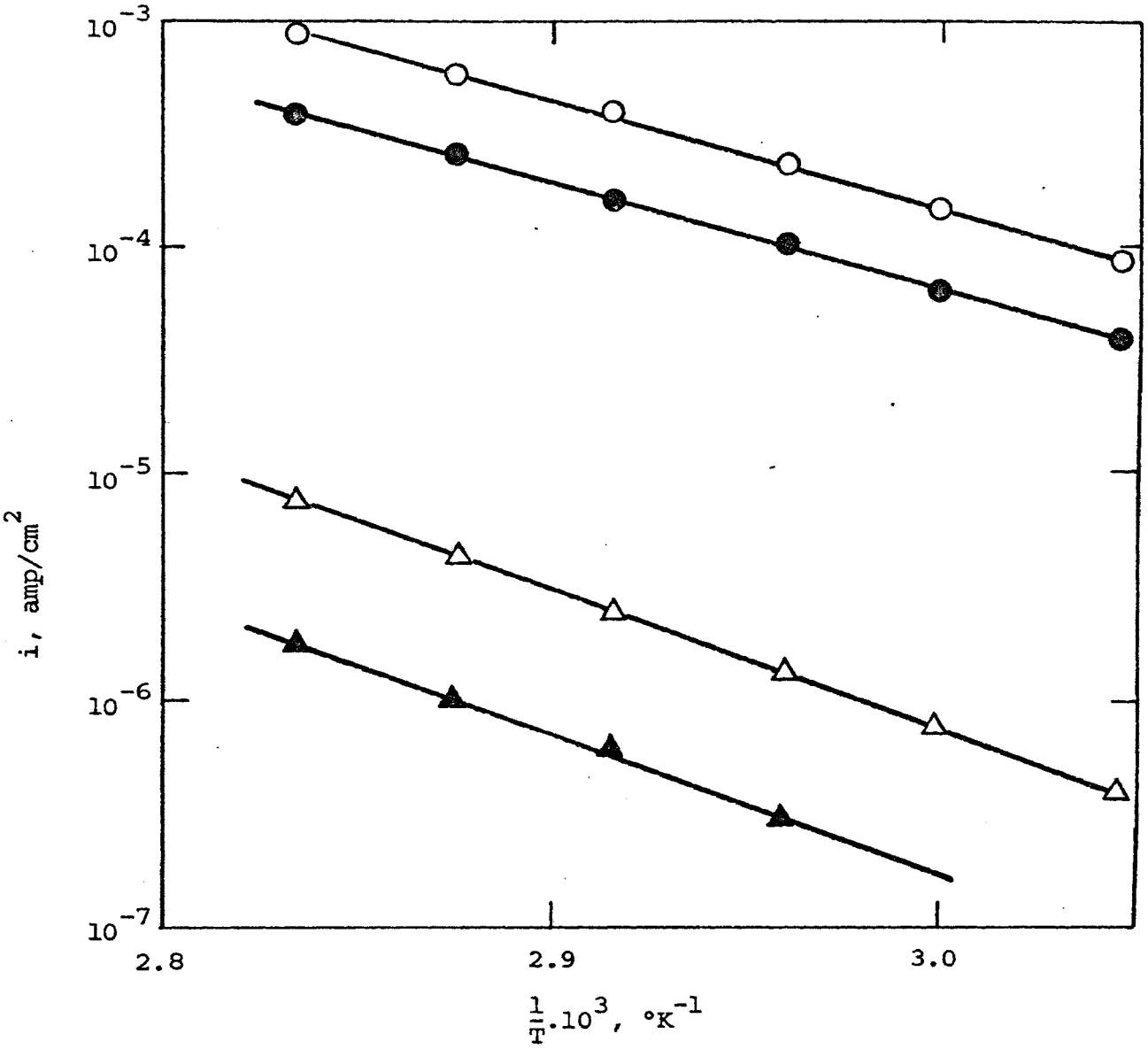

Figure 12. Current-temperature relation for the anodic oxidation of ethylene on 40Au-60Pt alloy (P_E = 1 atm). (○, 0.822 v, 1 N H_2SO_4; ●, 0.772 v, 1 N H_2SO_4; △, -0.071 v, 1 N KOH; ▲, -0.121 v, 1 N KOH)

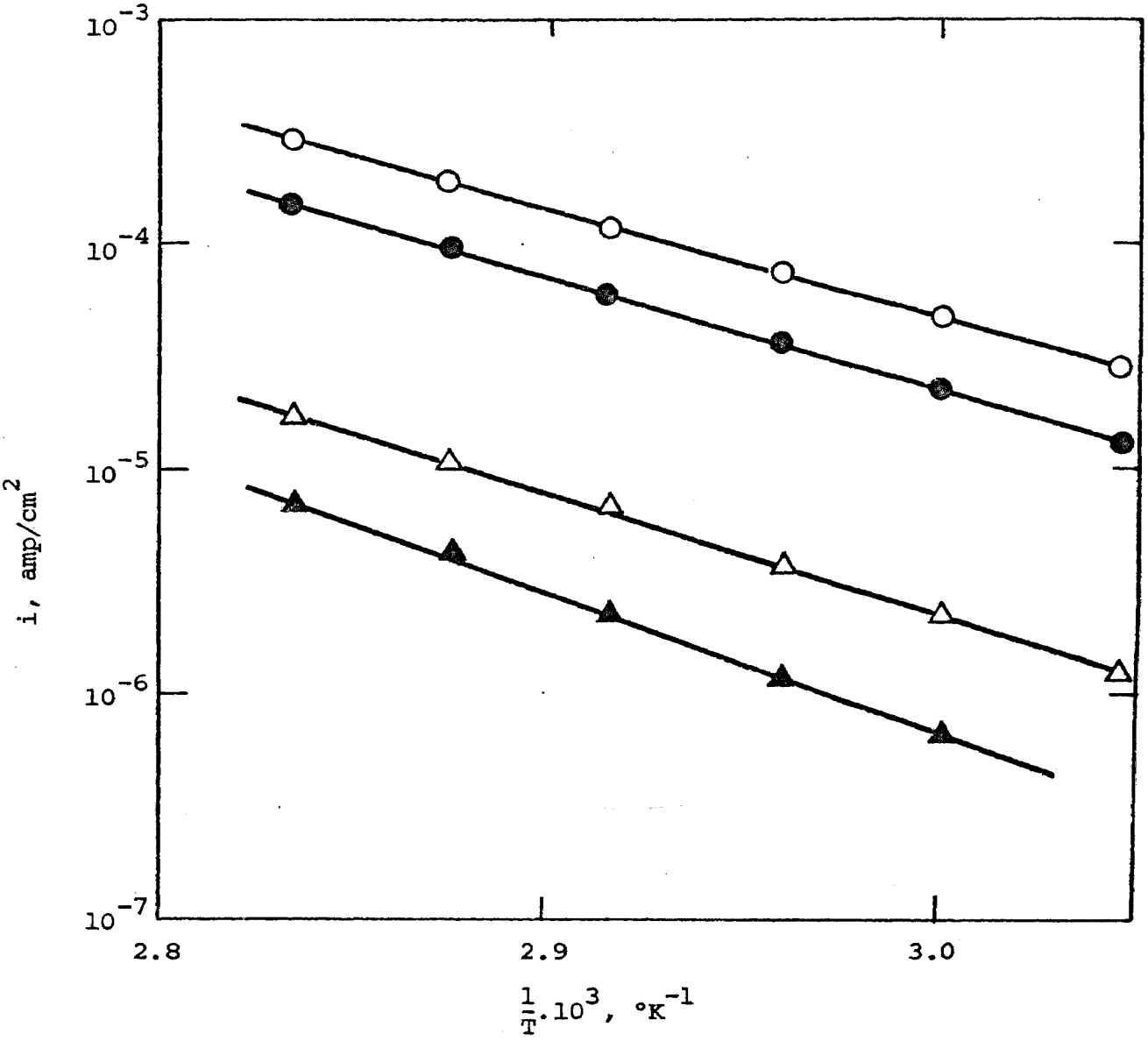

Figure 13. Current-temperature relation for the anodic oxidation of ethylene on 20Au-80Pt alloy (P_E = 1 atm).
(○, 0.847 v, 1 N H_2SO_4; ●, 0.797 v, 1 N H_2SO_4;
△, -0.096 v, 1 N KOH; ▲, -0.146 v, 1 N KOH)

TABLE V

APPARENT ACTIVATION ENERGIES FOR THE ANODIC OXIDATION OF ETHYLENE ON Au AND Au-Pt ALLOYS (P_E = 1 atm)

Electrode	Solution	Potential	Activation Energy	$-\partial E_a/\partial V$
		v(SHE)	Kcal	Kcal/volt
Au	1 N H_2SO_4	0.847	19.2	23.0
		0.897	18.05	
	1 N KOH	0.054	26.59	12.0
		0.104	25.99	
80Au-20Pt	1 N H_2SO_4	0.847*	19.61	21.6
		0.897*	18.53	
		0.547**	19.46	12.4
		0.597**	18.84	
	1 N KOH	-0.121	22.99	11.4
		-0.071	22.42	
60Au-40Pt	1 N H_2SO_4	0.822*	18.33	22.4
		0.872*	17.21	
		0.547**	18.26	12.8
		0.597**	17.62	
	1 N KOH	-0.121	23.33	12.6
		-0.071	22.70	
40Au-60Pt	1 N H_2SO_4	0.772	21.44	12.8
		0.822	20.80	
	1 N KOH	-0.121	28.28	11.4
		-0.071	27.71	
20Au-80Pt	1 N H_2SO_4	0.847	22.70	10.2
		0.897	22.19	
	1 N KOH	-0.146	27.25	11.4
		-0.096	26.68	

* a.t.r.

** b.t.r.

Since k is proportional to the rate, or current, E_a may be calculated from the slope of a plot of log i versus 1/T where,

$$\text{slope} = \frac{\log i_2 - \log i_1}{\frac{1}{T_2} - \frac{1}{T_1}} = -3,945°K$$

$$E_a = -(2.303)(R)(\text{slope})$$
$$= -(2.303)(1.987)(-3,945)$$
$$= 18,050 \text{ cal (or } 18.05 \text{ Kcal)}$$

E. Current-Partial Pressure Studies

1. Apparatus

The apparatus used was the same as that described previously.

2. Procedure

The procedure was essentially the same as discussed previously. However, after obtaining a rest potential, a potential inside the linear Tafel region was selected and a steady state current obtained at 1 atm ethylene partial pressure. The partial pressure then was reduced and the corresponding steady state current recorded. In order to get sizable current changes, the partial pressure was varied in the order 1.0, 0.3, 0.1, 0.03, and 0.01 atm. The partial pressures were obtained by diluting the ethylene with nitrogen using a dual-flow gas proportioner. The total gas flow rate was kept constant at 100 cm^3/min.

3. Data and Results

Two or three partial pressure studies were carried out in 1 N H_2SO_4 (both below and above the transition region) and in 1 N KOH at constant potential. The data obtained are listed in Appendix D and are also shown in Figures 14 to 18.

The current decreased as the partial pressure of ethylene decreased in acid and basic solutions on all electrodes, i.e., the system exhibited a positive pressure effect.

F. Coulombic Efficiency Studies

1. Apparatus

A sketch of the apparatus as used in this section is shown in Figure 19. The power for the constant current (galvanostatic) experiments was supplied by a constant voltage power supply. A large power resistor was placed in series with the cell to keep the current constant. A gas trap (maintained at 0°C) and a U-tube (filled with Ascarite) were used to collect the condensable components and to absorb the CO_2, respectively, from the gas coming from the anodic compartment of the cell.

2. Procedure

The rest potential was obtained in the same manner as for the potentiostatic experiments. The stopcock between compartments was closed and the current was adjusted to a desired value by varying the voltage applied with the power

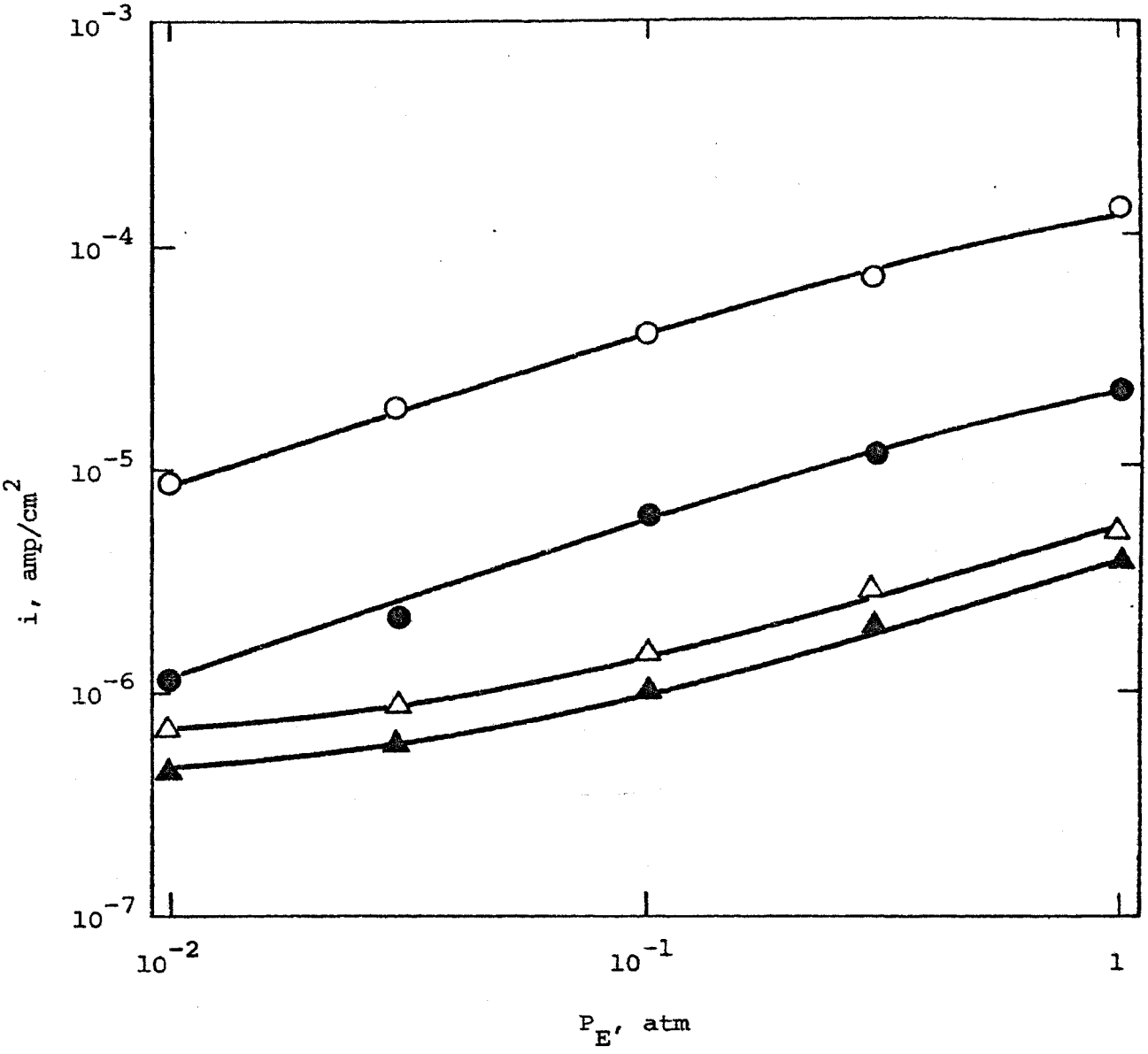

Figure 14. Current-partial pressure relation for the anodic oxidation of ethylene on Au at 80°C. (○ , 0.897 v, 1 N H_2SO_4; ● , 0.847 v, 1 N H_2SO_4; △ , 0.104 v, 1 N KOH; ▲ , 0.054 v, 1 N KOH)

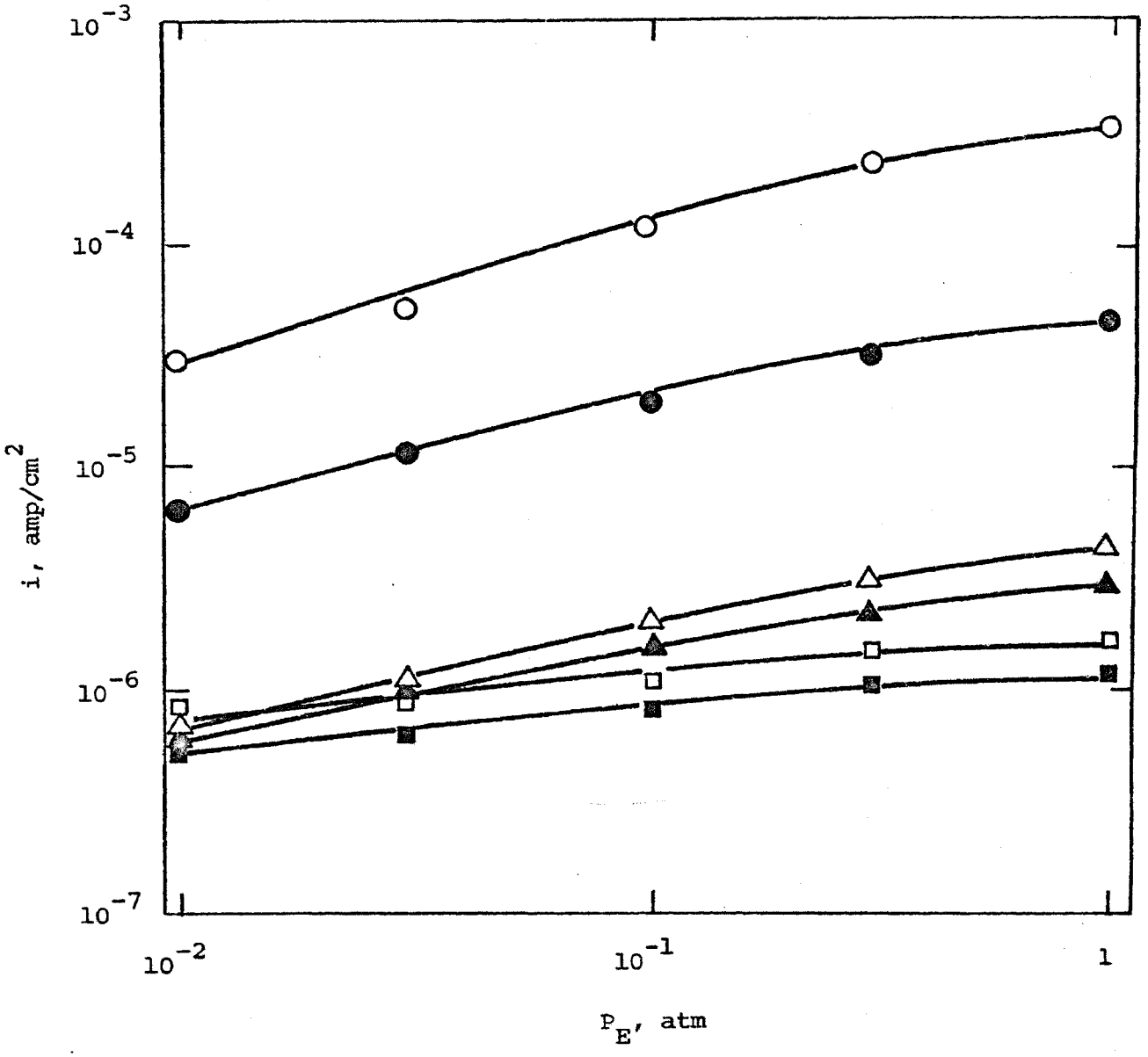

Figure 15. Current-partial pressure relation for the anodic oxidation of ethylene on 80Au-20Pt alloy at 80°C. (○ , 0.872 v, 1 N H_2SO_4; ● , 0.822 v, 1 N H_2SO_4; △ , -0.071 v, 1 N KOH; ▲ , -0.121 v, 1 N KOH; □ , 0.672 v, 1 N H_2SO_4; ■ , 0.622 v, 1 N H_2SO_4; ○ , ● , a.t.r.; □ , ■ , b.t.r.)

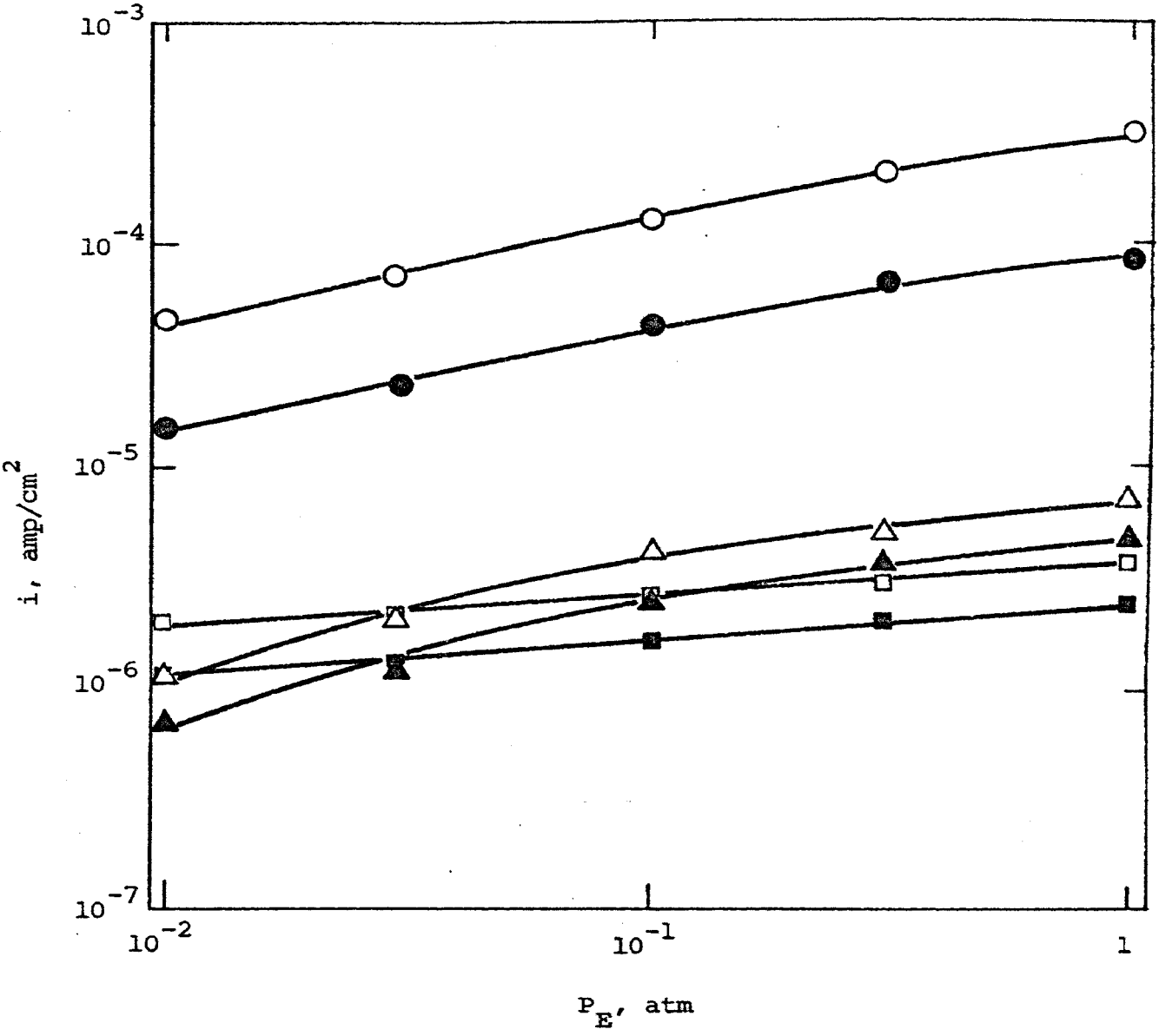

Figure 16. Current-partial pressure relation for the anodic oxidation of ethylene on 60Au-40Pt alloy at 80°C. (○ , 0.872 v, 1 N H_2SO_4; ● , 0.822 v, 1 N H_2SO_4; △ , -0.071 v, 1 N KOH; ▲ , -0.121 v, 1 N KOH; □ , 0.597 v, 1 N H_2SO_4; ■ , 0.547 v, 1 N H_2SO_4; ○ , ● , a.t.r.; □ , ■ , b.t.r.)

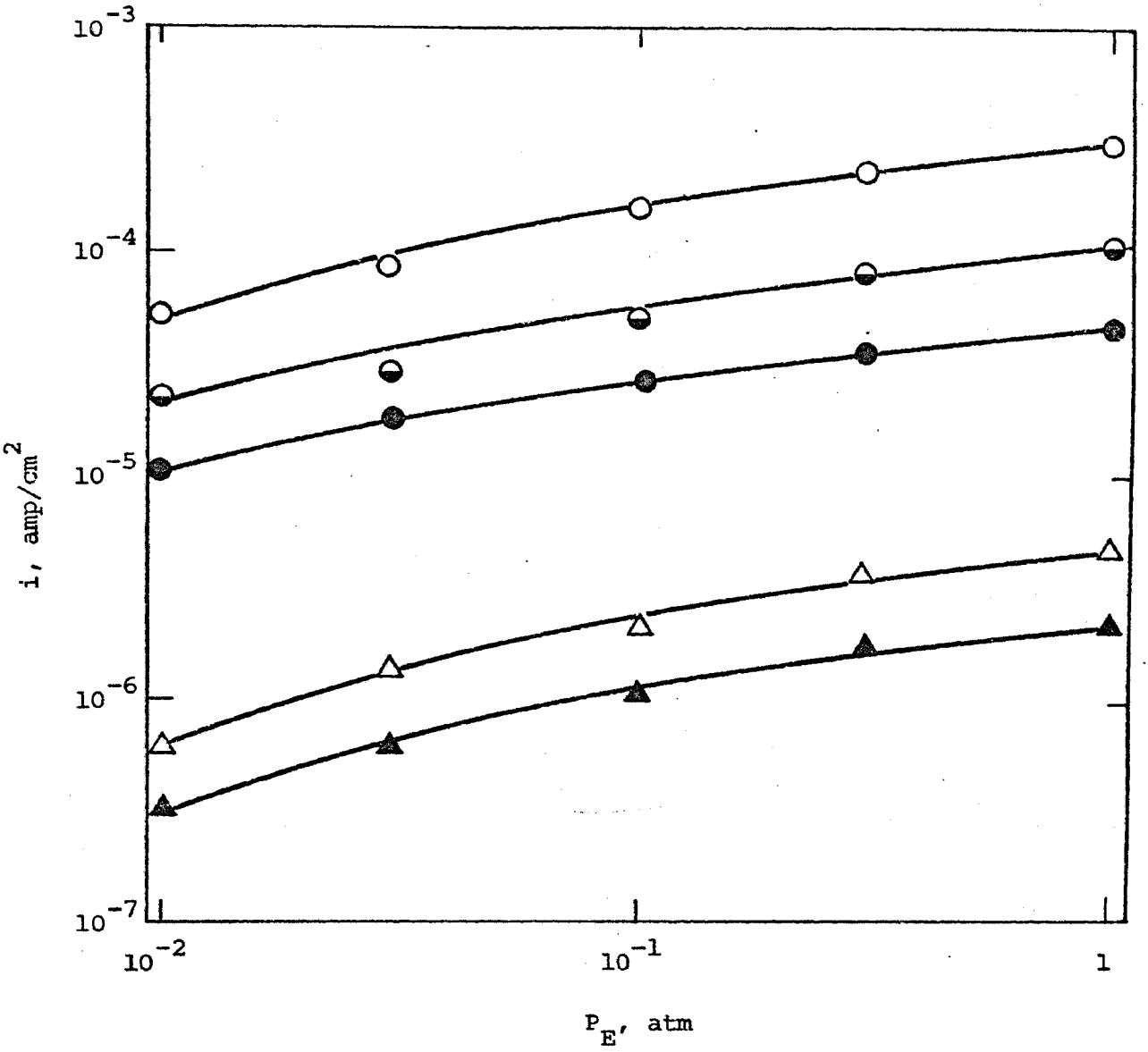

Figure 17. Current-partial pressure relation for the anodic oxidation of ethylene on 40Au-60Pt alloy at 80°C. (○ , 0.872 v, 1 N H_2SO_4; ◒ , 0.822 v, 1 N H_2SO_4; ● , 0.772 v, 1 N H_2SO_4; △ , -0.071 v, 1 N KOH; ▲ , -0.121 v, 1 N KOH)

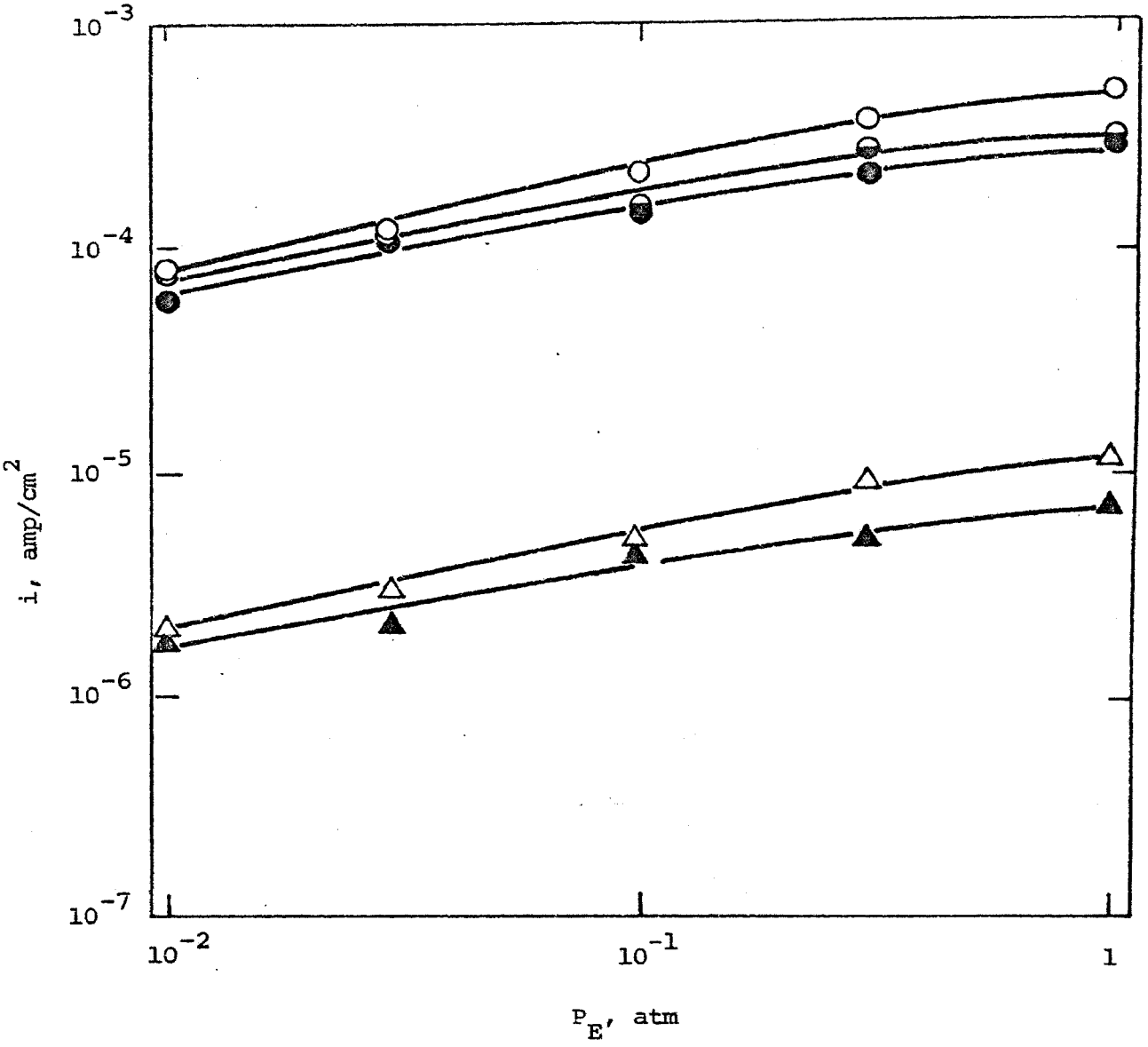

Figure 18. Current-partial pressure relation for the anodic oxidation of ethylene on 20Au-80Pt alloy at 80°C. (○, 0.897 v, 1 N H_2SO_4; ◒, 0.847 v, 1 N H_2SO_4; ●, 0.797 v, 1 N H_2SO_4; △, -0.096 v, 1 N KOH; ▲, -0.146 v, 1 N KOH)

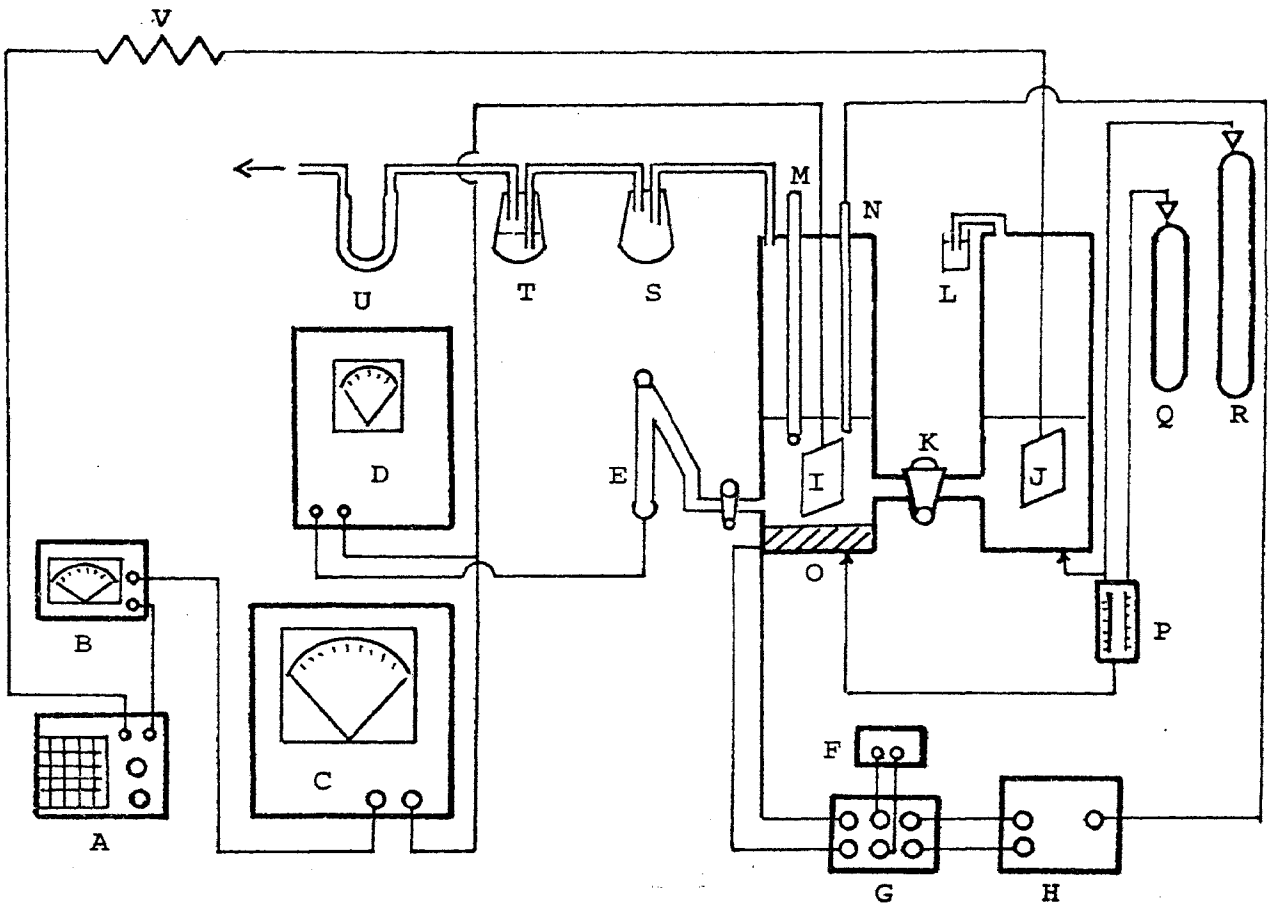

A. Recorder
B. Ammeter
C. Power Supply
D. Electrometer
E. Reference Electrode
F. Variac
G. Electrical Relay
H. Temperature Controller
I. Anode
J. Cathode
K. Electrolytic Cell
L. Water-sealed Gas Exit
M. Thermometer
N. Temperature Sensor
O. Heating Tape
P. Gas Proportioner
Q. Ethylene Tank
R. Nitrogen Tank
S. Gas Trap
T. Concentrated H_2SO_4
U. Ascarite
V. Power Resistor

Figure 19. Diagram of the apparatus used for galvanostatic studies in the anodic oxidation of ethylene.

supply. The efficiencies were determined at potentials in the linear Tafel region. The experiment was allowed to run for 10 hours to allow the system to reach steady state conditions. The exit gas from the anodic compartment was then passed through the gas trap, concentrated H_2SO_4 to remove any residual water, and a U-tube containing a measured amount of Ascarite. The weight gained by the Ascarite during the remaining period of experiment was equal to the amount of CO_2 produced by the oxidation.

It was necessary to pass current for a day or more in order to produce a quantity of CO_2 that could be measured with reasonable accuracy. Frequent checks of the potential were made to insure that it remained within the linear Tafel region.

The material collected in the trap and a sample of the anolyte were analyzed with a flame-ionization gas chromatograph.

3. Data and Results

All results of the coulombic efficiency studies in 1 N H_2SO_4 are reported in Table VI. It can be seen the efficiency of CO_2 production decreased as the amount of Pt in the alloy decreased. On the Au electrode, no CO_2 was produced. At 0.1 atm ethylene partial pressure in 1 N H_2SO_4 on the 20Au-80Pt alloy, the efficiency was about one third of that at 1 atm. In other words, as the partial pressure of ethylene decreased, the overall conversion to CO_2 also

TABLE VI

COULOMBIC EFFICIENCY OF CO_2 PRODUCTION FOR THE ANODIC OXIDATION OF ETHYLENE ON Au AND Au-Pt ALLOYS IN 1.0 N H_2SO_4 AT 80°C

Electrode	C_2H_4 Partial Pressure	Current	Time	CO_2 Oxidation Efficiency
	atm	ma	hours	percent
Au	1.0	6.0	40	0
	1.0	6.0	35	0
80Au-20Pt	1.0	5.0	36	5.1
	1.0	5.0	36	4.55
60Au-40Pt	1.0	5.0	36	11.5
40Au-60Pt	1.0	5.0	30	43
20Au-80Pt	1.0	5.0	31	65.7
	1.0	5.0	35.5	68
	0.1	1.5	40	20.1

decreased. The anode surface was still clean and no discoloration occurred in the anolyte after the experiment had run for two or three days. Due to the abbreviated Tafel region, no measurable amounts of CO_2 could be produced in alkaline solution even after operation for several days.

4. By-Product Analysis

The by-products from the anodic compartment collected in the trap and analyzed by g.c. were found to be acetaldehyde. It was produced on both Au and Au-Pt alloy electrodes. There apparently is a branching in the reaction by which either a partial oxidation product, acetaldehyde, or the total oxidation product, CO_2, can be formed. This branching probably occurs after the rate determining step.

5. Sample Calculations

The calculations in this section are based on the following equation for complete oxidation of ethylene to CO_2 in acid solution:

$$C_2H_4 + 4H_2O \longrightarrow 2\ CO_2 + 12\ H^+ + 12\ e \qquad (3.2)$$

The data used are taken from Table VI for the 31-hour efficiency study in 1 N H_2SO_4 at 1 atm ethylene pressure on the 20Au-80Pt electrode.

The theoretical amount of CO_2 formed per Faraday of charge can be calculated by an expression derived from Faraday's law:

$$W_t = \frac{2\ it}{12\ F}\ (44) \qquad (3.3)$$

The faradaic efficiency is defined as the actual amount of CO_2 formed during an experiment divided by the theoretical amount formed if the oxidation were complete. Substituting numerical values:

$$W_t = \frac{(2)(0.005)(31)(3600)}{(12)(96{,}500)}\ (44) = 0.04241 \text{ gm}$$

$$W_e = 0.02785 \text{ gm}$$

Faradaic efficiency $= \frac{W_e}{W_t} = \frac{0.02785}{0.04241} = 0.6567$ or 65.67 percent.

Chapter IV

DISCUSSION

It is evident from the experimental work that there is a transition region (inflection point) in some of the Tafel curves. This indicates a change in the reaction mechanism. Thus, in acid solutions on Au and above the transition region on Au-rich alloys, the mechanism is different from that in basic solutions on other electrodes of the Au-Pt system. Phenomenologically, the Au-rich alloys behaved similarly to Au as did the Pt-rich alloys to Pt. This has also been observed in surface oxidation studies[25].

The discussion is presented in three major sections. (1) Summary of experimental results, (2) deduction of the mechanism, and (3) correlation of experimental data with the proposed mechanism. Due to the nature of the observations, it seems expedient to discuss separately the experimental observations above and below the transition region.

A. Summary of Experimental Results

1. Current-Potential Studies

Tafel slopes obtained in acid solutions on Au and above the transition region on Au-rich alloys were found to be ∿70 mv. In basic solutions and below the transition region, the slopes were ∿140 mv. These normally fix the rate determining steps as a chemical reaction following the first electron transfer in the former case and as the first electron

transfer in the latter. Since the products of this study were varied, neither the reversible potentials nor the corresponding exhange currents could be calculated. The pH dependence of current, ∂ log i/∂ pH, was approximately zero in strong acid solutions and unity in strong base solutions on the Au-Pt alloys.

2. Temperature Studies

Apparent activation energies calculated from the temperature studies ranged from 17 to 28 Kcal. They were consistently higher in basic solutions than in acid. Values of (∂ E_a/∂ V) fell into two groups corresponding to F and αF Kcal/volt. This is in agreement with the different Tafel slopes which suggest some change or alteration in the reaction mechanism. The chemical (zero over-potential) activation energies could not be evaluated because of the inability to calculate the reversible potentials as mentioned previously.

3. Partial Pressure Studies

The partial pressure studies showed that the current decreased as the partial pressure of ethylene decreased in all solutions on all electrodes, i.e., $\partial i/\partial p > 0$.

4. Carbon Dioxide Efficiency Studies

It was found from the efficiency studies in 1 N H_2SO_4 that the relative amounts of the CO_2 produced decreased as

the Pt content of the alloy decreased. On Au, no CO_2 was produced. Due to the small amounts of CO_2 involved as a consequence of the small limiting currents, it was not possible to determine efficiencies in basic solutions.

5. By-Product Analysis

Acetaldehyde (identified by gas chromatograph) was found to be the only other product. It was produced on both Au and Au-Pt alloys in acid solutions. No analyses were possible in basic solutions due to reasons stated previously.

B. Postulation of a Reaction Mechanism

1. Adsorption of Ethylene

Two modes of ethylene adsorption, associative and dissociative, have been examined from the point of view of the energetics of adsorption[6,26]. In associative adsorption, the double bond is opened and the orbitals are released to form bonds with the metal, i.e.,

$$H_2C = CH_2 \longrightarrow \begin{array}{l} H_2C \text{ —— } CH_2 \\ \quad | \qquad\quad | \\ \quad M \qquad M \end{array} \tag{4.1}$$

Alternatively, hydrogen may be split off with the double bond remaining intact (dissociative adsorption), i.e.,

$$H_2C = CH_2 \longrightarrow \begin{array}{l} HC \text{ ═══ } CH + 2\ M\text{-}H \\ \quad | \qquad\quad | \\ \quad M \qquad M \end{array} \tag{4.2}$$

Evidence of both associative and dissociative adsorption in the gas phase has been reported, although associative adsorption is favored on the basis of energy considerations.

In electrosorption, the process of dissociative adsorption may be better represented as

$$H_2C = CH_2 \longrightarrow \underset{\underset{M}{|}}{HC} = \underset{\underset{M}{|}}{CH} + 2\,H^+ + 2\,e \qquad (4.3)$$

in the potential region where hydrocarbon oxidation occurs. Thus, the energies of ionization and solvation of hydrogen and a proton respectively, as well as the electronic work function of the metal, have to be considered. Taking all these factors into account, the associative mode of adsorption is still found to be more probable[26].

Further support for associative adsorption of ethylene is obtained from comparison of the kinetics of the anodic oxidation of ethylene and acetylene. The species left on the surface in the dissociative adsorption of ethylene would be an adsorbed acetylene molecule. Thus, dissociative adsorption should lead to the same kinetic behavior for ethylene and acetylene, which has not been found experimentally[6,27].

Based on steric considerations as well as taking into account the covalence with d-band vacancies as being responsible for ethylene chemisorption, the model of adsorption involves four surface sites of Pt per molecule of ethylene[6]. The adsorption isotherm (assuming Langmuir-type adsorption) is then of the form

$$\frac{\theta_E}{(1-\theta_E)^4} = K_c C_E \qquad (4.4)$$

or, $$= k_p P_E$$

the values of K_p have been estimated as $2.3 \leq K_p \leq 150$.

It has also been shown that the physical properties of Au and Pd and their behavior for the anodic oxidation of ethylene are similar[7]. Pd has 0.55 vacant d-orbitals per atom available for covalent bonding as does Pt, but Au has none. Thus, if d-orbitals are important for adsorption, one would expect Pd and Pt to behave similarly in oxidation studies and for no reaction to occur on Au. Such is not the case as studies with acetylene on Au showed both high currents and coverages of acetylene[24]. This may be associated with the energy required for d-s promotion which is uniquely small (3.25 ev) for Au. It is possible that such promotion accompanies chemisorption, creating d-band vacancies and hence allowing covalent bonding[28].

The mechanism of associative adsorption postulated for ethylene on Au would involve a two point attachment. However, due to the size of the ethylene molecule and the inter-atomic distances of the Au atoms, it is probable that the ethylene blocks two or more adjacent sites. Therefore, Langmuir isotherm for the adsorption of ethylene on Au and Au-Pt alloys is taken as

$$\frac{\theta_E}{(1-\theta_E)^n} = K_p P_E \qquad (4.5)$$

where n can be equal to 2 or more (possibly 4, 6, or 8).

The heat of adsorption of ethylene on various metal films from the gas phase has been found to depend on the position of the metal in the periodic table[29]. No data are available for Pt but values of -21 and -58 Kcal/mole have been obtained for Au and Ni, respectively. The low value of the heat of adsorption on Pt from solution, 0 ± 4 Kcal/mole, observed by Gileadi et al., was interpreted in terms of the replacement of water molecules from the surface and, to a small extent, the energy of solvation of ethylene[26]. It was represented as

$$C_2H_4 \text{ (sol)} + 4\ H_2O \text{ (ads)} \longrightarrow C_2H_4 \text{ (ads)} + 4\ H_2O \text{ (sol)} \qquad (4.6)$$

These hypotheses will be considered later in testing the pressure relationship that results from the proposed reaction mechanism.

2. Reaction Mechanism

The rate determining step in acid solutions on Au and above the transition region on Au-rich alloys* must have the following characteristics (1) be a chemical reaction following the first electron transfer since the Tafel slope is 2.3 RT/F, (2) involve adsorbed ethylene, or species derived

*It should be kept in mind that the transition region existed only on alloy electrodes in strong acid solutions.

therefrom since $\partial i/\partial p > 0$, and (3) exhibit no pH dependence in strong acid solutions.

In basic solutions and below the transition region on Au and Au-Pt alloys*, the rate determining step must: (1) be the first electron transfer since the Tafel slopes are 2(2.3 RT/F), (2) involve adsorbed ethylene, or species derived therefrom since $\partial i/\partial p > 0$, and (3) exhibit no pH dependence in strong acid solutions but show a unity pH dependence in basic solutions.

There is apparently branching in the reaction or parallel reactions by which acetaldehyde (partial oxidation product) and/or CO_2 (total oxidation product) are produced. If branching is the case, it most likely occurs after the rate determining step since the r.d.s. apparently occurs in the early part of the reaction sequence.

In the kinetics of simplified open reaction sequences, each step in the sequence is taken to be simple and first order with respect to the involved species. All steps prior to the r.d.s. are considered to be in equilibrium. Steps after the r.d.s. are not considered to be in equilibrium as their forward rates are greater than that of the r.d.s.

The following reaction scheme was proposed by Dahms et al.[7], and has been applied here to the reaction sequence in acid solutions on Au and above the transition region on Au-rich alloys.

$$C_2H_4\ (sol) \rightleftharpoons C_2H_4\ (ads) \qquad (4.7)$$

$$C_2H_4\ (ads) \rightleftharpoons C_2H_4^+\ (ads) + e \qquad (4.8)$$

$$C_2H_4^+\ (ads) + H_2O\ (sol) \xrightarrow{r.d.s.} C_2H_4OH\ (ads) + H^+ \qquad (4.9)$$

$$C_2H_4(OH)\ (ads) \longrightarrow CH_3CHO + H^+ + e \qquad (4.10a)$$

or

$$C_2H_4(OH)\ (ads) \xrightarrow{H_2O} \cdots \longrightarrow CO_2,\ CH_3CHO,\ H^+,\ \text{and electrons} \qquad (4.10b)$$

This mechanism involves the assumption of a $C_2H_4^+$ (carbonium ion) intermediate. Evidence that reactions with these species could be slow arise from their stabilization by solvation[7].

From the quasi-equilibrium in reaction 4.8

$$\Theta_{C_2H_4^+} = K_{4.8}\ \Theta_E\ \exp\left(\frac{FV}{RT}\right) \qquad (4.11)$$

Thus, the rate of anodic oxidation of ethylene can be expressed as

$$i = nF\ k_{4.9}\ K_{4.8}\ a_{H_2O}\ \Theta_E\ \exp\left(\frac{FV}{RT}\right) \qquad (4.12)$$

In basic solutions and below the transition region on Au and Au-Pt alloys, the first electron transfer is the r.d.s. A reaction sequence which is qualitatively consistent with all requirements is represented by

$$C_2H_4\ (sol) \rightleftharpoons C_2H_4\ (ads) \qquad (4.13)$$

$$\text{r.d.s.}\begin{cases} C_2H_4\ (ads) + H_2O \longrightarrow C_2H_4OH\ (ads) + H^+ + e & (4.14a) \\ C_2H_4\ (ads) + OH^- \longrightarrow C_2H_4OH\ (ads) + e & (4.14b) \end{cases}$$

$$C_2H_4OH\ (ads) \xrightarrow{H_2O} CO_2,\ CH_3CHO,\ H^+,\ \text{and electrons} \qquad (4.15)$$

Using this sequence the rate of the anodic oxidation of ethylene in basic solutions and below the transition region on all electrodes can be expressed as

$$i = nF\ (k_{4.14a}\ a_{H_2O} + k_{4.14b}\ a_{OH^-})\ \theta_E\ \exp\left(\frac{\alpha FV}{RT}\right) \qquad (4.16)$$

Equation 4.12 and 4.16 can now be tested by their ability to correlate the experimental data.

C. Correlation of Experimental Results with the Theoretical Rate Equations

This section consists of correlating the experimental data with derived rate equations. An ability of these equations to correlate the data would lend support to the validity of the proposed mechanisms.

1. Current-Potential Relationship

Taking the logarithm of both sides of equation 4.12

$$\log i = \log\ (nF\ k_{4.9}\ K_{4.8}\ a_{H_2O}\ \theta_E) + \frac{FV}{2.3\ RT} \qquad (4.17)$$

The partial differential of V with respect to log i from

equation 4.17 gives the Tafel slope

$$\frac{\partial V}{\partial \log i} = \frac{2.3\ RT}{F} = 70 \text{ mv (for 80°C)} \qquad (4.18)$$

A similar treatment of equation 4.16 yields

$$\frac{\partial V}{\partial \log i} = \frac{2.3\ RT}{\alpha F} = 140 \text{ mv (for 80°C)} \qquad (4.19)$$

Thus, the values of the theoretical and experimental Tafel slopes agree.

2. Current-pH Relationship

Values of current density determined from the experimental data on the alloys and the corresponding pH for a potential of 0.4 v are shown in Figures 20 to 23. These values were obtained by extrapolating the linear Tafel regions to a potential of 0.4 v.

Equation 4.12 shows the rate to be independent of pH, i.e.,

$$\frac{\partial \log i}{\partial\ pH} = 0 \qquad (4.20)$$

Considering the term $[nF\ \theta_E \exp\left(\frac{\alpha FV}{RT}\right)]$, in equation 4.16 to be constant, then

$$i = \text{constant}\ (k_{4.14a}\ a_{H_2O} + k_{4.14b}\ a_{OH^-})\ \theta_E \exp\left(\frac{\alpha FV}{RT}\right) \qquad (4.21)$$

and

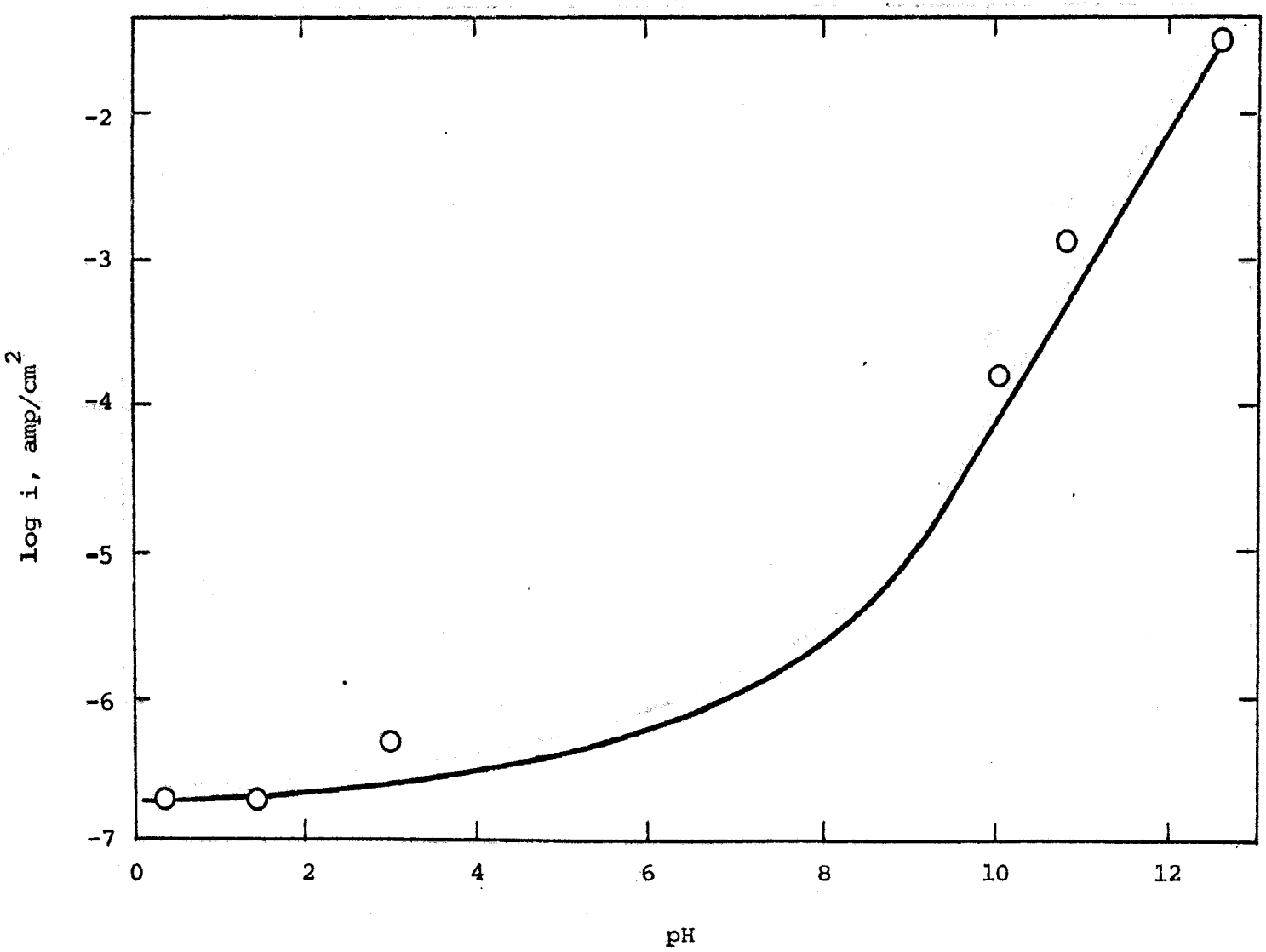

Figure 20. Comparison of the theoretical and experimental effect of electrolyte pH on current density (V = 0.40 v) for the anodic oxidation of ethylene on 80Au-20Pt alloy at 80°C. (O , equation 4.16; —, experimental data)

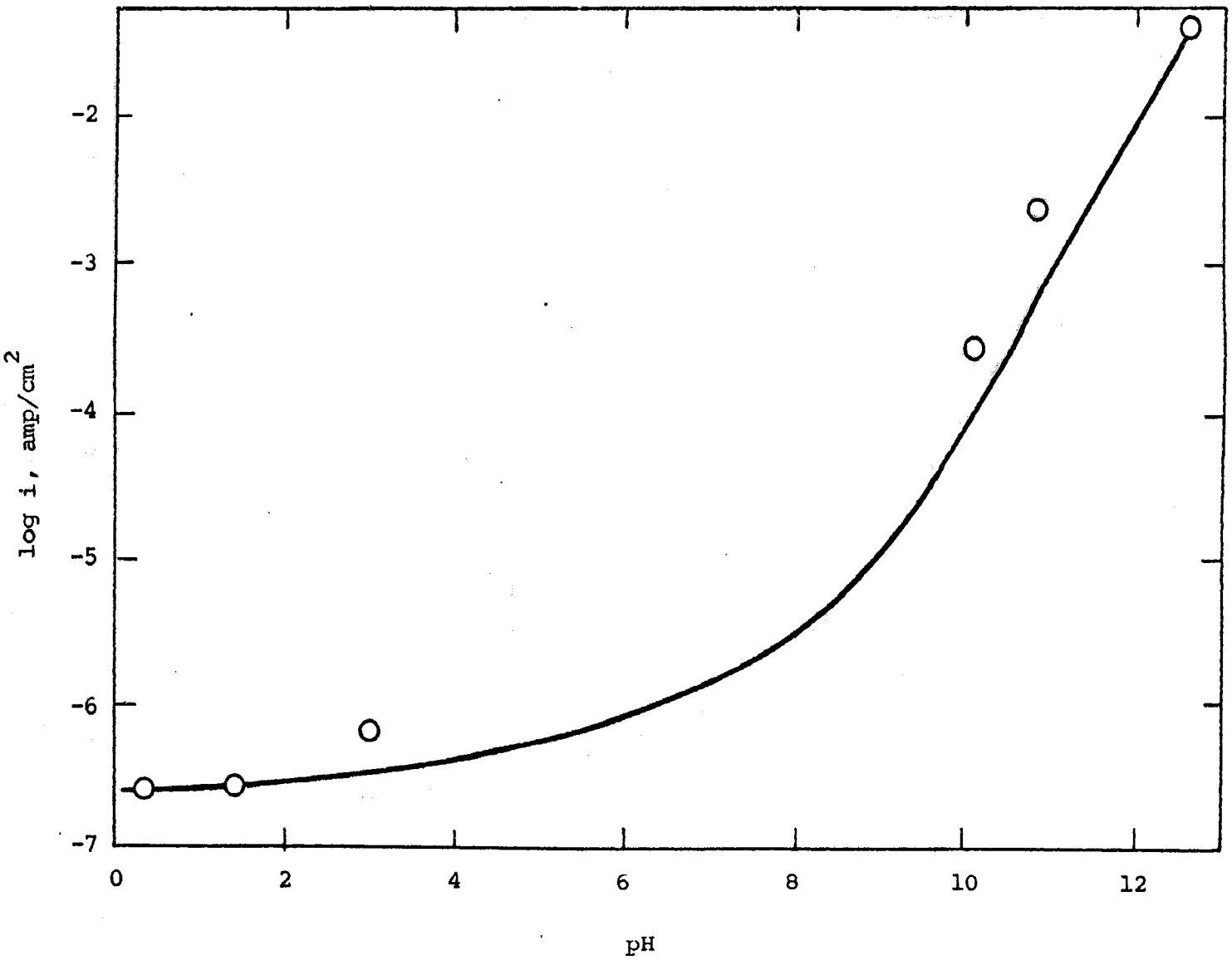

Figure 21. Comparison of the theoretical and experimental effect of electrolyte pH on current density (V = 0.40 v) for the anodic oxidation of ethylene on 60Au-40Pt alloy at 80°C. (O, equation 4.16; ——, experimental data)

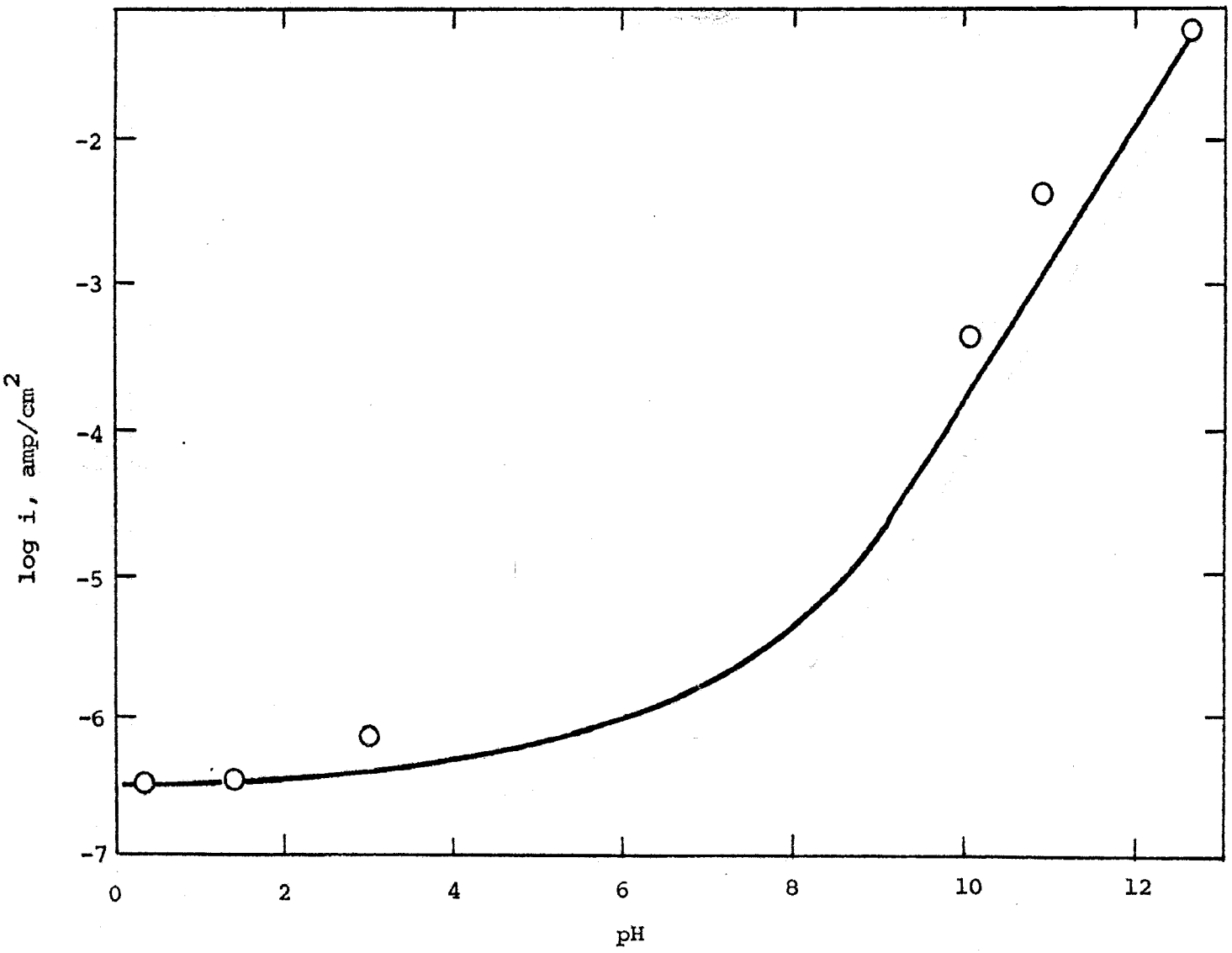

Figure 22. Comparison of the theoretical and experimental effect of electrolyte pH on current density (V = 0.40 v) for the anodic oxidation of ethylene on 40Au-60Pt alloy at 80°C. (O , equation 4.16; ——, experimental data)

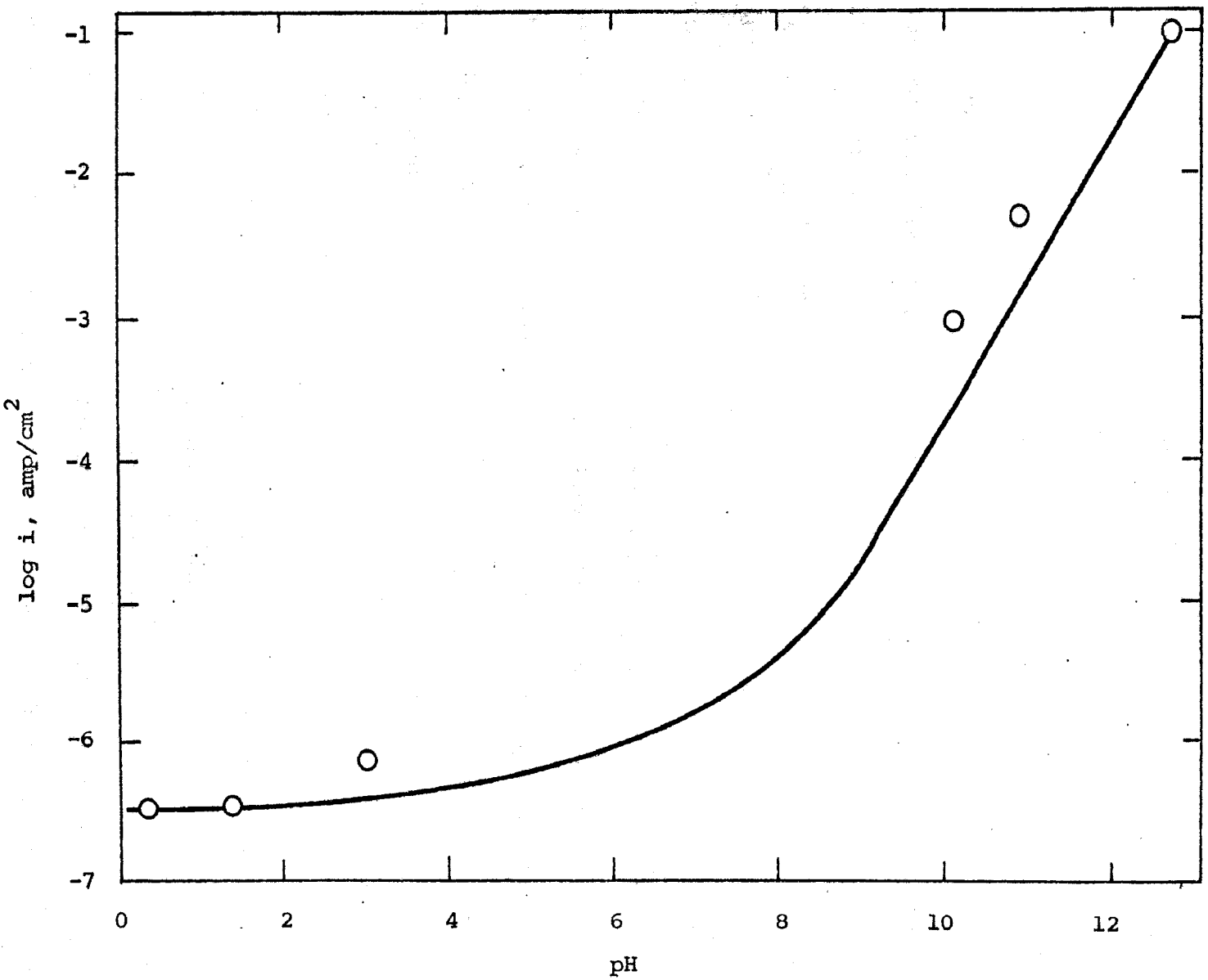

Figure 23. Comparison of the theoretical and experimental effect of electrolyte pH on current density (V = 0.40 v) for the anodic oxidation of ethylene on 20Au-80Pt alloy at 80°C. (O , equation 4.16; ——, experimental data)

$$\frac{\partial \log i}{\partial pH} = \frac{1}{\frac{k_{4.14a}\ a_{H_2O}}{k_{4.14b}\ a_{OH^-}} + 1} \qquad (4.22)$$

The value of $k_{4.14a}\ a_{H_2O}$ can be calculated from the experimentally measured current in 1 N H_2SO_4 where the contribution to the current from OH^- discharge would be negligible due to its low concentration. The term $k_{4.14b}$ can be calculated using similar data from 1 N KOH assuming the value of $k_{4.14a}\ a_{H_2O}$ to be correspondingly insignificant. These predicted current-pH dependence are also shown in Figures 20 to 23.

The experimental values differ slightly from the theoretical values. However, the trend is correct and errors of these magnitudes could easily arise from the extrapolation of the Tafel curves and from the assumption that θ_E was independent of potential.

3. Temperature Studies

The variation of the apparent activation energy with potential in acid solutions on Au and above the transition region on Au-rich alloys can be found from equation 4.12. The term $k_{4.9}$ is equivalent to a chemical rate constant which, by use of the Arrhenius relationship, can be expressed as $A \cdot \exp(-E_a'/RT)$. Substituting for $k_{4.9}$ and taking the derivtive of the log of both sides of equation 4.12 with respect to (1/T), one obtains

$$\frac{\partial \log i}{\partial (1/T)} = \frac{-E_a'}{2.3\ R} + \frac{FV}{2.3\ R} = \frac{-E_a}{2.3\ R} \qquad (4.23)$$

Using this expression, the variation of the apparent activation energy with potential is found to be

$$\frac{\partial E_a}{\partial V} = -F = -23.06 \text{ Kcal/volt} \qquad (4.24)$$

A similar treatment of equation (4.16) gives

$$\frac{\partial E_a}{\partial V} = -\alpha F = -11.53 \text{ Kcal/volt} \qquad (4.25)$$

for basic solutions and below the transition region on all electrodes. These values agree well with that obtained experimentally (See Table V).

4. Partial Pressure Studies

The mode of ethylene adsorption during the reaction has already been discussed. Qualitatively, a positive pressure effect was observed on Au and Au-Pt alloys in both acidic and basic solutions.

For the case represented by equation 4.12 (in acid solutions on Au and above the transition region on Au-rich alloys), the reaction rate depends on the coverage of $C_2H_4^+$, which can be related to θ_E. Since carbonium ions readily react with water (not necessarily adsorbed), the number of points of attachment of ethylene to the electrode surface can be assumed to be either two or four.

In the case of equation 4.16, H_2O (or OH^-) may undergo

discharge only when it is adsorbed adjacent to an adsorbed ethylene molecule, so the rate of reaction also depends on Θ_E. However, the Θ_E term will include not only the sites occupied by the ethylene, but also those next to it that are necessary for water discharge. Therefore, an adsorption isotherm involving four to eight adjacent sites would be feasible.

In order to correlate the ethylene partial pressure with current, Θ_E was calculated as a function of pressure using equation 4.5. Appropriate values of n and K_p were found by trial and error. For illustration, the results from an adsorption isotherm using four point attachment (n = 4) are shown in Figure 24 for various values of K_p. The current was calculated with the appropriate value of Θ_E for each case and compared to the experimental value . This procedure has been described previously[30] and was used to find values of n and K_p that would best correlate the data.

For equation 4.12, n = 4 and K_p = 1 and 5 for Au and Au-rich alloys, respectively, give the best agreement with the experimental data.

For equation 4.16, it was found that both four and eight point attachment with appropriate values of K_p fit the data within experimental limits. Eight point attachment would seem more feasible considering the additional sites required for H_2O (or OH^-) discharge. A further decrease in pressure might assist in selecting the best value of n if

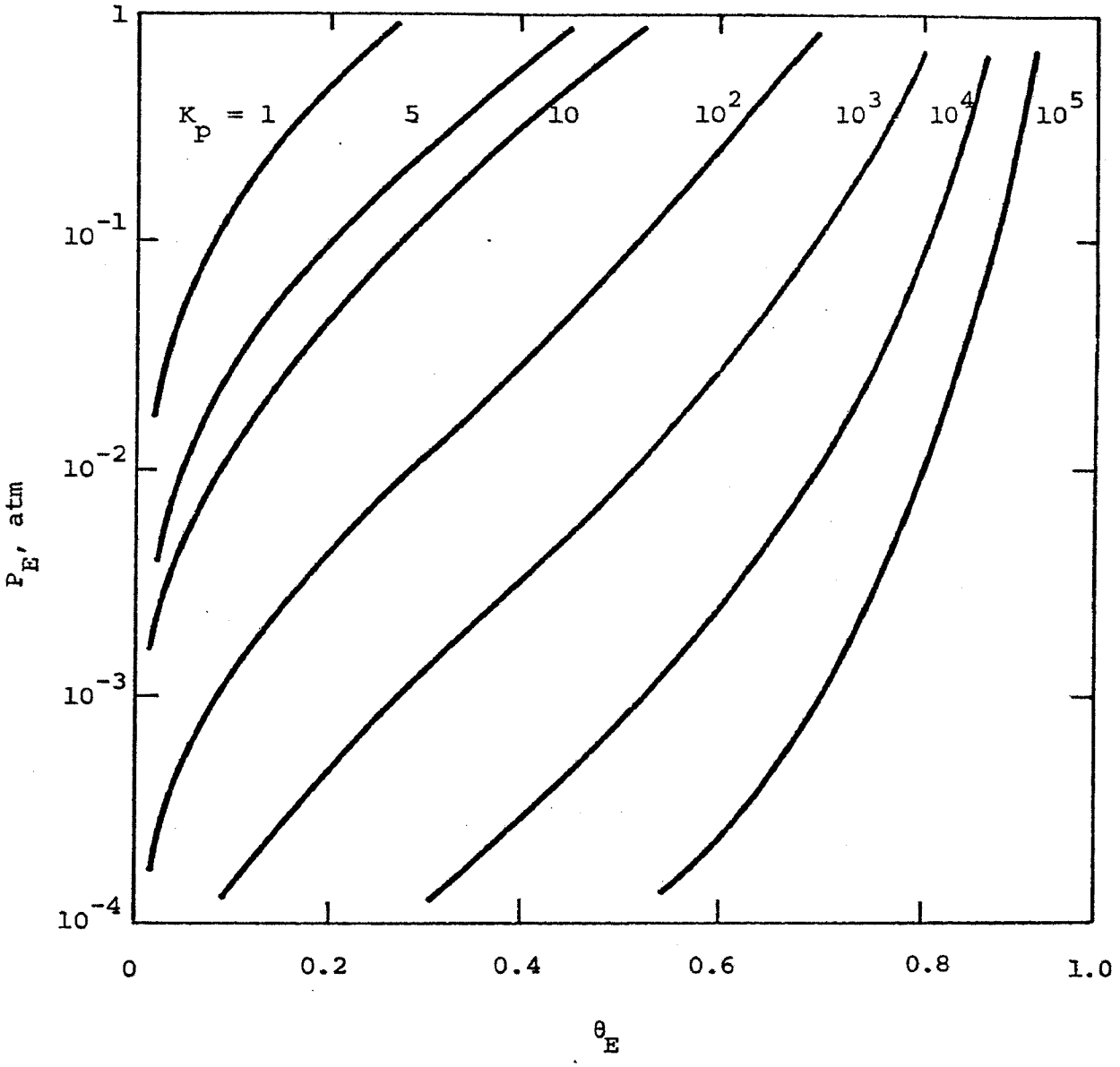

Figure 24. Ethylene adsorption isotherms for a four point attachment.

there were not current limitations on the experiments.

The calculated values of current versus partial pressure are shown in Figures 25 to 29 along with the experimental data for comparison. The agreement is considered to be quite good.

Adsorption of ethylene in basic solutions is thought to depend on potential with desorption occurring at higher potentials[30]. This is consistent with the abbreviated Tafel curves and a greater ease of formation of passivation oxides observed in these studies in basic solutions.

The different reaction parameters in acid and basic solutions on Au arise from the r.d.s. changing from the first electron transfer to a chemical reaction following the first electron transfer. In acid solutions, the potential is high (positive) enough to cause the adsorbed ethylene molecules to give up an electron, thereby forming the $C_2H_4^+$ intermediate. At lower potentials, H_2O (or OH^-) is discharged when adsorbed adjacent to an adsorbed ethylene molecule, such is the case in basic solutions. A phenomena similar to this has been observed for oxygen reduction on Au[32].

The observed change in the reaction from one r.d.s. occurring at lower potentials to another at high potentials occurs on Au-Pt alloys. At lower potentials, H_2O (or OH^-) is discharged when adjacent to adsorbed ethylene molecules and further reacts with the ethylene. When the potential has been increased to a certain point, the behavior is as if

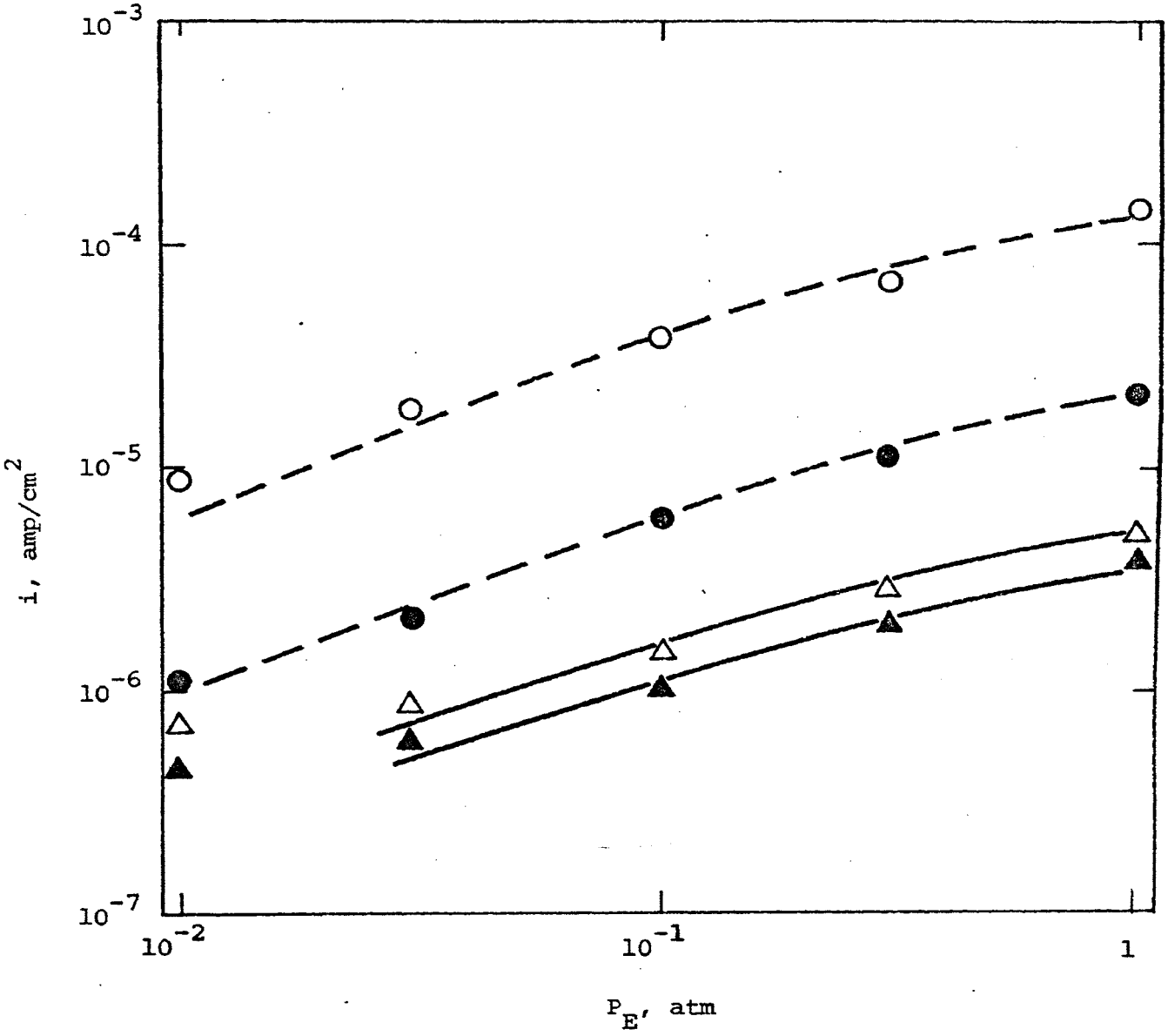

Figure 25. Comparison of the theoretical and experimental effect of partial pressure on current density for the anodic oxidation of ethylene on Au at 80°C. (---, equation 4.12, n = 4, K_p = 1; ——, equation 4.16, n = 8, K_p = 1; ○, ●, △, ▲, experimental data)

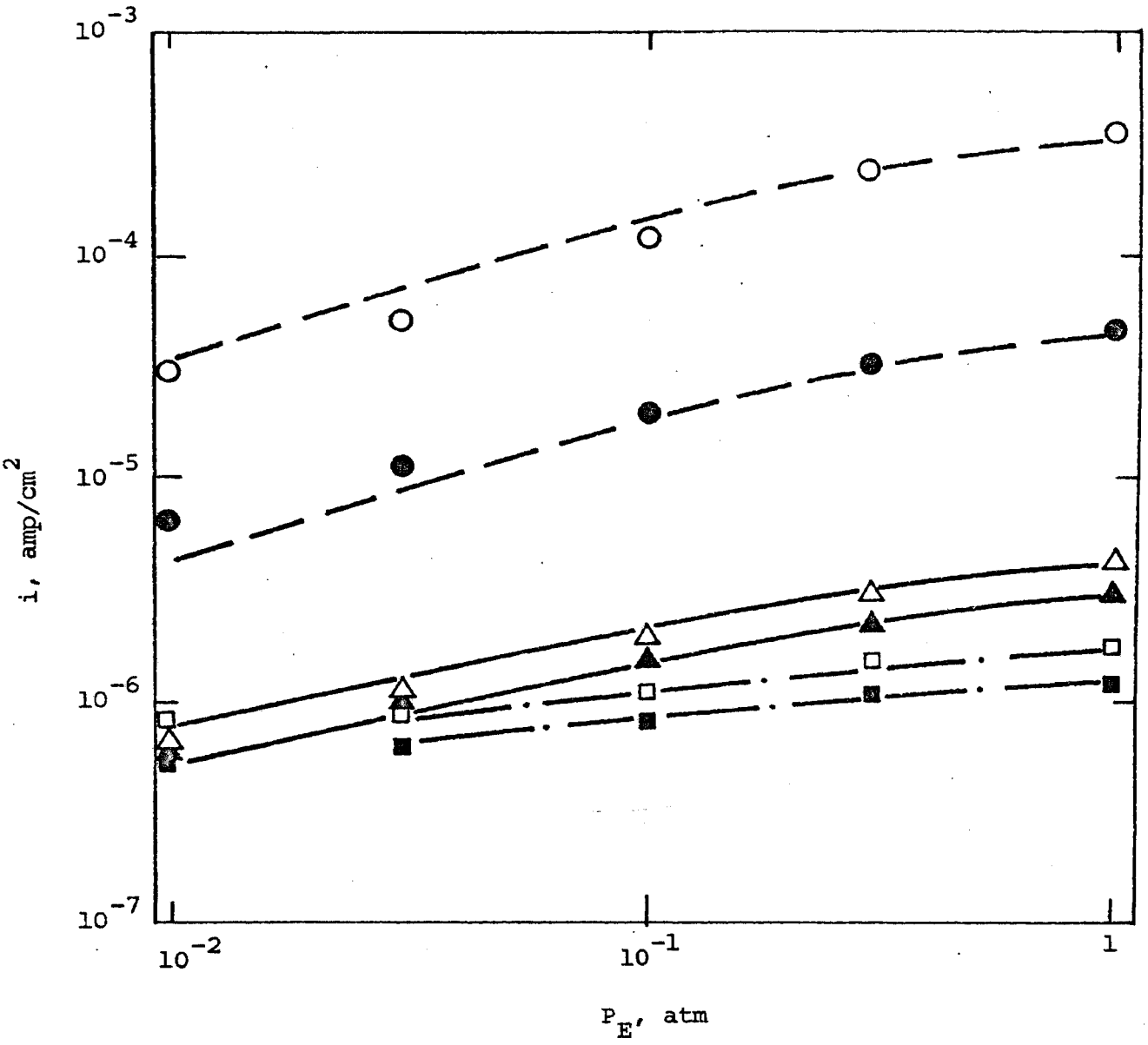

Figure 26. Comparison of the theoretical and experimental effect of partial pressure on current density for the anodic oxidation of ethylene on 80Au-20Pt alloy at 80°C. (---, equation 4.12, n = 4, K_p = 5; ——, equation 4.16, n = 8, K_p = 10;—·—, equation 4.16, n = 8, K_p = 100; ○, ●, △, ▲, □, ■, experimental data)

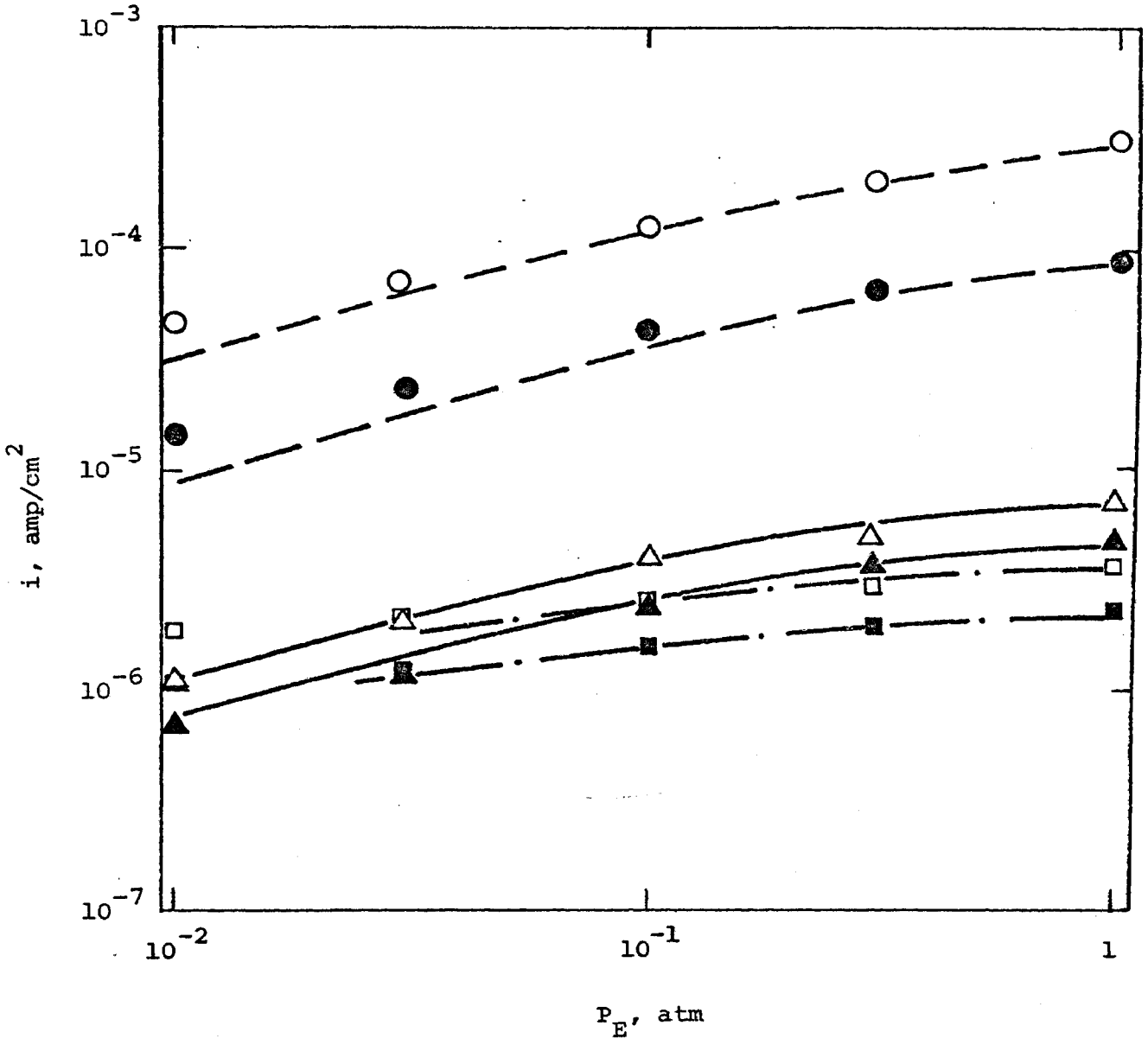

Figure 27. Comparison of the theoretical and experimental effect of partial pressure on current density for the anodic oxidation of ethylene on 60Au-40Pt alloy at 80°C. (---, equation 4.12, n = 4, K_p = 5; ——, equation 4.16, n = 8, K_p = 10; —·—, equation 4.16, n = 8, K_p = 100; ○, ●, △, ▲, □, ■, experimental data)

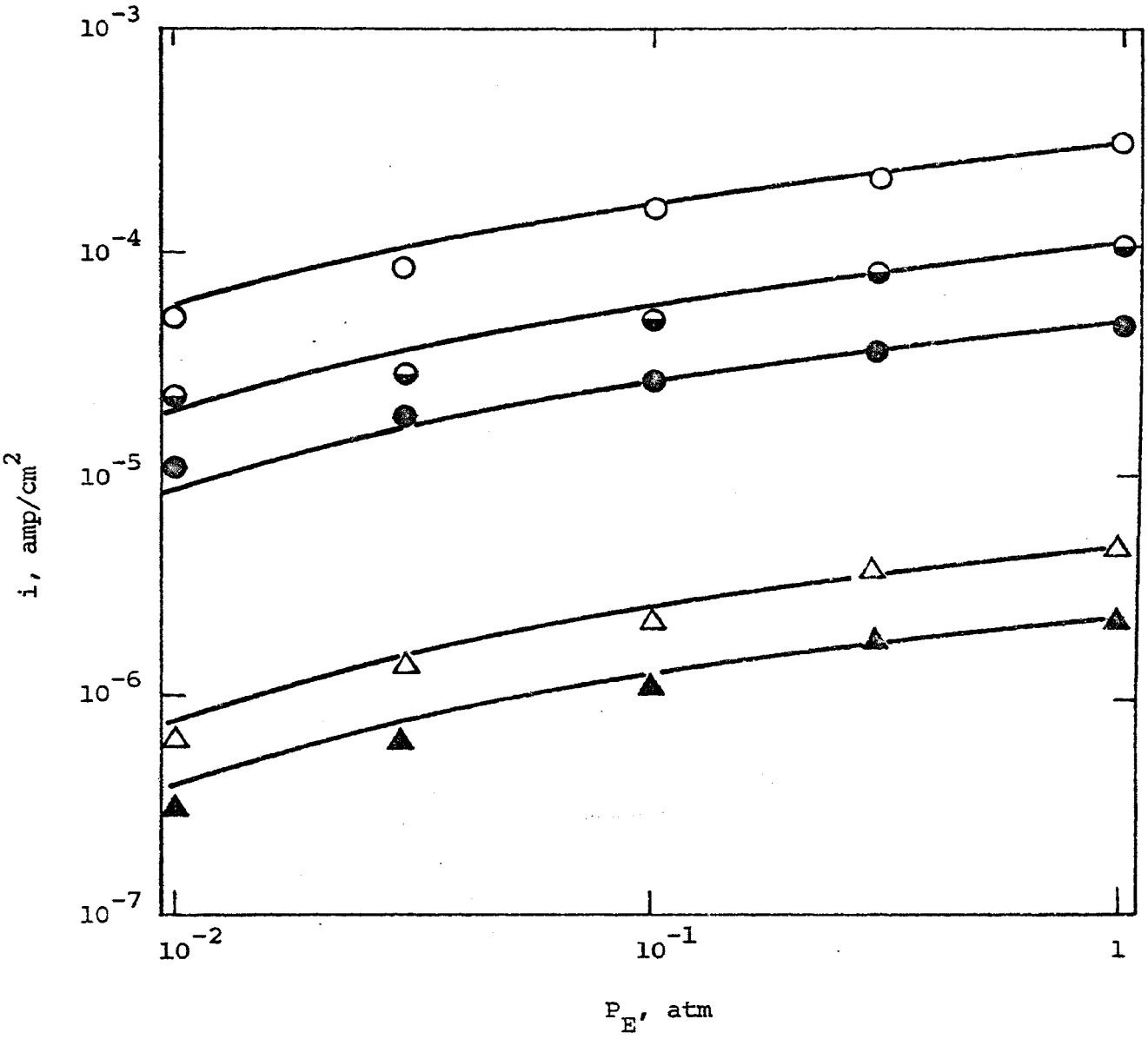

Figure 28. Comparison of the theoretical and experimental effect of partial pressure on current density for the anodic oxidation of ethylene on 40Au-60Pt alloy at 80°C. (——, equation 4.16, n = 8, K_p = 10; ○ , ◒ , ● , △ , ▲, experimental data)

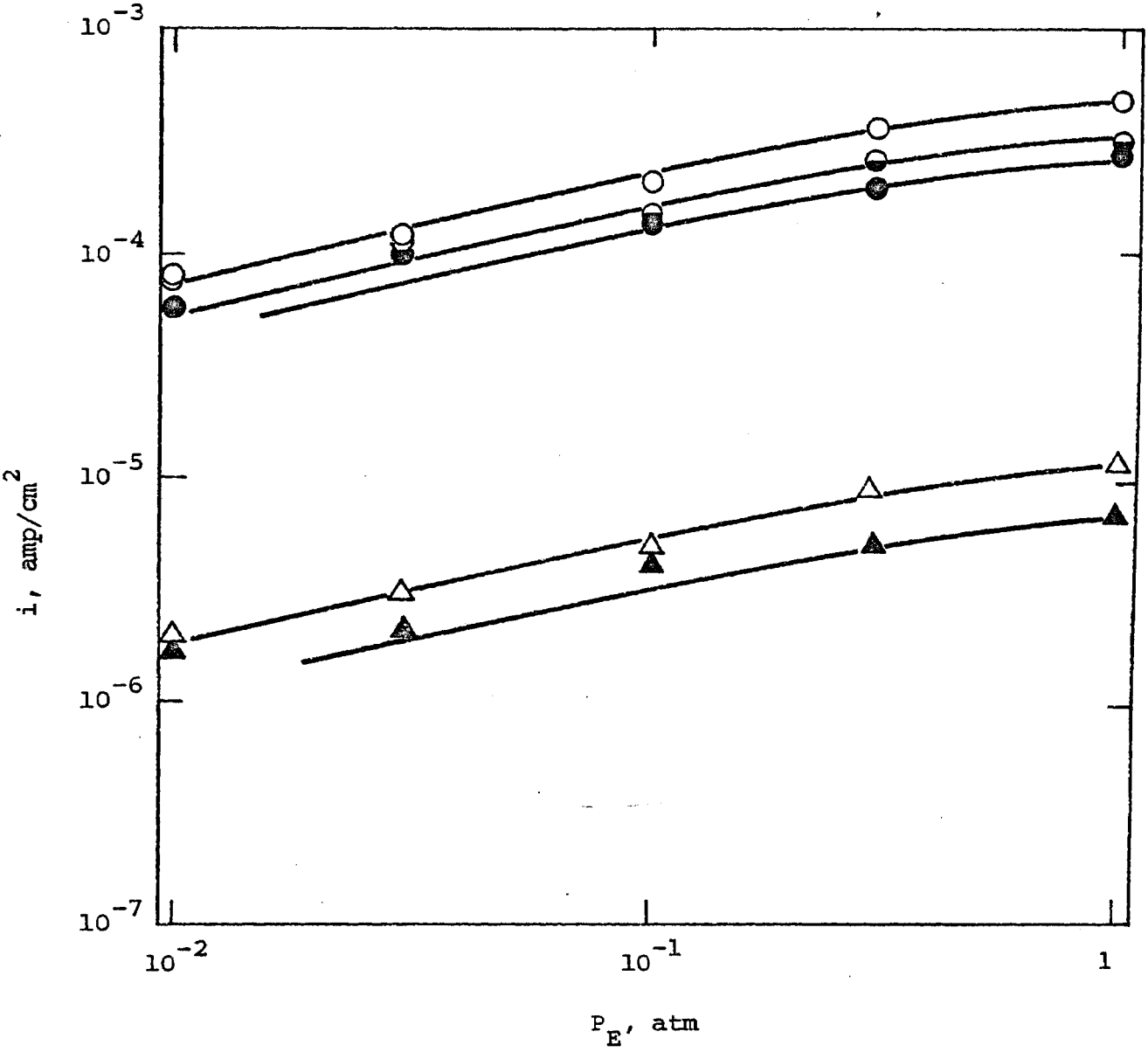

Figure 29. Comparison of the theoretical and experimental effect of partial pressure on current density for the anodic oxidation of ethylene on 20Au-80Pt alloy at 80°C. (——, equation 4.16, n = 8, K_p = 5; ○, ◒, ●, △, ▲, experimental data)

the reaction with $OH^{\cdot}$ is inhibited possibly due to the potential influence in removing electrons from adsorbed ethylene to form the carbonium ions. This is the transition region. Further increases of potential supply the required energy to completely remove the electrons to form the $C_2H_4^+$ on the electrode surface. The deficiency of electrons in the carbonium ion which are necessary for covalent bonding retards the reaction with $OH^{\cdot}$, thus allowing the reaction to proceed directly between the carbonium ion and water.

The Tafel slopes above the transition region are observed to increase in going from Au-rich to Pt-rich alloys. This can be explained on the basis of separate reactions occurring on the Au-rich and Pt-rich phases present in the alloys in which the compositions are the same but their relative amounts are changing from one electrode to another. This indicates the carbonium ion to be formed primarily on Au-rich phases (where the electron can be most easily removed) leading to acetaldehyde as a product and reaction by H_2O (or OH^-) discharge to form CO_2 on Pt-rich phases (where electrons could only very difficultly be removed). The geometric summation of currents on these phases with Tafel slopes of 70 and 140 mv respectively would give pseudo Tafel curves with slopes varying between 70 to 140 mv in going from predominately α_2-phase to predominately α_1-phase. This is consistent with the experimental observations on Au, Pt and Au-Pt alloy electrodes.

5. Reaction Products

The explanation for the incomplete oxidation of ethylene on Au and Au-Pt alloys is probably that presented by Dahms et al.[7] Their reasoning involved the bond strength between the metal electrodes and the adsorbing hydrocarbons. Using Pauling's equation, the covalent bond strength between a metal and a carbon atom is[16]

$$E_{M-C} = \frac{1}{2} (E_{M-M} + E_{C-C}) + 23.06 (X_C - X_M)^2 \qquad (4.26)$$

The heats of sublimation for Au and Pt, approximately equal to their bond energies, are given in Table II. The electronegativities of Au, Pt, and C are 2.54, 2.28 and 2.55 respectively[33]. Ethylene has one π bond and one σ bond. One may assume, as an approximation, that the energy required to break the π bond is $\sim$ 63 Kcal (the difference in the bond energy of C = C and C-C)[33]. According to the associative adsorption model, the π bond is broken when ethylene is adsorbed. The strengths of the respective metal-carbon bonds on Au and Pt are:

$$E_{Au-C} = \frac{1}{2} (84 + 63) + 23.06 (2.55 - 2.54)^2$$

$$= 73.5 \text{ Kcal} \qquad (4.27)$$

$$E_{Pt-C} = \frac{1}{2} (135 + 63) + 23.06 (2.55 - 2.28)^2$$

$$= 100.68 \text{ Kcal} \qquad (4.28)$$

There are two metal-carbon bonds formed in each case from the

ethylene π bond rupture. This leaves for the adsorbed ethylene, one C-C σ bond and two carbon-metal bonds. In the case of Pt, the next most probable bond rupture would be the C-C σ bond ($\sim$ 83 Kcal versus $\sim$ 101 Kcal for Pt-C bond). The Au-C bond strength ($\sim$ 74 Kcal) is less than that of C-C σ bond. Therefore, it is possible that the metal-carbon bond for Au could be broken before the C-C σ bond, thus allowing a partially oxidized ethylene molecule to be desorbed.

The intermediate oxidation product of Au is acetaldehyde and no CO_2 is produced. The CO_2 produced on Au-Pt alloys is proportional to the Pt content and is apparently balanced by the acetaldehyde.

6. Comparison of Electrocatalytic Activity

The Au-Pt system, studied by Darling et al., is shown in Figure 30[34]. It indicates that below 1260°C, the mutual solubility of Au and Pt becomes limited and the solid solutions separates into Pt-rich (α_1) and Au-rich (α_2) phases. At lower temperatures, it can be seen that the composition of the α_1-phase approaches that of pure Pt, and the α_2-phase that of about 80 percent Au. (Relative amounts of these phases for the alloys studied were given in section B, Chapter II).

It is likely that the reaction rates on the alloys are related to the relative amounts of the individual phases. This allows the reaction to be expressed as

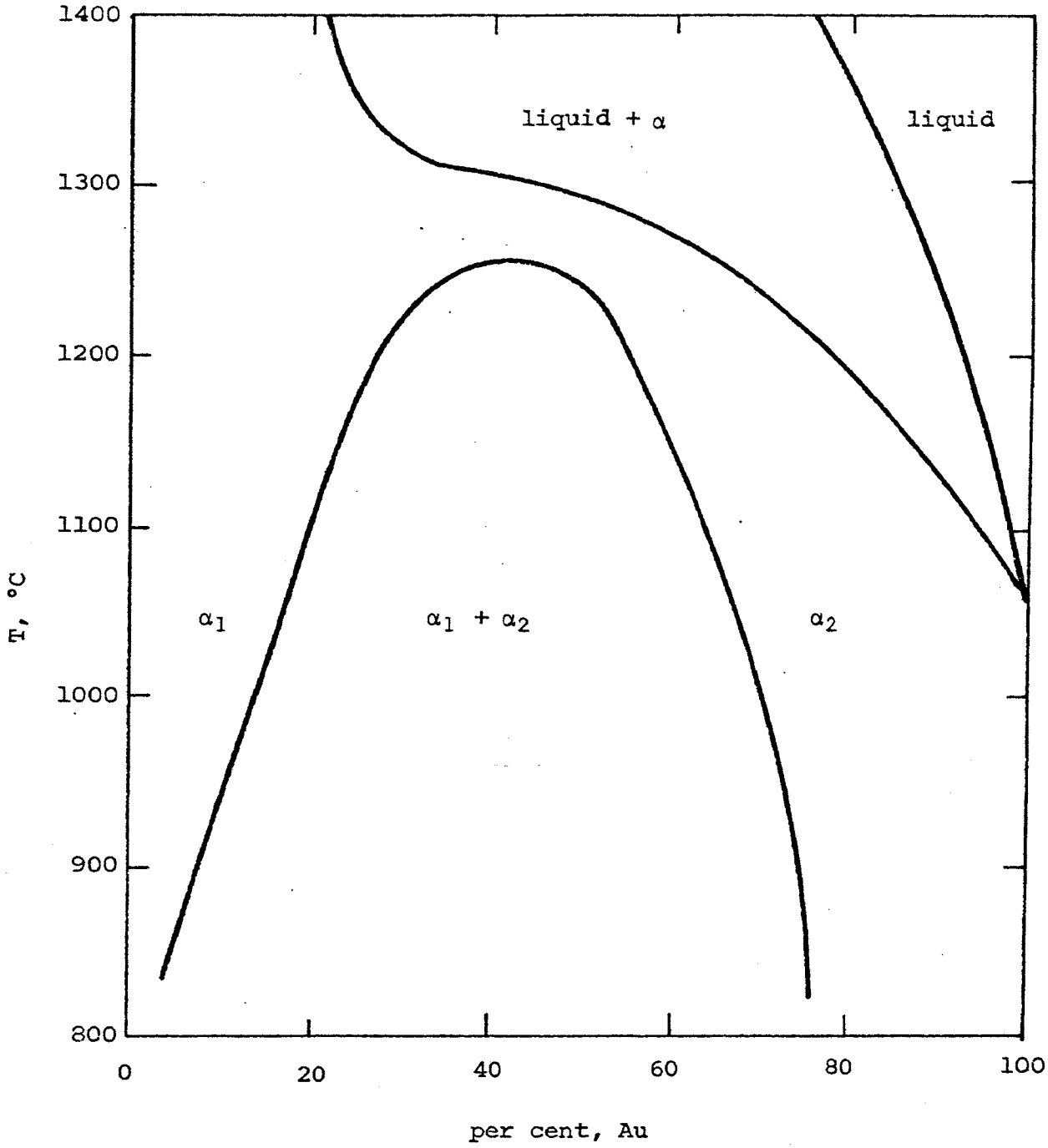

Figure 30. Equilibrium diagram for the Au-Pt system.[34]

$$i_T = f_1 i_1 + f_2 i_2 \qquad (4.29)$$

Values of i_T have been calculated for each alloy at 0.4 v and are shown in Figure 31. The reaction rates on the metals are also included for comparison.

Comparison of the theoretical and experimental values shows fair agreement considering the approximations used to evaluate the rates on the separate phases. It can be seen that a small amount of Pt added to Au increases the electro-activity of the metal over ten times in basic solution and over 10^4 times in acid solution. A further increase of the Pt component increases the activity to some extent, but not so dramatically.

Due to the heterogeneity of the alloys, it does not seem possible to relate the d-band vacancies to the bulk compositions, therefore, one has not been attempted. It is contemplated that an extension of this work will be an attempt to produce solid-solution alloys for use in such studies.

7. Comparison of the Electro-Oxidation Rates of Ethylene and Acetylene

A comparison of the studies on Au[24] and Pt[6,27] shows that the currents resulting from acetylene electro-oxidation are significantly higher than those from ethylene. As this is of considerable interest, a brief discussion of possible explanations follows:

(1) Relative Solubilities. Solubility of ethylene in

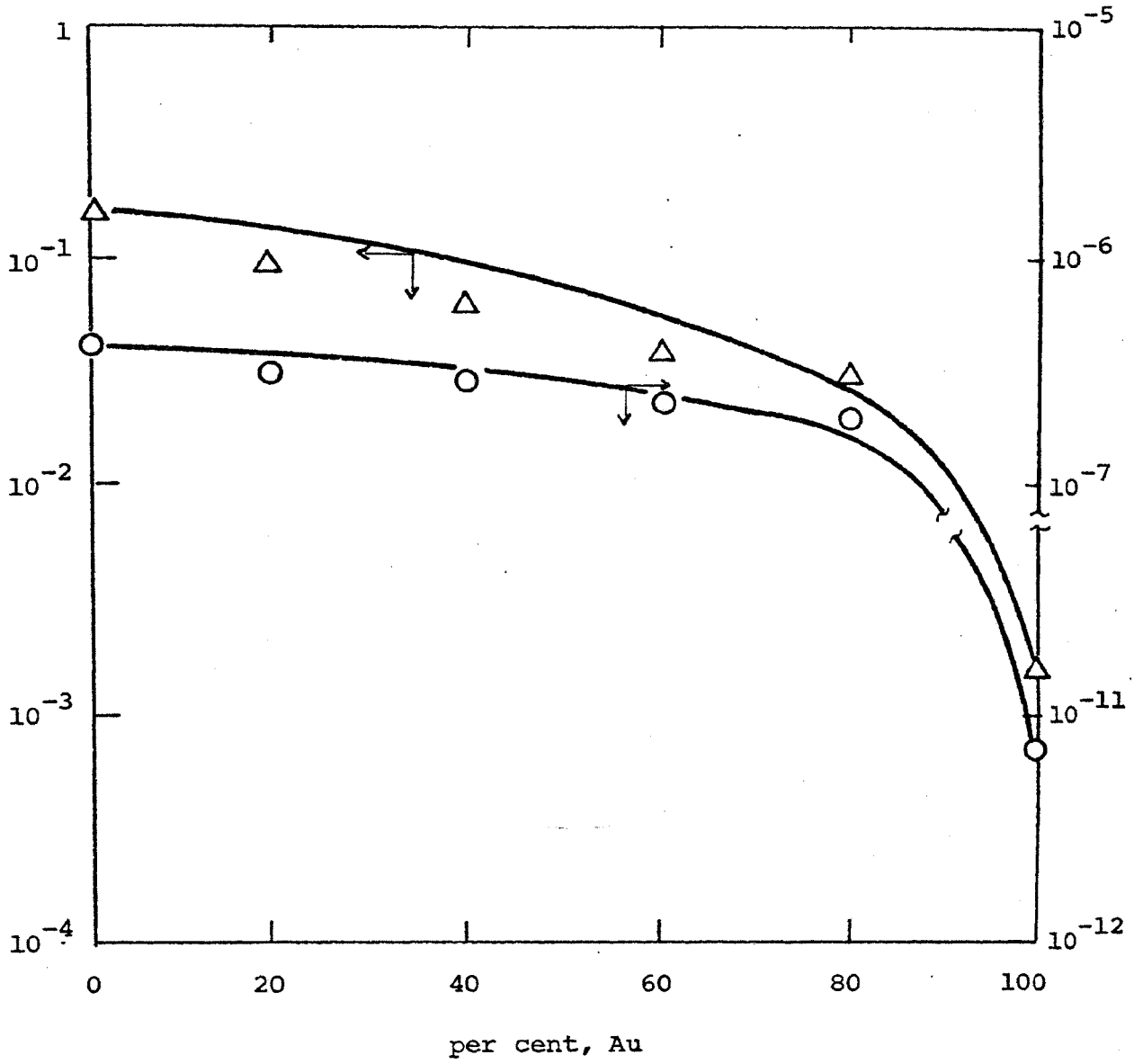

Figure 31. Comparison of the electrocatalytic activity of electrodes from the Au-Pt system for the anodic oxidation of ethylene at 80°C. (——, equation 4.29, ○, 1 N H_2SO_4, △, 1 N KOH)

aqueous solutions is smaller than that of acetylene[35]. Since the coverage of a species is related to its bulk concentration in solution, it is expected that the coverage of adsorbed acetylene would be higher than ethylene possibly giving higher currents on Au.

(2) Accessibility to Adsorption Sites. Acetylene is more accessible to the active sites on the metal surface than ethylene due to the size of the molecules. The low value of limiting coverage is often claimed to be due to inactive sites or small crevices on the surface. A fraction of the sites may be unavailable for adsorption, either due to a different degree of affinity of the surface atoms for the adsorbent (inactive sites) or due to some of the sites being inside small crevices inaccessible to the larger organic molecules. The relative number of inactive sites would be expected to increase as the size of the adsorbing molecules increases.

(3) Mode of Adsorption. As discussed previously, the adsorption by hydrocarbon from solution can be interpreted in terms of replacement of water molecules on the metal surface. Within limits, the lower the energy required for hydrocarbon adsorption, the easier it is for the hydrocarbon to replace the adsorbed water molecules on the surface. Acetylene has two π bonds and one σ bond. The energy required to break the first π bond is $\sim$ 54 Kcal (the difference in bond energy of C≡C and C=C). Assuming that the first π bond is broken when acetylene is adsorbed, and using Pauling's equation,

the bond strength of Au-C for acetylene adsorption is ∿ 69 Kcal. Therefore, acetylene molecules could replace water molecules on the metal surface more easily than ethylene (∿ 74 Kcal). Unfortunately, no reliable data on the adsorption energy of water on Au are available. Similar arguments can be applied to Pt.

Chapter V

RECOMMENDATIONS

It may be expected on the basis of the equilibrium diagram for Au-Pt alloys that different methods of preparation or heat treatment lead to different phase compositions within the alloy. Thus, correlations between catalytic or electrochemical properties and certain properties of the bulk, for instance, the d-band character, is not possible. Attempts should be made to produce electrodes that consist of a homogeneous solution of Au and Pt to see if d-band character is an important consideration. Alloys of Au with other noble and non-noble metals which show catalytic activity (e.g., Fe, Co, Ni, etc.) might give valuable insight to the effect of d-band filling on the electrocatalytic activity.

Further studies with other hydrocarbons should be of interest. In order to take advantage of the reactiveness of compounds with unsaturated bonds, substituted acetylenic and ethylenic compounds should be used as far as possible. The reaction products should be particularly scrutinized for possible syntheses using electrochemical oxidation. This could be one of the more important aspects of the study. It was recently emphasized by Dr. G. E. Evans of Union Carbide Corporation, that fuel cells will ultimately be used primarily as reactors to produce various chemicals and that the electricity generated during the process will be considered only a by-product.[36]

BIBLIOGRAPHY

1. Justi, E.W. and A.W. Winsel, "Cold Combustion, Fuel Cell", Franz Steiner Verlag Weisbaden (1963).

2. Young, G.J., "Fuel Cell", Vol. I & II, Reinhold Pub. Corp. N.Y. (1960 & 1963).

3. Breiter, M. and S. Gilman, J. Electrochem. Soc., 109, 622 (1962).

4. Buck, R.P. and L.R. Griffith, J. Electrochem. Soc., 109, 1007 (1962).

5. Green, M., J. Weber, and V. Drazic, J. Electrochem. Soc., 111, 721 (1964).

6. Wroblowa, H., B.J. Piersma, and J.O'M Bockris, J. Electroanal. Chem., 6, 401 (1963).

7. Dahms, H. and J.O'M Bockris, J. Electrochem. Soc. 111, 6, (1964).

8. Adlhart, O.J., Proceeding 19th Power Sources Conference (1965).

9. Mattews, D.B., Ph.D. thesis, Univ. of Pennsylvania (1965).

10. Conway, B.E. and J.O'M Bockris, J. Chem. Phys., 26, 532 (1957).

11. Bockris, J.O'M and S. Srinivasan, J. Electroanal. Chem., 11, 350 (1966).

12. Conway, B.E., E.M. Beatty, and P.A.D. DeMaine, Electrochim. Acta, 7, 39 (1962).

13. Rao, M.L.B., A. Damjanovic, and J.O'M Bockris, J. Phys. Chem., 67, (1963).

14. Damjanovic, A., V. Brusic and J.O'M Bockris, J. Electroanal. Chem., 15, 29, (1967).

15. Kuhn, A.T., H. Wroblowa, and J.O'M Bockris, Trans. Faraday Soc., 63, 1458 (1967).

16. Pauling, L., " The Nature of the Chemical Bond", Cornell Univ. Press, Ithaca, N.Y. (1960).

17. Prontelli, L., Peraldo Bicelli, and A. Lavecchia, Rend. Accad. Naz-Lincei, VIII, 27, 312 (1959).

18. Reddy, A.K.N., A. Pannovic, and J.O'M Bockris, Univ. of Pennsylvania Report (NASA Contract No. NSG 325).

19. Gottlieb, J. Electrochem. Soc., 111, 465 (1964).

20. Piersma, B.J., Ph.D. thesis, Univ. of Pennsylvania (1965).

21. Drazic, V. and J.O'M Bockris, Electrochem. Acta, 7, 293 (1962).

22. Glasstone, S., K.J. Laidler, and H. Eyring, " The Theory of Rate Process", McGraw-Hill, N.Y. (1941).

23. Bagotsky, V.S. and Yu. B. Vasiliev, Electrochim. Acta, 9, 869, (1964).

24. Johnson, J.W., J.L. Reed, and W.J. James, J. Electrochem. Soc., 114, 572 (1967).

25. Breiter, M.W., J. Phys. Chem., 69, 901 (1965).

26. Gileadi, E., B.T. Rubin, and J.O'M Bockris, J. Phys. Chem., 69, 3335 (1965).

27. Johnson, J.W., H. Wroblowa, and J.O'M Bockris, J. Electrochem. Soc., 111, 864 (1964).

28. Trapnell, B.M.W., " Chemisorption", Academic Inc., N.Y. (1955).

29. Bond, G.C., "Catalysis by Metals", Academic Press Inc., London (1962).

30. Reed, J.L., "A Study of the Anodic Oxidation of Acetylene on Gold", Ph.D. thesis, Univ. of Missouri-Rolla (1966).

31. Dahms, H., M. Green, and J. Weber, Nature, 195, 1310 (1962).

32. Gnanamuthu, D.S. and J.V. Petrocelli, J. Electrochem. Soc., 114, 1036 (1967).

33. Gray, H.B., "Electrons and Chemical Bonding", W.A. Benjamin, Inc., Amsterdam, N.Y. (1965).

34. Darling, A.S., R.A. Mintern, and J.C. Chaston, J. Inst. of Metals, 81, 1424 (1952-1953).

35. "Handbook of Chemistry and Physics", 4th edition, published by CRC, Clevend, Ohio (1962).

36. Evans, G.E., "Future Commercial Application for Fuel Cells in the Chemical Industry", Paper presented at St. Louis, the AIChE National Meeting (1968).

APPENDIX A

NOTATIONS

A = Frequency factor in Arrhenius equation

a.t.r.= Above transition region

b.t.r.= Below transition region

C_E = Concentration of ethylene in solution, gmole/cm^3

E_a = Apparent activation energy, Kcal

E'_a = Chemical activation energy, Kcal

E_{C-C} = Carbon-carbon bond energy, Kcal

E_{M-C} = Metal-carbon bond energy, Kcal

E_{M-M} = Metal-metal bond energy, Kcal

F = Faraday constant, 96,500 coulombs/equiv.= 23.06/v·equiv.

f_1 = Fraction of α_1-phase in solid solution

f_2 = Fraction of α_2-phase in solid solution

i_T = Total current density, amp/cm^2

i_1 = Current density contributed by α_1-phase, amp/cm^2

i_2 = Current density contributed by α_2-phase, amp/cm^2

k = Rate constant, sec^{-1}

K_C = Concentration equilibrium constant

K_P = Pressure equilibrium constant

P.Z.C.= Potential of zero charge

P_E = Partial pressure of ethylene, atm

R = Gas constant, 1.987 cal/gmole·K°

r.d.s.= Rate determing step

SHE = Standard hydrogen electrode

T = Absolute temperature °K

V = Potential, volt

W_e = Experimental CO_2 formed for oxidation, gm

W_t = Theoretical CO_2 formed for complete oxidation, gm

α_1 = Pt-rich phase in solid solution

α_2 = Au-rich phase in solid solution

Θ_E = Fraction of total active sites covered with ethylene

Θ_T = Fraction of total active sites covered with chemisorbed species

APPENDIX B

MATERIALS

The following is a list of the materials and reagents used in this investigation. A detailed analysis of the reagents may be obtained from the chemical catalogue of the respective supplier.

1. Acid, Sulfuric. Reagent grade, Fisher Scientific Co., Fairlawn, N.J.

2. Ascarite. 8 to 20 Mesh, Arthur H. Thomas Co., Philadelpha, Pa.

3. Ethylene. C.P. grade, 99.0 % min., Matheson Scientific Co., Joliet, Ill.

4. Gold. (0.003 in. thick sheet) Engelhard Industries Inc., Newark, N.J.

5. Gold-Platinum Alloy. (0.003 in. thick sheet) Engelhard Industries Inc., Newark, N.J.

6. Mercurous Chloride. Reagent grade, Fisher Scientific Co., Fairlawn, N.J. (used in reference electrode)

7. Mercurous Sulfate. Reagent grade, Fisher Scientific Co., Fairlawn, N.J. (used in reference electrode)

8. Nitrogen. Prepurified grade, Matheson Scientific Co. Joliet, Ill.

9. Potassium Chloride. Reagent grade, Fisher Scientific CO., Fairlawn, N.J. (used in reference electrode)

10. Potassium Hydroxide. Reagent grade, Fisher Scientific Co., Fairlawn, N.J.

11. Potassium Sulfate. Reagent grade, Fisher Scientific Co., Fairlawn, N.J.

APPENDIX C

APPARATUS

The following is a list of the principal components used in this investigation.

1. Ammeter. Ultra high sensitivity volt-ohm-microammeter, Simpson 269, Simpson Electric Co., Chicago, Ill.

2. Electrometer. Multi-range type, Model 610B, Keithley Instruments Inc., Cleveland, Ohio.

3. Gas Chromatograph. Model 810 Research Chromatograph, F & M Scientific Corp., Avondale, Pa.

4. Gas Proportioner. Matheson Model 665, Dual-flow control, Matheson Scientific Co., East Rutherford, N.J.

5. Potentiostat. Wenking 66TS1, Gerhard Bank Elektronik, Gottinger, West Germany.

6. Power Supply. Sorensen, QRB (0.75 amp, 40 v) D.C. power supply, Raytheon Co., South Norwalk, Conn.

7. Recorder. Laboratory Recorder V.O.M.-5, Bausch & Lomb Incorp., Rochester, N.Y.

8. Temperature Controller. YSI Thermistemp Model 71, Yellow Springs Instrument Co., Yellow Springs, Ohio.

APPENDIX D

DATA

The following tables include the data obtained in the current-potential studies, current-temperature studies, and current-partial pressure studies. The listed current can be converted to current density by dividing by the geometric surface area of the electrode.

TABLE VII

CURRENT-POTENTIAL VALUES FOR THE ANODIC OXIDATION OF ETHYLENE ON Au AT 80°C (P_E = 1 atm)

1 N H_2SO_4 pH = 0.35		H_2SO_4-K_2SO_4 Mixture pH = 1.4		H_2SO_4-K_2SO_4 Mixture pH = 3.0	
Potential v(SHE)	Current ma	Potential v(SHE)	Current ma	Potential v(SHE)	Current ma
0.747	0.010	0.747	0.011	0.547	0.008
0.794	0.042	0.797	0.040	0.597	0.013
0.822	0.110	0.822	0.090	0.647	0.020
0.847	0.295	0.847	0.240	0.697	0.038
0.872	0.750	0.872	0.560	0.747	0.138
0.897	2.60	0.897	1.50	0.797	0.400
0.947	5.90	0.947	3.70	0.847	0.770
0.997	13.0	0.997	7.50	0.897	1.20
1.047	22.0	1.047	14.0	0.947	1.63

TABLE VIII

CURRENT-POTENTIAL VALUES FOR THE ANODIC OXIDATION OF ETHYLENE ON Au AT 80°C (P_E = 1 atm)

K_2SO_4-K_2CO_3 Mixture pH = 10.1		1 N K_2CO_3 pH = 10.9		1 N KOH pH = 12.7	
Potential v(SHE)	Current ma	Potential v(SHE)	Current ma	Potential v(SHE)	Current ma
0.122	0.010	0.047	0.009	-0.071	0.006
0.172	0.012	0.097	0.015	-0.046	0.008
0.197	0.014	0.122	0.019	-0.021	0.012
0.222	0.018	0.147	0.026	0.004	0.020
0.247	0.022	0.172	0.039	0.029	0.037
0.272	0.030	0.197	0.064	0.054	0.059
0.297	0.045	0.222	0.088	0.079	0.093
0.322	0.065	0.247	0.100	0.104	0.120
0.347	0.093	0.272	0.090	0.129	0.145
0.372	0.117			0.154	0.14
0.397	0.125				
0.422	0.120				

TABLE IX

CURRENT-POTENTIAL VALUES FOR THE ANODIC OXIDATION OF ETHYLENE ON 80Au-20Pt ALLOY AT 80°C (P_E = 1 atm)

1 N H_2SO_4 pH = 0.35		H_2SO_4-K_2SO_4 Mixture pH = 1.4		H_2SO_4-K_2SO_4 Mixture pH = 3.0	
Potential v(SHE)	Current ma	Potential v(SHE)	Current ma	Potential v(SHE)	Current ma
0.422	0.0055	0.397	0.004	0.347	0.0045
0.447	0.011	0.447	0.009	0.397	0.010
0.497	0.025	0.497	0.0165	0.447	0.0195
0.547	0.0505	0.547	0.029	0.497	0.039
0.597	0.103	0.597	0.090	0.547	0.100
0.647	0.195	0.647	0.180	0.647	0.470
0.697	0.200	0.697	0.225	0.697	0.440
0.747	0.210	0.747	0.245	0.722	0.430
0.797	0.640	0.797	0.430		
0.847	2.70	0.847	1.15		
0.872	6.0	0.897	2.80		
0.897	8.80	0.922	2.70		
0.922	8.50				

TABLE X

CURRENT-POTENTIAL VALUES FOR THE ANODIC OXIDATION OF ETHYLENE ON 80Au-20Pt ALLOY AT 80°C (P_E = 1 atm)

K_2SO_4-K_2CO_3 Mixture pH = 10.1		1 N K_2CO_3 pH = 10.9		1 N KOH pH = 12.7	
Potential v(SHE)	Current ma	Potential v(SHE)	Current ma	Potential v(SHE)	Current ma
0.029	0.005	-0.096	0.0045	-0.171	0.010
0.054	0.008	-0.071	0.007	-0.146	0.017
0.079	0.012	-0.046	0.012	-0.121	0.026
0.104	0.015	-0.021	0.0165	-0.096	0.048
0.129	0.018	0.004	0.024	-0.071	0.068
0.154	0.018	0.029	0.040	-0.046	0.082
0.179	0.016	0.054	0.045	-0.021	0.086
		0.079	0.043	0.004	0.082
		0.129	0.042		

TABLE XI

CURRENT-POTENTIAL VALUES FOR THE ANODIC OXIDATION OF ETHYLENE ON 60Au-40Pt ALLOY AT 80°C (P_E = 1 atm)

1 N H_2SO_4 pH = 0.35		H_2SO_4-K_2SO_4 Mixture pH = 1.4		H_2SO_4-K_2SO_4 Mixture pH = 3.0	
Potential v(SHE)	Current ma	Potential v(SHE)	Current ma	Potential v(SHE)	Current ma
0.447	0.006	0.397	0.004	0.347	0.006
0.497	0.016	0.447	0.008	0.397	0.012
0.547	0.043	0.497	0.016	0.447	0.024
0.597	0.100	0.547	0.030	0.497	0.048
0.647	0.182	0.597	0.060	0.547	0.128
0.697	0.225	0.647	0.170	0.597	0.320
0.722	0.235	0.697	0.200	0.647	0.570
0.747	0.260	0.747	0.300	0.672	0.720
0.772	0.400	0.797	0.640	0.697	0.690
0.797	0.850	0.847	1.650		
0.822	1.480	0.897	3.60		
0.847	2.750	0.922	3.50		
0.872	5.50				
0.897	8.70				
0.922	10.0				
0.947	8.0				

TABLE XII

CURRENT-POTENTIAL VALUES FOR THE ANODIC OXIDATION OF ETHYLENE ON 60Au-40Pt ALLOY AT 80°C (P_E = 1 atm)

K_2SO_4-K_2CO_3 Mixture pH = 10.1		1 N K_2CO_3 pH = 10.9		1 N KOH pH = 12.7	
Potential v(SHE)	Current ma	Potential v(SHE)	Current ma	Potential v(SHE)	Current ma
0.004	0.007	-0.096	0.009	-0.196	0.013
0.029	0.010	-0.071	0.013	-0.146	0.025
0.054	0.016	-0.046	0.022	-0.121	0.050
0.079	0.022	-0.021	0.037	-0.096	0.082
0.104	0.027	0.004	0.050	-0.071	0.120
0.129	0.027	0.029	0.060	-0.046	0.140
0.154	0.026	0.054	0.062	-0.021	0.135
		0.079	0.060		
		0.129	0.050		

TABLE XIII

CURRENT-POTENTIAL VALUES FOR THE ANODIC OXIDATION OF ETHYLENE ON 40Au-60Pt ALLOY AT 80°C (P_E = 1 atm)

1 N H_2SO_4 pH = 0.35		H_2SO_4-K_2SO_4 Mixture pH = 1.4		H_2SO_4-K_2SO_4 Mixture pH = 3.0	
Potential v(SHE)	Current ma	Potential v(SHE)	Current ma	Potential v(SHE)	Current ma
0.447	0.0075	0.447	0.010	0.347	0.004
0.497	0.016	0.497	0.020	0.397	0.008
0.547	0.029	0.547	0.046	0.447	0.016
0.597	0.070	0.597	0.084	0.497	0.032
0.647	0.175	0.647	0.240	0.547	0.094
0.697	0.285	0.697	0.500	0.597	0.230
0.722	0.365	0.747	0.780	0.647	0.480
0.747	0.470	0.797	1.10	0.697	0.780
0.772	0.760	0.847	2.10	0.747	0.800
0.797	1.20	0.897	2.40	0.797	0.700
0.822	1.95	0.922	2.20		
0.847	3.10				
0.872	6.0				
0.897	9.0				
0.922	8.5				

TABLE XIV

CURRENT-POTENTIAL VALUES FOR THE ANODIC OXIDATION OF ETHYLENE ON 40Au-60Pt ALLOY AT 80°C (P_E = 1 atm)

K_2SO_4-K_2CO_3 Mixture pH = 10.1		1 N K_2CO_3 pH = 10.9		1 N KOH pH = 12.7	
Potential v(SHE)	Current ma	Potential v(SHE)	Current ma	Potential v(SHE)	Current ma
0.004	0.005	-0.071	0.012	-0.171	0.013
0.029	0.008	-0.046	0.020	-0.146	0.018
0.054	0.016	-0.021	0.032	-0.121	0.034
0.079	0.023	0.004	0.049	-0.096	0.067
0.104	0.031	0.029	0.055	-0.071	0.098
0.129	0.033	0.079	0.054	-0.046	0.110
0.154	0.034			-0.021	0.100
0.179	0.034				
0.229	0.039				
0.329	0.036				

TABLE XV

CURRENT-POTENTIAL VALUES FOR THE ANODIC OXIDATION OF ETHYLENE ON 20Au-80Pt ALLOY AT 80°C (P_E = 1 atm)

1 N H_2SO_4 pH = 0.35		H_2SO_4-K_2SO_4 Mixture pH = 1.4		H_2SO_4-K_2SO_4 Mixture pH = 3.0	
Potential v(SHE)	Current ma	Potential v(SHE)	Current ma	Potential v(SHE)	Current ma
0.447	0.013	0.447	0.0075	0.447	0.026
0.497	0.024	0.497	0.015	0.497	0.050
0.547	0.043	0.547	0.035	0.547	0.110
0.597	0.082	0.597	0.077	0.597	0.245
0.647	0.152	0.647	0.150	0.647	0.460
0.697	0.280	0.697	0.283	0.697	0.700
0.747	0.530	0.747	0.500	0.747	0.900
0.797	0.860	0.797	0.960	0.797	1.60
0.847	2.20	0.847	2.80	0.847	2.00
0.872	3.90	0.897	4.40	0.897	1.40
0.922	7.20	0.922	3.30		
0.947	5.00				

TABLE XVI

CURRENT-POTENTIAL VALUES FOR THE ANODIC OXIDATION OF ETHYLENE ON 20Au-80Pt ALLOY AT 80°C (P_E = 1 atm)

K_2SO_4-K_2CO_3 Mixture pH = 10.1		1 N K_2CO_3 pH = 10.9		1 N KOH pH = 12.7	
Potential v(SHE)	Current ma	Potential v(SHE)	Current ma	Potential v(SHE)	Current ma
-0.053	0.011	-0.103	0.018	-0.221	0.014
-0.028	0.015	-0.078	0.027	-0.196	0.024
-0.003	0.023	-0.053	0.046	-0.171	0.042
0.022	0.031	-0.028	0.072	-0.146	0.073
0.047	0.049	-0.003	0.110	-0.096	0.220
0.072	0.075	0.022	0.140	-0.071	0.290
0.097	0.120	0.045	0.130	-0.046	0.310
0.122	0.157			-0.021	0.300
0.147	0.163				
0.172	0.150				

TABLE XVII

CURRENT-POTENTIAL VALUES FOR THE ANODIC OXIDATION OF ETHYLENE ON SMOOTH Pt* AT 80°C (P_E = 1 atm)

1 N H_2SO_4 pH = 0.35		1 N KOH pH = 12.7	
Potential v(SHE)	Current ma	Potential v(SHE)	Current ma
0.447	0.017	-0.196	0.015
0.497	0.034	-0.171	0.025
0.547	0.092	-0.146	0.038
0.597	0.260	-0.121	0.086
0.647	0.610	-0.096	0.155
0.697	1.10	-0.071	0.220
0.722	1.40	-0.046	0.180
0.747	1.80	0.029	0.140
0.797	2.60		
0.822	3.00		
0.847	3.40		
0.872	3.60		
0.897	3.00		

*Surface area = 12.5 cm^2

TABLE XVIII

CURRENT-TEMPERATURE VALUES FOR THE ANODIC OXIDATION OF ETHYLENE ON Au IN 1.0 N H_2SO_4 (P_E = 1 atm)

Potential v(SHE)	Temperature °C	Current ma
0.847	80	0.730
	75	0.525
	70	0.360
	65	0.250
	60	0.170
	55	0.105
0.897	80	2.50
	75	1.75
	70	1.135
	65	0.79
	60	0.54
	55	0.37

TABLE XIX

CURRENT-TEMPERATURE VALUES FOR THE ANODIC OXIDATION OF ETHYLENE ON Au IN 1.0 N KOH (P_E = 1 atm)

Potential V(SHE)	Temperature °C	Current ma
0.054	80	0.095
	75	0.067
	70	0.032
	65	0.018
	60	0.0115
0.104	80	0.285
	75	0.165
	70	0.098
	65	0.067
	60	0.035
	55	0.018

TABLE XX

CURRENT-TEMPERATURE VALUES FOR THE ANODIC OXIDATION OF ETHYLENE ON 80Au-20Pt ALLOY IN 1.0 N H_2SO_4 (P_E = 1 atm)

Potential v(SHE)	Temperature °C	Current ma
	Above Transition Region	
0.847	80	2.25
	75	1.40
	70	1.0
	65	0.73
	60	0.50
	55	0.30
0.897	80	7.5
	75	5.6
	70	3.5
	65	2.32
	60	1.53
	55	1.0
	Below Transition Region	
0.547	80	0.026
	75	0.018
	70	0.012
	65	0.0075
	60	0.005
0.597	80	0.043
	75	0.030
	70	0.020
	65	0.014
	60	0.0095
	55	0.006

TABLE XXI

CURRENT-TEMPERATURE VALUES FOR THE ANODIC OXIDATION OF ETHYLENE ON 80Au-20Pt ALLOY IN 1.0 N KOH (P_E = 1 atm)

Potential v(SHE)	Temperature °C	Current ma
-0.121	80	0.041
	75	0.028
	70	0.019
	65	0.012
	60	0.0067
-0.071	80	0.138
	75	0.096
	70	0.059
	65	0.035
	60	0.021
	55	0.012

TABLE XXII

CURRENT-TEMPERATURE VALUES FOR THE ANODIC OXIDATION OF ETHYLENE ON 60Au-40Pt ALLOY IN 1.0 N H_2SO_4 (P_E = 1 atm)

Potential v(SHE)	Temperature °C	Current ma
	Above Transion Region	
0.822	80	1.81
	75	1.28
	70	0.90
	65	0.54
	60	0.42
	55	0.28
0.872	80	5.6
	75	4.3
	70	3.2
	65	2.0
	60	1.2
	55	0.76
	Below Transition Region	
0.547	80	0.047
	75	0.035
	70	0.025
	65	0.0175
	60	0.012
	55	0.008
0.597	80	0.107
	75	0.075
	70	0.052
	65	0.036
	60	0.024
	55	0.016

TABLE XXIII

CURRENT-TEMPERATURE VALUES FOR THE ANODIC OXIDATION OF ETHYLENE ON 60Au-40Pt ALLOY IN 1.0 N KOH (P_E = 1 atm)

Potential v(SHE)	Temperature °C	Current ma
-0.121	80	0.052
	75	0.031
	70	0.0185
	65	0.011
	60	0.0078
-0.071	80	0.145
	75	0.105
	70	0.066
	65	0.040
	60	0.022
	55	0.0135

TABLE XXIV

CURRENT-TEMPERATURE VALUES FOR THE ANODIC OXIDATION OF ETHYLENE ON 40Au-60Pt ALLOY IN 1.0 N H_2SO_4 (P_E = 1 atm)

Potential v(SHE)	Temperature °C	Current ma
0.772	80	0.55
	75	0.37
	70	0.24
	65	0.155
	60	0.098
	55	0.059
0.822	80	1.35
	75	0.91
	70	0.59
	65	0.36
	60	0.212
	55	0.135

TABLE XXV

CURRENT-TEMPERATURE VALUES FOR THE ANODIC OXIDATION OF ETHYLENE ON 40Au-60Pt ALLOY IN 1.0 N KOH (P_E = 1 atm)

Potential v(SHE)	Temperature °C	Current ma
-0.121	80	0.025
	75	0.016
	70	0.009
	65	0.0045
-0.071	80	0.110
	75	0.070
	70	0.038
	65	0.0205
	60	0.012
	55	0.006

TABLE XXVI

CURRENT-TEMPERATURE VALUES FOR THE ANODIC OXIDATION OF ETHYLENE ON 20Au-80Pt ALLOY IN 1.0 N H_2SO_4 (P_E = 1 atm)

Potential v(SHE)	Temperature °C	Current ma
0.797	80	2.20
	75	1.40
	70	0.87
	65	0.54
	60	0.33
	55	0.20
0.847	80	4.10
	75	2.70
	70	1.70
	65	1.11
	60	0.68
	55	0.38

TABLE XXVII

CURRENT-TEMPERATURE VALUES FOR THE ANODIC OXIDATION OF ETHYLENE ON 20Au-80Pt ALLOY IN 1.0 N KOH (P_E = 1 atm)

Potential v(SHE)	Temperature °C	Current ma
-0.146	80	0.105
	75	0.065
	70	0.035
	65	0.0195
	60	0.009
-0.096	80	0.250
	75	0.160
	70	0.105
	65	0.057
	60	0.032
	55	0.018

TABLE XXVIII

CURRENT-PRESSURE VALUES FOR THE ANODIC OXIDATION OF ETHYLENE ON Au IN 1.0 N H_2SO_4 AT 80° C

Potential v(SHE)	C_2H_4 Partial Pressure atm	Current ma
0.847	1.0	0.33
	0.3	0.165
	0.1	0.090
	0.03	0.033
	0.01	0.016
0.897	1.0	2.10
	0.3	1.07
	0.1	0.57
	0.03	0.25
	0.01	0.127

TABLE XXIX

CURRENT-PRESSURE VALUES FOR THE ANODIC OXIDATION OF ETHYLENE ON Au IN 1.0 N KOH AT 80°C

Potential v(SHE)	C_2H_4 Partial Pressure atm	Current ma
0.054	1.0	0.061
	0.3	0.035
	0.1	0.016
	0.03	0.009
	0.01	0.007
0.104	1.0	0.075
	0.3	0.041
	0.1	0.020
	0.03	0.013
	0.01	0.011

TABLE XXX

CURRENT-PRESSURE VALUES FOR THE ANODIC OXIDATION OF ETHYLENE ON 80Au-20Pt ALLOY IN 1.0 N H_2SO_4 AT 80°C

Potential v(SHE)	C_2H_4 Partial Pressure atm	Current ma
	Above Transition Region	
0.822	1.0	0.68
	0.3	0.50
	0.1	0.29
	0.03	0.16
	0.01	0.10
0.872	1.0	5.3
	0.3	3.5
	0.1	1.7
	0.03	0.76
	0.01	0.44
	Below Transition Region	
0.622	1.0	0.018
	0.3	0.016
	0.1	0.0125
	0.03	0.0095
	0.01	0.0070
0.672	1.0	0.025
	0.3	0.022
	0.1	0.0165
	0.03	0.0135
	0.01	0.0120

TABLE XXXI

CURRENT-PRESSURE VALUES FOR THE ANODIC OXIDATION OF ETHYLENE ON 80Au-20Pt ALLOY IN 1.0 N KOH AT 80°C

Potential v(SHE)	C_2H_4 Partial Pressure atm	Current ma
-0.121	1.0	0.045
	0.3	0.035
	0.1	0.025
	0.03	0.014
	0.01	0.008
-0.071	1.0	0.063
	0.3	0.045
	0.1	0.027
	0.03	0.016
	0.01	0.010

TABLE XXXII

CURRENT-PRESSURE VALUES FOR THE ANODIC OXIDATION OF ETHYLENE ON 60Au-40Pt ALLOY IN 1.0 N H_2SO_4 AT 80°C

Potential v(SHE)	C_2H_4 Partial Pressure atm	Current ma
	Above Transition Region	
0.822	1.0	1.30
	0.3	1.0
	0.1	0.64
	0.03	0.34
	0.01	0.22
0.872	1.0	4.5
	0.3	3.0
	0.1	1.87
	0.03	1.08
	0.01	0.69
	Below Transition Region	
0.547	1.0	0.034
	0.3	0.030
	0.1	0.0255
	0.03	0.0215
	0.01	0.019
0.597	1.0	0.054
	0.3	0.0455
	0.1	0.0375
	0.03	0.034
	0.01	0.030

TABLE XXXIII

CURRENT-PRESSURE VALUES FOR THE ANODIC OXIDATION OF ETHYLENE ON 60Au-40Pt ALLOY IN 1.0 N KOH AT 80°C

Potential v(SHE)	C_2H_4 Partial Pressure atm	Current ma
-0.121	1.0	0.072
	0.3	0.055
	0.1	0.035
	0.03	0.019
	0.01	0.011
-0.071	1.0	0.105
	0.3	0.08
	0.1	0.06
	0.03	0.03
	0.01	0.016

TABLE XXXIV

CURRENT-PRESSURE VALUES FOR THE ANODIC OXIDATION OF ETHYLENE ON 40Au-60Pt ALLOY IN 1.0 N H_2SO_4 AT 80°C

Potential v(SHE)	C_2H_4 Partial Pressure atm	Current ma
0.772	1.0	0.69
	0.3	0.53
	0.1	0.37
	0.03	0.24
	0.01	0.16
0.822	1.0	1.65
	0.3	1.20
	0.1	0.73
	0.03	0.41
	0.01	0.32
0.872	1.0	4.6
	0.3	3.6
	0.1	2.2
	0.03	1.3
	0.01	0.71

TABLE XXXV

CURRENT-PRESSURE VALUES FOR THE ANODIC OXIDATION OF ETHYLENE ON 40Au-60Pt ALLOY IN 1.0 N KOH AT 80°C

Potential v(SHE)	C_2H_4 Partial Pressure atm	Current ma
-0.121	1.0	0.034
	0.3	0.026
	0.1	0.017
	0.03	0.009
	0.01	0.005
-0.071	1.0	0.068
	0.3	0.052
	0.1	0.034
	0.03	0.020
	0.01	0.009

TABLE XXXVI

CURRENT-PRESSURE VALUES FOR THE ANODIC OXIDATION OF ETHYLENE ON 20Au-80Pt ALLOY IN 1.0 N H_2SO_4 AT 80°C

Potential v(SHE)	C_2H_4 Partial Pressure atm	Current ma
0.797	1.0	4.3
	0.3	3.4
	0.1	2.2
	0.03	1.45
	0.01	0.95
0.847	1.0	5.35
	0.3	3.90
	0.1	2.50
	0.03	1.60
	0.01	1.20
0.894	1.0	7.50
	0.3	5.40
	0.1	3.30
	0.03	1.90
	0.01	1.20

TABLE XXXVII

CURRENT-PRESSURE VALUES FOR THE ANODIC OXIDATION OF ETHYLENE ON 20Au-80Pt ALLOY IN 1.0 N KOH AT 80°C

Potential v(SHE)	C_2H_4 Partial Pressure atm	Current ma
-0.146	1.0	0.105
	0.3	0.082
	0.1	0.059
	0.03	0.035
	0.01	0.028
-0.096	1.0	0.188
	0.3	0.133
	0.1	0.078
	0.03	0.048
	0.01	0.028

VITA

San-Cheng Lai was born on December 8, 1940, in Taichung, Formosa. He received his elementary and high school education in Taichung, and graduated from high school in June, 1959.

He entered the National Taiwan University in September, 1959, and graduated in June, 1963, with a B.S. degree in Chemical Engineering. After graduation, he served in the Nationalist Chinese Army for one year of military service as a Second Lieutenant.

He came to the United States and enrolled in the Graduate School of the University of Missouri - Rolla, in January, 1965. In August, 1966 he received the M.S. degree in Chemical Engineering.

He held a Teaching Assistantship in the Mathematics Department while pursuing studies to the M.S. degree. He received a Research Assistantship from the Space Sciences Research Center during his study for the Ph.D. degree in Chemical Engineering.